HEINRICH HEINE
UNIVERSITÄT
DÜSSELDORF

The importance of the integrity of phytochromes for their biochemical and physiological function

Inaugural Dissertation

zur

Erlangung des Doktorgrades der

Mathematisch-Naturwissenschaftlichen Fakultät

der Heinrich-Heine-Universität Düsseldorf

vorgelegt von

Rashmi Shah

aus Kathmandu (Nepal)

May 2011

angefertigt am Max Planck Institut für Bioanorganische Chemie
(Performed at Max Planck Institute for Bioinorganic Chemistry)

Gedruckt mit der Genehmigung der
Mathematisch-Naturwissenschaftlichen Fakultät der
Heinrich-Heine-Universität Düsseldorf

Referent: Prof. Dr. Wolfgang Gärtner *(first referee)*

Koreferent: Prof. Dr. Karl-Erich Jaeger *(second referee)*

Tag der mündlichen Prüfung: 30.05.2011 *(date of the oral examination)*

Acknowledgement

First of all I would like to express my sincere gratitude to Prof. Dr. Wolfgang Gärtner for giving me the opportunity to work in his group and providing superb guidance during the period of investigation. Furthermore, I am grateful to him for the critical readings and corrections of the manuscript in spite of his busy schedules, after which this thesis has come out in this form.

I would like to thank Prof. Dr. Karl-Erich Jaeger (Institute for Molecular Enzyme Technology, University of Düsseldorf, Forschungszentrum Jülich) for kindly accepting to be the second referee of this dissertation.

My sincere thanks go to Dr. Thomas Drepper (Institute for Molecular Enzyme Technology, University of Düsseldorf, Forschungszentrum Jülich) for valuable suggestions during the generation of the knockout mutants. Many thanks also go to Prof. Jorge Casal (Institute for Agricultural Plant Physiology and Ecology, Buenos Aires, Argentina) for helping with the infectivity experiments of knockout mutants.

I would like to thank Dr. Shivani Sharda for generously sharing her expertise and labor in phytochrome expression and conducting the protein-purification experiments. Special thanks go to colleagues Dr. Amrit Pal Kaur, Björn Zorn, Dr. Cao Zhen, Dr. Christina Alessandra Hoppe, Jana Riethausen, Dr. Madina Mansurova, Sarah Raffelberg and Sebastian Gandor for good working and the inspiring atmosphere. It was a pleasant and unforgettable environment in the lab because of cooperative and supportive attitude of all of the group members. I extend my appreciation to Ms. Gülümse Koc-Weier and Mrs. Helene Steffen for maintaining the order and providing support for keeping things functional in the laboratory.

I am deeply and forever indebted to my parents for their love, support and encouragement throughout my entire life. My deepest gratitudes are to my sisters for their love, belief and eternal support. A special thank to my son Garbit whose smile always inspired me and coming home to him everyday made my life sweet. Finally, a great thanks to my husband Gopal with whom I would like to share this work, for his patience, support and above all for his love.

Publications and manuscripts

Sharda, S., Shah, R., and Gärtner, W., (2007) Domain interaction in cyanobacterial phytochromes as a prerequisite for spectral integrity. Eur Biophys J.; 36(7) : 815-21.

Shah, R., Pathak, G., Drepper, T., and Gärtner, W. An Efficient, Linear DNA-based *in vivo* Mutagenesis System for *Pseudomonas syringae* (Manuscript)

Shah, R., and Gärtner, W., Complex formation between heme oxygenase and phytochrome during biosynthesis in *Pseudomonas syringae* pv *tomato* (Manuscript).

Summary

Phytochrome pigments were first characterized in higher plants in the 1950's [1]. These red/far red sensing biological photoreceptors were later reported also for cyanobacteria [2], and also in other non-photosynthetic bacteria and fungi [3]. Phytochromes interconvert between red light (664/704 nm, P_R states) and far-red light (707/750 nm, P_{FR} states) absorbing forms. This photoconversion represents a double bond photoisomerization of the covalently bound bilin chromophores

In this work, four different research projects from the area of biological photoreceptors were followed:

(i) The phytochromes CphA and CphB from the cyanobacterium *Calothrix* PCC7601 were investigated for the essential protein domains required to maintain the spectral integrity. Both proteins fold into PAS-, GAF-, PHY-, and Histidine-kinase (HK) domains. CphA binds phycocyanobilin (PCB) as chromophore and CphB binds biliverdin (BV) IXα. Removal of the HK domains had no effect on the absorbance maxima of the resulting PAS–GAF–PHY constructs (CphA: 663/ 707 nm, CphB: 704/750 nm, P_R/P_{FR}, respectively); these values are similar to the full length protein CphA and CphB. Further deletion of the "PHY" domains caused a blue-shift of the P_R and P_{FR} absorption of CphA (λ_{max}: 658/698 nm) and increased the amount of unproperly folded apoprotein, seen as a reduced capability to bind the chromophore in a photoconvertible manner. In CphB, however, this deletion practically impaired the formation of $P_{FR.}$ The intermediate that can be generated shows an absorption band with very low oscillator strength, whereas the spectral features of the P_R form remain unchanged.

(ii) In an approach to generate non-naturally existing hybrid proteins, the blue-light sensor kinase module (PAS motif) of *P. syringae pv tomato* was fused with the red/far red photoreceptor HK from the cyanobacterial phytochrome CphA to study the kinase activity of such a reprogrammed (swapped) sensor kinase. This

reprogrammed sensor LOV-kinase retained the typical photochemical properties of *Pst*LOV.

(iii) Recent genome sequence data of the model plant pathogen *Pseudomonas syringae* pv tomato DC3000 have revealed the presence of two red/far red sensing putative phytochrome photoreceptors (*Pst*BphP1 and *Pst*BphP2) and one blue-light photoreceptor (*Pst*LOV). The bacterial phytochromes from *P. syringae pv tomato* (*Pst*BphPs) were recombinantly expressed in *E. coli* and characterized *in vitro.* Both phytochromes show the general modular architecture of a three domain chromophore-binding region (PAS-GAF-PHY) that is followed by a histidine kinase domain at the C-terminal part. *PstbphP1* is arranged in an operon with a preceding gene encoding a heme oxygenase (*PstbphO*), whereas *PstbphP2* is followed by a response regulator. Heterologous expression of the heme oxygenase yielded a green protein (λ_{max} = 650 nm), indicative for bound biliverdin. Heterologous expression of *PstbphP1* and *PstbphP2* yielded the apoproteins for both phytochromes, however, only in case of *Pst*BphP1 a holoprotein was formed upon addition of biliverdin. The two phytochromes were also co-expressed with *Pst*bphO as a two-plasmid approach yielding a fully assembled holoprotein for *Pst*BphP1, whereas again for *Pst*BphP2 no chromophore absorbance could be detected. An even further increased yield for *Pst*BphP1 was obtained when the operon *PstbphO: PstbphP1* was expressed in *E. coli*. A construct placing the gene for *Pst*BphP2 exactly at the position of *PstbphP1* in this operon again gave the negative result such that no phytochrome-2 chromoprotein was formed. The reason for the improved yield for the operon expression *PstbphO: PstbphP1* is the formation of a complex formed between both proteins during biosynthesis.

(iv) The regulatory functions of these red/ far red genes and of the also present blue light photoreceptor gene were studied by generating insertional knockout mutants. As the commonly applied protocol of gene transfer by conjugation/homologous recombination is a time-consuming process of low-efficiency, an alternative method was developed in this study to create interposon- as well as point mutations of the

corresponding photoreceptors genes by employing linear DNA constructs. Four single mutant strains, *bphP1Δ*, *bphP2Δ*, *bphOΔ*, pspto_2896 (*LOVΔ*) and one double mutant strain, *bphP1ΔbphP2Δ* were generated using the new method. The bphO- and the pspto_2896 (LOV) genes encode the heme oxygenase and the blue light-sensitive photoreceptor, described in sub-project (iii). The pspto_2896 mutant strain was tested for the motility in blue light (447 nm), and all the other mutants were tested under red/ far red (625, 660, 720, 740 nm) light for changes in their motility. All mutant strains showed photokinesis response to the blue/red/ far red light. Further, the effect of mutations on infectivity on plants was studied for the phytochrome mutant strain (*bphP1Δ*), and the blue-light photoreceptor (*LOVΔ*) mutant strain. Our preliminary experiments of plant-mutant interaction indicate that light perceived by the LOV-domain photoreceptor reduces bacterial growth (this behavior is not observed for the mutant strain), whereas no such effect is observed for the phytochrome photoreceptor.

Zusammenfassung

Die Existenz von Phytochromen wurde zuerst in den fünfziger Jahren des vorigen Jahrhunderts in höheren Pflanzen nachgewiesen [1]. Diese rot/dunkelrot sensitiven Photorezeptoren wurden später dann für Cyanobakterien berichtet [2], und im Folgenden auch in nicht-photosynthetischen Bakterien und Pilzen [3]. Phytochrome konvertieren bei Belichtung zwischen Rotlicht-absorbierenden (664/704 nm, P_R Zustände) und Dunkelrot-absorbierenden Formen (707/750 nm, P_{FR} Zustände). Diese Photokonversion beruht auf einer Doppelbindung-Photoisomerisierung des Chromophors.

In dieser Dissertation wurden vier verschiedene Aspekte dieser biologischen Photorezeptoren bearbeitet:

(i) Die Phytochrome CphA und CphB aus dem Cyanobakterium *Calothrix* PCC7601 wurden dahin gehend untersucht, zu bestimmen, welche Proteindomänen essentiell sind, um die spektrale Integrität dieser Chromoproteine aufrecht zu erhalten. Beide Proteine bilden PAS-, GAF-, PHY-, und Histidine-kinase (HK) Domänen. CphA bindet Phycocyanobilin (PCB) als Chromophor und CphB bindet Biliverdin (BV) IXα. Es zeigte sich, dass die Entfernung der HK-Domäne keinen Effekt auf die Absorptionsmaxima der verbleibenden PAS-GAF-PHY Konstrukte hatte (CphA: 663/ 707 nm, CphB: 704/750 nm, für jeweils P_R/P_{FR}; diese Werte sind praktisch identisch zu denen der Volllängenproteine). Eine weitergehende Entfernung der „PHY“-Domänen führte zu einer Blauverschiebung beider Maxima für CphA (λ_{max}: 658/698 nm) und zu einer größeren Menge an ungefaltetem Protein; dies ließ sich aus der geringeren Menge an assemblierbarem Protein ableiten. Im Fall von CphB führte die gleiche Deletion jedoch zum fast vollständigen Verlust der P_{FR}-Absorption, während die spektralen Eigenschaften der P_R-Form erhalten

blieben. Wahrscheinlich bildet sich stattdessen ein Intermediat mit einer deutlich geringeren Oszillatorstärke.

(ii) Im zweiten projekt wurde der Versuch unternommen, nicht-natürlich vorkommende hybride Proteine zu erzeugen. Hierzu wurde die Blaulicht-sensitive LOV-Domäne eines Photorezeptors aus *Pseudomonas syringae* (pv. tomato) mit der HK-Domäne eines Rotlicht-sensitiven Phytochroms (aus CphA) fusioniert. Ziel dieses Ansatzes war die Frage, ob sich die Kinaseaktivität auch mit einer veränderten Lichtdetektions-Domäne steuern lässt. Die im Rahmen dieses Projekts erhaltenen Ergebnisse zeigen zunächst den Erhalt der typischen Blaulicht-Photochemie.

(iii) Im dritten projekt wurden Untersuchungen an dem Pflanzen-pathogenen Modellorganismus *P. syringae* (pv. tomato DC3000) durchgeführt. Genomsequenz-Analysen ergaben die Existenz zweier Gene für Rot-/Dunkelrot-sensitiven Phytochrome (*Pst*BphP1 und *Pst*BphP2) und eines weiteren Gens für einen Blaulicht-sensitiven Photorezeptor (*Pst*LOV). Die Phytochrome wurden rekombinant in *E. coli* exprimiert und *in vitro* charakterisiert. Beide Proteine zeigen die typische modulare Struktur einer Dreidomänen Chromophor-Binderegion (PAS-GAF-PHY), an die sich C-terminal eine Histidinkinase anschließt. *PstbphP1* liegt in einem Operon vor, in dem ein Hämoxygenase- (HO) kodierendes Gen vorangeht, während *PstbphP2* von einem Gen gefolgt wird, das für einen response regulator kodiert. Heterologe Expression des HO-Gens ergab ein grünes Protein (λ_{max} = 650 nm), dessen Farbe charakteristisch für gebundenes Biliverdin ist. Die heterologe Expression von *PstbphP1* und *PstbphP2* ergaben in beiden Fällen die Apoproteine, allerdings ließ sich nur im Fall von *Pst*bphP1 das Holoprotein durch Zugabe von Biliverdin erzeugen. Beide Phytochrome wurden auch mit der Hämoxygenase ko-exprimiert, aber auch in diesem Falle konnte nur für *Pst*bphP1 das Holoprotein nachgewiesen werden, während für sein Paralog *Pst*bphP2 keine

Chromophorabsorption nachgewiesen werden konnte. Eine noch mehr erhöhte Ausbeute an Protein mit verbesserten spektralen Eigenschaften wurde erhalten, wenn die vorhandene Operonstruktur ausgenutzt wurde, allerdings versagte dieser Ansatz wiederum für *Pst*bphP2 (hier wurde Basen-genau das kodierende Gen für *Pst*bphP2 an die Stelle von *PstbphP1* gesetzt). Als Ursache für die deutlich verbesserte Ausbeute von *Pst*bphP1 konnte eine Komplexbildung dieses Proteins mit der HO während der Expression nachgewiesen werden, die offensichtlich stabilisierend auf das Phytochrom wirkt.

(iv) Die regulatorische Funktion der Rot-/Dunkelrot-sensitiven Phytochrome und auch des Blaulicht-sensitiven Rezeptors für das Bakterium wurden im vierten Teilprojekt durch knock-out insertierte Mutanten nachgewiesen. Da die üblicherweise angewandte Methode des Gentransfers mittels Konjugation/homologer Rekombination sehr zeitaufwändig und von geringer Effizienz ist, wurde in dieser Arbeit eine alternative Methode entwickelt, um nun mit Hilfe linearer doppelsträngiger DNA Interposon- und Punktmutationen dieser Photorezeptoren zu erzeugen. Vier Einzelmutanten, *bphP1Δ*, *bphP2Δ*, *bphOΔ*, pspto_2896 (*LOVΔ*) und eine Doppelmutante, *bphP1ΔbphP2Δ*, wurden auf diese Weise erzeugt. Die bphO- und pspto_2896 (LOV) Gene kodieren die bereits in (iii) diskutierten Hämoxygenase und den Blaulicht-sensitiven Photorezeptor. Der pspto_2896 Mutant-Stamm wurde auf seine Motilität in blauem Licht getestet (447 nm), während alle anderen Mutanten in rotem bzw. dunkelrotem Licht (625, 660, 720, 740 nm) auf Änderungen ihrer Motilität untersucht wurden. Es wurden für alle Mutanten Änderungen in ihrer Photokinese gefunden. Darüber hinaus wurde untersucht, ob die Mutantenstämme (*bphP1Δ* und der Blaulicht-Photorezeptor defiziente Stamm, *LOVΔ*) eine veränderte Infektivität gegenüber Pflanzen aufwiesen (*Arabidopsis thaliana*). Erste Ergebnisse zeigen, dass der Blaulicht-Photorezeptor im Wildtyp-Stamm im Vergleich zur Mutante unter

Belichtung zu verringertem Wachstum führt, während kein entsprechender Effekt für den Phytochrom-Rezeptor nachweisbar war.

Table of contents

Abbreviations

aa	Amino acid(s)
Abs	Absorbance
Amp	Ampicillin
AP	Alkaline phosphatase
ATP	Adenosin 5'-triphosphate
BBP	Bilin binding pocket
BL	Blue light
BLUF	Light Using FAD domain
bp	Base pairs
BphP	Bacteriophytochrome ("P" is photoreceptor)
BSA	Bovine serum albumin
BV	Biliverdin
^{0}C	Degree Celsius
CBD	Chromophore binding domain
CCA	Complementary chromatic adaptation
cDNA	Complementary DNA
CikA	Circadian input kinase A
CIP	Calf intestinal phosphatase
Cm	Chloramphenicol
Cph	Cyanobacterial phytochrome
CRY	Cryptochrome
Cys	Cysteine
DMSO	Dimethyl sulfoxide
DNA	Deoxyribonucleic acid
dNTP	Deoxynucleoside-triphosphate mix
DTT	Dithiothreitol
EDTA	Ethylene diamine tetra-acetic acid
FAD	Flavin Adenine Dinucleoctide (Riboflavin 5'-diphosphate)
FKF1	Flavin –Binding Kelch Repeat F-Box Protein

FMN	Flavin Mononucleotide (Riboflavin 5'-monophosphate)
GAF	cGMP Phosphodiestrase, Adenylate cyclase and Formate hydrogen lyase transciption activator
His_6-tag	attachment of six histidine residues
HisKA	Histidine kinase
HKRD	Histidine kinase related domain
HO	Heme oxygenase
IMAC	Immobilized metal affinity chromatography
IPTG	Isopropyl-β-D-thiogalactopyranoside
Kan	Kanamycin
KB	King's broth B
kb	Kilobase
kDa	Kilodalton
LB	Luria Bertani media
LOV	Light, oxygen, voltage domain
MCS	multiple cloning site
min	Minute
mg	Milligram
MOPS	3-(N-morpholino) propanesulfonic acid
MW	Molecular weight
NBT	Nitro blue tetrazolium
nm	Nanometer
ns	Nanosecond
OD	Optical density
ORF	Open reading frame
PAC	Pas associated /C-terminal PAS domain
PAGE	Polyacrylamide gel electrophoresis
PAS	Period clock (Per) protein, aromatic hydrocarbon receptor nuclear translocator (Arndt) and single minded (Sim).
PCB	Phycocyanobilin
PCC	Pasteur Culture Collection

PCR	Polymerase chain reaction
PE	Phycoerythrin
PEB	Phycoerythrobilin
Pefabloc	4-(2-aminoethyl)-benzene-sulfonylfluoride hydrochloride
P_{FR}	Far-red absorbing form of phytochrome
Phy	Phytochrome
PHY	Phytochrome specific GAF related domain
Phot	Phototropin
P_R	Red absorbing form of phytochrome
PRD	PAS repeat domain
Pst/PSPTO	*Pseudomonas syringae pv tomato* DC3000
PVDF	Polyvinylidene difluoride
PYP	Photoactive yellow protein
PΦB	Phytochromobilin
RBS	Ribosome binding site
RNA	Ribonucleic acid
rpm	Rotations per minute
RR(s)	Response regulator(s)
RT	Room temperature
SAP	Shrimp alkaline phosphatase
SAR	Specific absorbance ratio (ratio between the absorbance at the P_R maximum and at 280 nm)
SDS	Sodium dodecyl sulphate
SDS-PAGE	Sodium dodecyl sulphate polyacrylamide gel electrophoresis
SDM	Site directed mutagenesis
sec	Second
TAE	Tris-acetate/EDTA
TBY	Terrific broth/ yeast extract excess
TCEP	Tris (2-carboxyethyl)phosphine HCl
TE	Tris/ EDTA
TIGR	The Institute of Genomic Research

Tris	2-amino-2-(hydroxymethyl)-1,3-propanediol
UV-Vis	absorption spectroscopy in the ultraviolet and visible light range
X-Gal	5-bromo-3-chloro-3-Indolyl-β-D-galactopyranoside
ZTL	ZEITLUPE
β-ME	ß-mercaptoethanol
ΔA	Absorbance difference
ε	Extinction coefficient (in $M^{-1}cm^{-1}$)
λ	Wavelength
λ_{max}	Absorption maximum

1. Introduction

Light is probably the most important environmental factor in nearly all ecosystems. However, only a small part of the overall solar radiation (Figure 1) reaches the earth surface. The solar radiation is limited at both “ends” of the visible spectrum: most of the biologically harmful UV radiation (below 295 nm) is absorbed by the atmospheric ozone layer, whereas a large portion of the infrared radiation is absorbed by water and CO_2 in atmosphere [4;5].

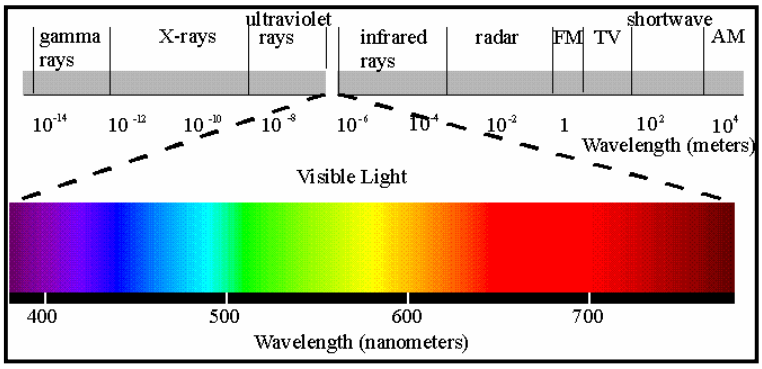

Figure 1: Solar radiation. Visible light extends from ca. 380 nm to ca. 780 nm and is detected through different photoreceptors of different organism.

Living organisms are directly or indirectly dependent on solar radiation for their survival and maintenance. In case of humans, the “visible” spectral range extends from 380 nm to nearly 780 nm. An even wider range has been reported for a number of animal species: their visual sensitivity extends far into the UV region. In order to monitor the quality of the incident light, nearly all living species have developed photoreceptors in order to sense and to respond to light. As the most obvious example, such properties are critical for photosynthetic organisms to optimize their growth behavior and metabolism. Ultimately, practically all life on earth originates from photosynthetic activity, in a direct or an indirect dependence [6;7].

1.1 Photoreceptors

Nature has developed a number of different photoreceptor families which allow monitoring the quality, quantity, direction, and duration of light. In general, photoreceptors are composed of the light-absorbing entity, the chromophore (from the Greek word *chromos*=color), and a protein moiety [7;8].

The biological photoreceptors can be classified into six major families: rhodopsins, the phytochromes, the xanthopsins, the cryptochromes, the phototropins and the BLUF proteins (Figure 2). In the following, all classes of photoreceptors will be briefly presented; as the phytochromes were the topic of this thesis, they will be described at the end in greater detail.

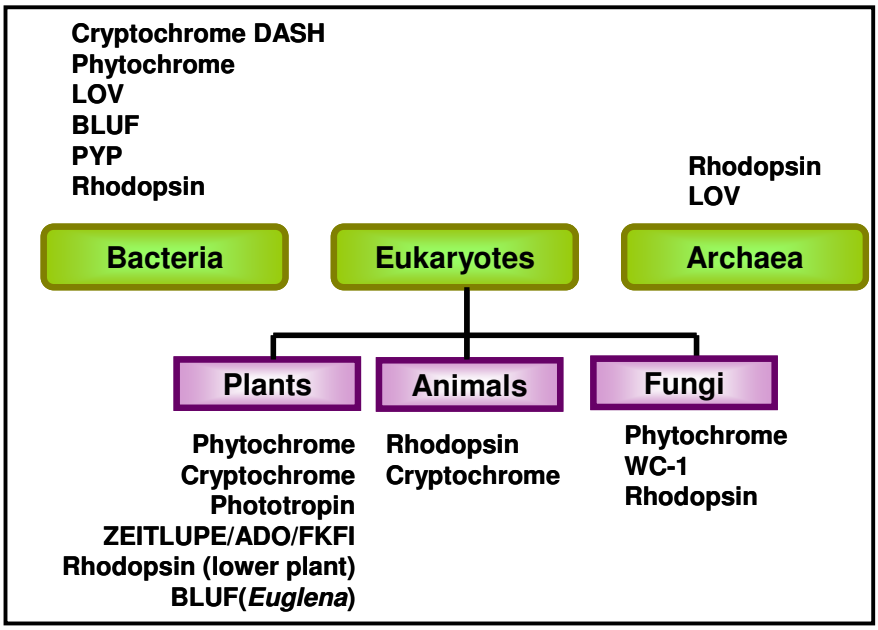

Figure 2: Distribution of photoreceptor proteins in the three domains of life. These photoreceptor proteins of six well characterized photoreceptor families function in nature to mediate light induced signal transduction. Rhodopsins are nearly ubiquitous. The phytochromes can be found in bacteria, fungi, and plants. A number of blue light-sensitive receptor families have been identified: the xanthopsin-type PYP-proteins in bacteria, and the blue light-sensing flavin-binding receptors; the LOV

domain-containing photoreceptor proteins are present in archaea, bacteria and eukaryotes (except animals; LOV: Light, Oxygen, Voltage); the BLUF-proteins are found in plants and bacteria (photosensory proteins carrying a Blue Light Using FAD domain), and the cryptochrome DASH family: cryptochromes in *Drosophila*, *Arabidopsis*, *Synechocystis* and *Homo*. PYP: Photoactive Yellow Protein; ZEITLUPE (ZTL)/ADAGIO(ADO)/ Flavin Binding Kelch Repeat F-Box proteins.

1.1.1 Rhodopsins

Rhodopsins are found in higher and lower animals (vertebrates as well as invertebrates) as the principal visual pigment. In this function, the chromophore in all cases is the 11-*cis* isomer of retinal (vitamin-A aldehyde) [9]. Light-sensing, retinal based pigments are also found in a great number of bacteria and archaea. In contrast to the eukaryotic rhodopsins, in the prokaryotic (bacterial) rhodopsins, the chromophore in all cases known so far is the all-*trans* isomer of retinal. In addition, another classification has to be made for the bacterial rhodopsins: based on the same building principle, two functionally different types of rhodopsins can be identified: light driven energy pumps and sensory rhodopsins. Bacteriorhodopsin (BR) and halorhodopsin (HR) are light driven energy pumps, and sensory rhodopsins I (SRI) and sensory rhodopsin II (SRII) perform light-sensing functions. These receptors, BR, HR, SRI and SRII, were initially reported for an archaeon, *Halobacterium salinarum*, [10].

All rhodopsins are membrane-embedded proteins and consist of a bundle of seven membrane-spanning alpha helices that form an internal pocket in which the retinal chromophore is bound [11]. Binding is always accomplished via the formation of a Schiff base built with the side chain of a lysine residue. The Schiff base is protonated, adding positive charge to the polyene chain of the chromophore and thus providing an easy tuning of the absorption maximum by the surrounding amino acids of the binding pocket. The retinal chromophore, when activated by light undergoes a double bond photo-isomerization and thus induces a conformational change in the protein, rendering the photoreceptor active. The retinal molecule can adapt several *cis-trans* isomeric forms. Rhodopsins found in prokaryotes and algae

commonly contain (in their dark or resting state) an all-*trans* retinal isomer that isomerizes to 13-*cis* upon light activation. On the other hand, rhodopsins of the animal kingdom bind an 11-*cis* isomer of retinal that photo-isomerizes to the all-*trans* isomer [9;12] (Figure 3a and b). This change acts as a molecular switch to activate a downstream signaling pathway within the cell. Thus these retinal-binding proteins are the molecular basis for a variety of light-sensing systems from phototaxis in algae to visual perception and circadian clock in animals [13].

1.1.2 Xanthopsins

Xanthopsins use p-coumaric acid as their light sensitive chromophore, which is linked by a thioester bond to a cysteine side chain [14] (Figure 3c). Xanthopsis are also knows as “photoactive yellow proteins” (PYP) and they were first isolated from an archaeon, *Ectothiorhodospira halophila* [15]. PYPs are water-soluble proteins and undergo a light-induced photocycle triggered by the photo-isomerization of its chromophore [14]. They are photochemically and spectroscopically well characterized proteins. This class of receptor proteins is thought to be responsible for a negative phototactic response [16]. It is also involved in the expression of chalcone synthase [17], which is a key enzyme for the synthesis of photo-protective pigments. In *Rhodospirillum centenum* and *Thermochromatium tepidum,* genes encoding PYP domains have been found to be followed by genes encoding bacteriophytochrome [17;18].

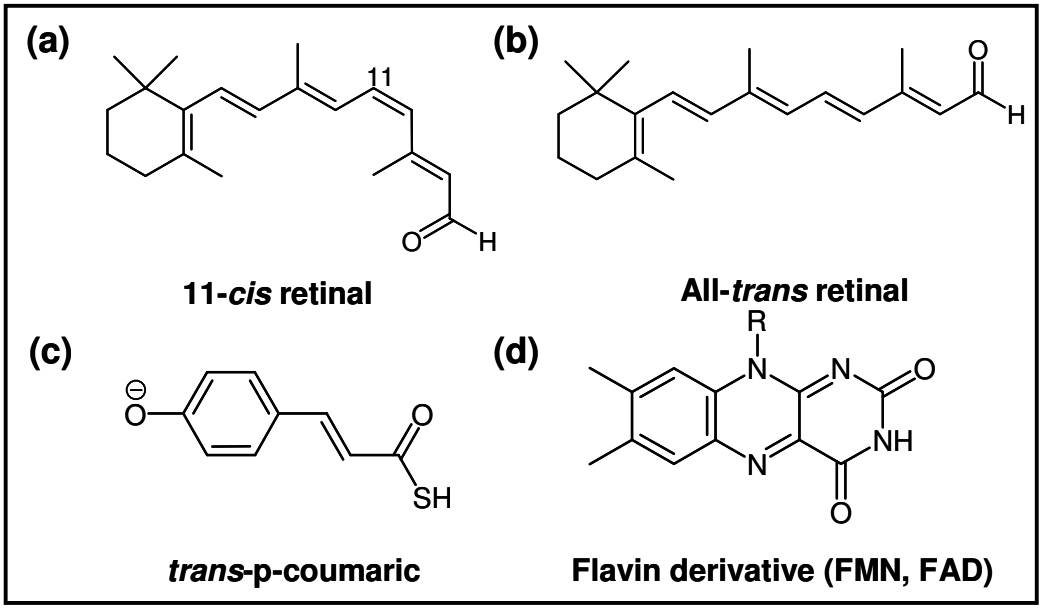

Figure 3: Chromophores of different photoreceptors utilized for photon-capture. (a) 11-*cis* retinal, chromophore of rhodopsins found in the dark states in animals, (b) all-*trans* retinal, chromophore of rhodopsins found in the dark state in prokaryotes and algae, (c) trans-p-coumaric acid, chromophore of xanthopsin undergoes as photochemical reaction a *cis/trans* isomerization of its double bond upon photon-capture; (d) Flavin derivatives (FMN, FAD), found in cryptochromes, phototropins, ZTL/ADO/FKF1, and the BLUF photoreceptors; all these blue light-sensitive photoreceptors bind similar flavin co-factors (flavin adenine dinucleotide (FAD) or flavin mononucleotide (FMN). Phytochromes chromophores are explained on 1.2.1 and Figure 6.

1.1.3 Flavin containing photoreceptors

The blue region of the spectra (430-500 nm) provides the highest energy content in the visible spectrum. On the one hand, higher energy content can facilitate energy utilization in photosynthetic processes, but on the other hand it also represents a caution signal for the avoidance of energy-rich blue/UV light, which may cause severe damage in living organisms. Three major types of flavin-containing photoreceptors, viz. cryptochromes, BLUF domains and LOV domains (of phototropins) are found in the different forms of life.

1.1.4 Cryptochromes

Cryptochromes (from the Greek word *krypto chroma* = hidden color) were the first identified group of flavin-containing photoreceptors (Figure 3d). These proteins use FAD as chromophore. Cryptochromes share a high degree of sequential and structural similarity to DNA photolyases but lack the activity of typical DNA photolyase enzymes; instead, they carry a C-terminal tail for signal transduction [19]. These blue-light photosensors are present in lower and higher eukaryotes, including algae, plants, insects and animals [20-23]. Cryptochromes play a pivotal role in the generation and maintenance of circadian rhythms. In higher plants they are involved in the processes that regulate germination, hypocotyls elongation, photoperiodism and pigment accumulation. Recently, a new family of cryptochrome protein, the CRY-DASH (DASH: *Drosophila*, *Arabidopsis*, *Synechocystis*, *Homo*) was reported from some eubacteria (*Synechocystis* sp PCC6803, *Vibrio cholerae*). CRY-DASH proteins do not possess the C-terminal tail found in typical cryptochromes and show DNA photolyase activity in single stranded DNA.

1.1.5 BLUF-Proteins

This family of photoreceptors was named BLUF according to their function and chromophore: “sensor for blue light using FAD (Flavin Adenine Dinucleotide)”. They have been reported from bacteria and lower eukaryotes [24]. Members of this family are known to be involved in photophobic responses in *Euglena gracilis* and *Synechocystis* [21] and in the transcriptional regulation in *Rhodobacter sphaeroides* [25]. Many BLUF domains are part of multidomain proteins involved in catalytic conversion of regulatory cyclic nucleotides, such as cAMP and c-di-GMP.

1.1.6 The LOV proteins: phototropin and ZTL/ADO/FKF1 families

Phototropin photoreceptors have been identified from a genetic analysis using the model plant *Arabidopsis thaliana*. The nph1- (non-phototropic hypocotyl) mutants of *Arabidopsis* lack the commonly found hypocotyl phototropism to blue light [26]. The NPH1 protein was named phototropin 1 (phot1) after its functional role in phototropism [27]. Phototropins regulate a number of blue light induced responses like chloroplast relocalization, stomatal opening and phototropism [28]. There are two phototropins (phot1 and phot2) in *Arabidopsis thaliana*.

A sequencial and biochemical characterization shows that these phototropins consist of two stretches of PAS domains in their N-terminal part that show light detection capability due to an incorporated FMN chromophore. Such domains can be regulated by light, oxygen and voltage, after which the name LOV domain was assigned to these blue light absorbing PAS domains of phototropins [29]. The LOV signaling module is widely distributed in all three kingdoms of life with the exception of animals. LOV modules are present not only in photosynthetic plants and prokayotes, but also in fungi, proteobacteria, varieties of plants and animal pathogens [30].

The LOV domain binds an oxidized FMN as chromophore. Blue light illumination causes the formation of a covalent bond between the C4a position of flavin and the SH-group of a conserved cysteine, and this photoadduct can slowly reconvert to the unbound state in a time scale from minutes to hours. The plant-derived phototropins possess two LOV domains (LOV1 and LOV2) in a tandem array that are functionally coupled with a downstream serine/threonine kinase. The covalent binding of FMN upon blue-light absorption leads to a conformational change in the protein and results in enhanced kinase activity, and this activation is dark reversible [28].

The **ZTL/ADO/FKF1** family is the last class of LOV domain-containing photoreceptors that has recently been identified mainly in higher plants. It comprises three members: Zeitlupe (ZTL, also referred to as Adagio, ADO); Flavin-binding,

Kelch Repeat, F-box 1 (FKF1); and LOV Kelch, Protein 2 (LKP2). These proteins are believed to play a key role in control of circadian rhythm in higher plants [31]. They possess an N-terminal LOV domain, followed by an F-box characteristic of this class of proteins that direct ubiquitin-mediated degradation, and six Kelch repeats predicted to fold into a β propeller. The LOV domain of this novel photoreceptor family also binds an FMN as chromophore, and displays analogous photochemical properties, but unlike the phototropin LOV domains, ZTL, FKF1, and LKP2, it does not recover to the ground state in the dark [28] or their decay may occur in a quite slow mode that will take several days [32]. This distinct photochemical property might correlate with the relatively slow responses triggered by FKF1, ZTL, and LKP2 (e.g. induction of flowering) in comparison to the rapid responses controlled by the phototropins (e.g. chloroplast movements) [33].

The LOV domains from different organisms regulate the activity of numerous output- or effector domains such as kinases, phosphodiesterases, zinc finger motifs or stress sigma factors. Plant phototropins play an important role in phototropism, hypocotyl development, chloroplast movement, stomata opening and leaf expansion with dependence on blue lights [29] (Figure 4). NPH1 encodes a plasma membrane-associated protein known to be essential for most of the phototropic responses in *Arabidopsis*. In fact, the involvement of the blue light photoreceptor in hypocotyl extension in green seedlings was already reported in 1984 [34]. The response to changes in light conditions involves a variety of photoreceptors that can modulate gene expression, enzyme activity and/or motility.

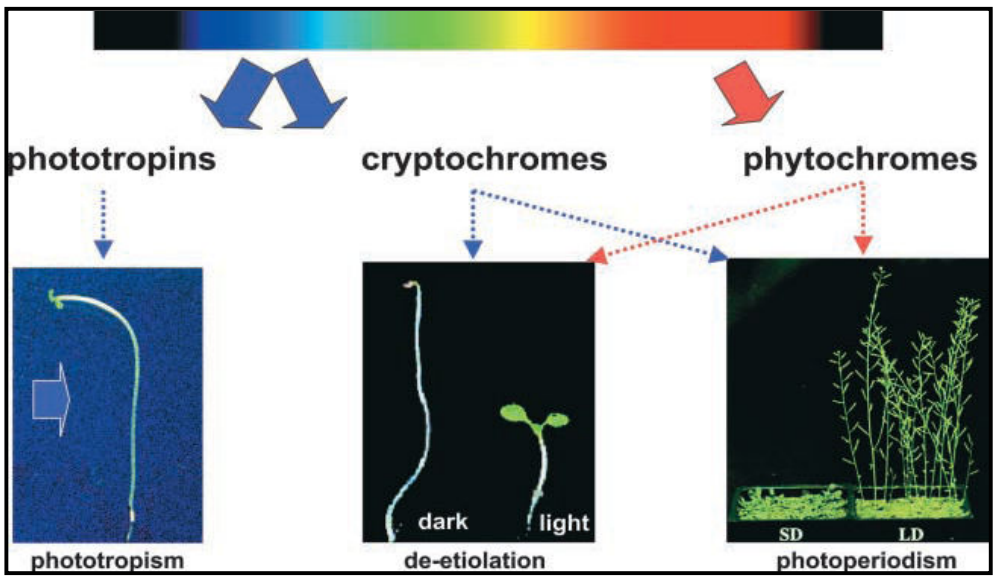

Figure 4: Depiction of the three types of photoreceptors comprehensible for plants with the assigned functions of each photoreceptor as described by various studies. The figure is adapted from Lin et al., 2002.

1.2 Phytochromes

Phytochromes, among the best characterized photoreceptors, comprise a widespread family of red/far-red light responsive photoreceptors. Phytochrome pigments were first characterized in higher plants in the 1950's [1]. Vierstra and Quail isolated the full length phytochrome protein from *Avena sativa* in 1982 [35] and the complete amino acid sequence of this phytochrome was obtained through the identification of the encoding gene in 1985 [36]. Phylogenetic and biochemical studies have dramatically expanded the phytochrome superfamily to other domains of life. Phytochromes have been discovered in bacteria [2;37;38], fungi [3] and slime molds [39]. In 2005 Karniol et al. organized the members of the phytochromes superfamily into distinct subfamilies that include plant phytochromes, bacteriophytochromes, cyanobacterial phytochromes, fungal phytochromes and phytochrome-like sequences (Figure 5) [40].

Some bacteria contain different families of phytochromes indicating that a variety of light-signaling systems can co-exist. For example, *Synechocystis* contains two Cphs (Cph1 and Cph2) and three Phy-like sequences (TaxD1, PlpA and RcaE) [37;40], while *Calothrix* contains two types of phytochromes, a Cph protein (CphA) and a BphP protein (CphB) [41].

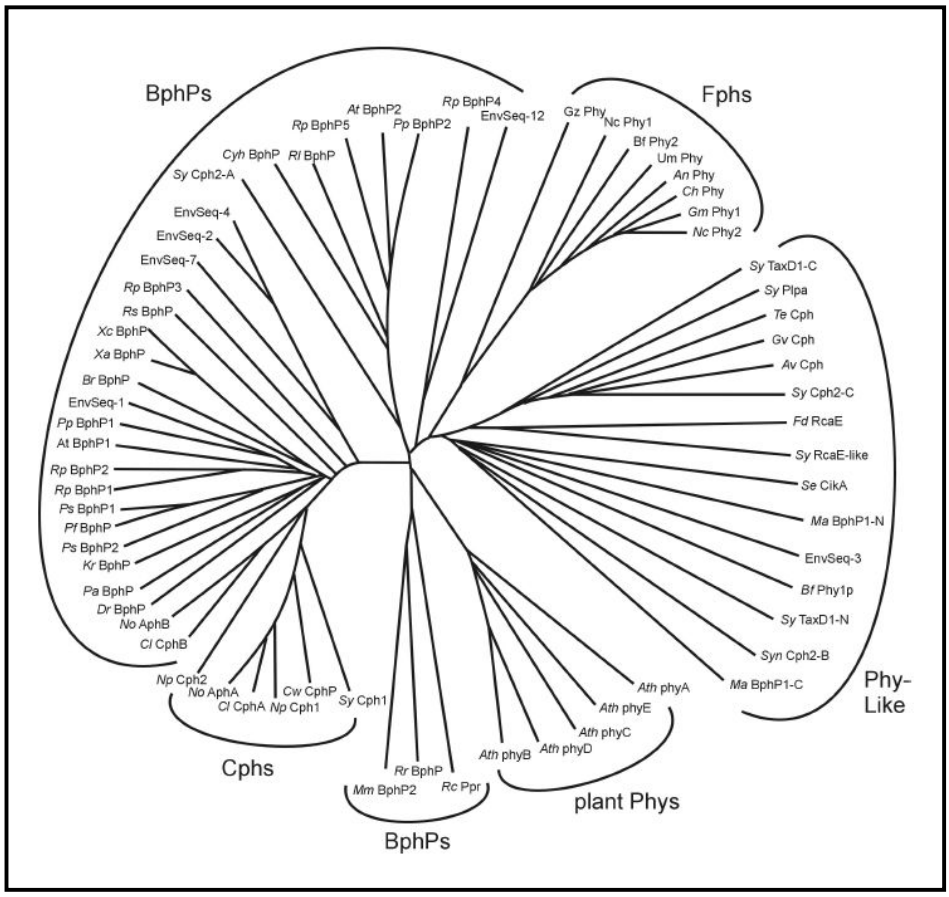

Figure 5: Phylogenetic analysis of the phytochrome superfamily. The phylogenetic organization of the Phy-superfamily is based on an alignment of the GAF domain (adapted from [40]. The major phytochrome classes are: Plants (Phy), cyanobacteria (Cph), Eubacteria (Bph), Fungi (Fph); Phy-like subfamilies of phytochrome are indicated.

1.2.1 The phytochrome chromophore

All phytochromes carry a covalently attached open-chain tetrapyrrole (bilin) chromophore that absorbs light in red and far-red region. Three different bilins have been identified as chromophores: Plants use phytochromobilin (PΦB), [42] and cyanobacteria use in their “canonical” phytochrome phycocyanobilin (PCB) [2;43]. PCB is also a chromophore of the light-harvesting pigment, phycocyanin, and differs from PΦB only by a further reduction of the vinyl group at the C18 position to an ethyl group [43], whereas other bacteria and fungi use biliverdin [3;44;45].

The bilin chromophores incorporated in all phytochromes derive from the oxidative metabolism of heme. First, a heme oxygenase converts the heme into biliverdin IXα (BV), which can be directly attached as chromophore of the BphPs and Fphs via a thioether linkage at $C3^2$ (Figure 6) to a conserved cysteine upstream of the P2/PAS domain [46;47].

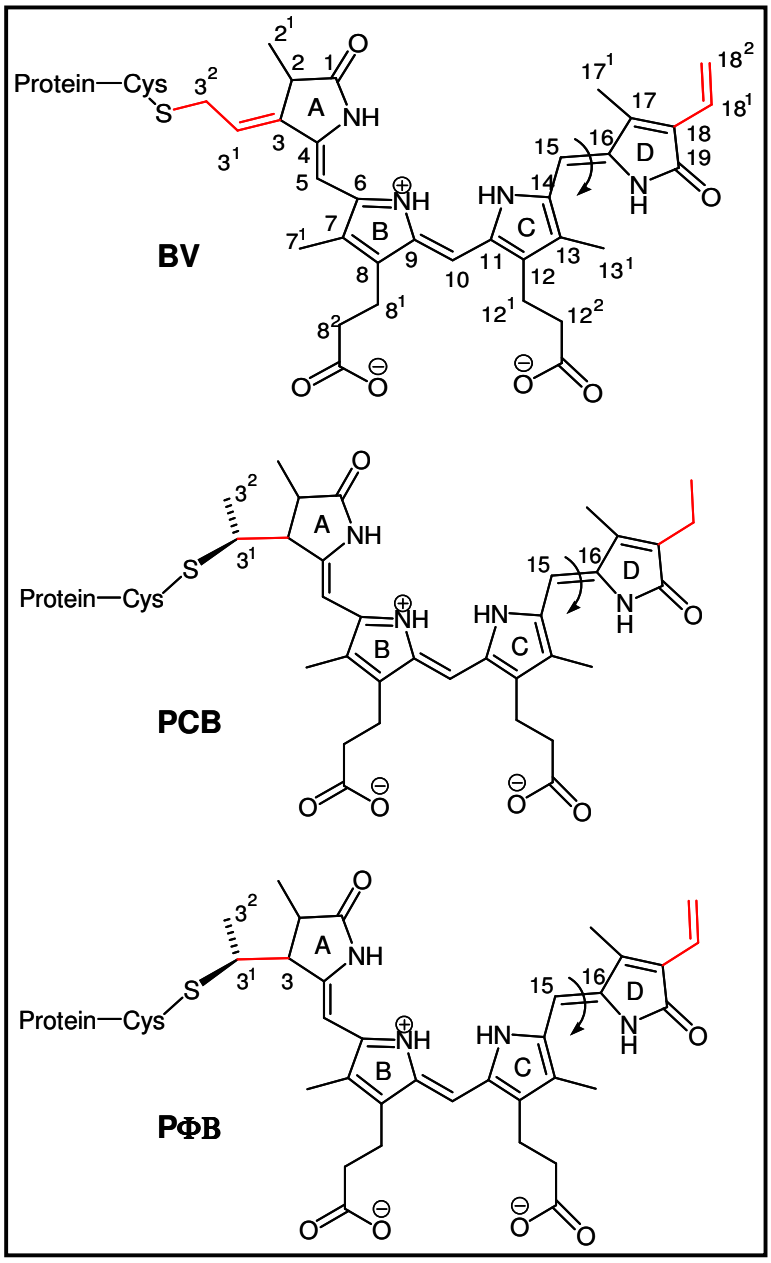

Figure 6: Structural formula of phytochrome chromophores. Biliverdin IXα (BV), the chromophore of the BphPs and Fphs, binds to the protein via a thioether linkage at position C3^2. Phycocyanobilin (PCB), the chromophore of cyanobacterial phytochromes and phytochromobilin (PΦB), the chromophore of phytochromes from plants, are covalently attached at position C3^1. BV and PΦB carry a vinyl group at the

C18 position, whereas PCB contains an ethyl group. The structural differences in the rings A and D are marked in red.

In cyanobacteria, BV is converted to phycocyanobilin (PCB) via a four electron reduction, mediated by ferrodoxin dependent bilin reductases of the PcyA subfamily [48]. In higher plants, BV is converted to phytochromobilin (PΦB) through the action of the homologous two–electron bilin reductase phytochromobilin synthase. The bilins PΦB and PCB are covalently attached to the protein at position $C3^1$ (Figure 6) of A-ring via the side chain of a conserved cysteine in the P3/GAF domain of the photosensory core [49;50]. The attachment of PΦB and PCB chromophores by Phy and Cph takes place via a common mechanism of thioether formation from the cysteine side chain to the ethylidene group present at the $C3^1$ carbon of the bilin A-ring. In contrast to PΦB and PCB, BV does not contain the A-ring ethylidene group required for formation of a thioether linkage with the GAF domain cysteine. Instead, BV carries a vinyl group at this position (Figure 6), to which the covalent binding is accomplished in a very similar manner (to position 3^2).

The chromophore triggers the conversion between two thermally stable states, P_R and P_{FR} (Figure 7). In the P_R ground state, the chromophore absorbs red light (λ_{max} ~ 660/700 nm) triggering a *Z*-to-*E* photoisomerization of the C15=C16 double bond, and thus converting the protein into the far-red light absorbing P_{FR} state (λ_{max} ~ 710/750 nm). The P_R state reverts to P_{FR} either in the dark at ambient temperature or instantaneously by a light-induced sequence of reactions [51].

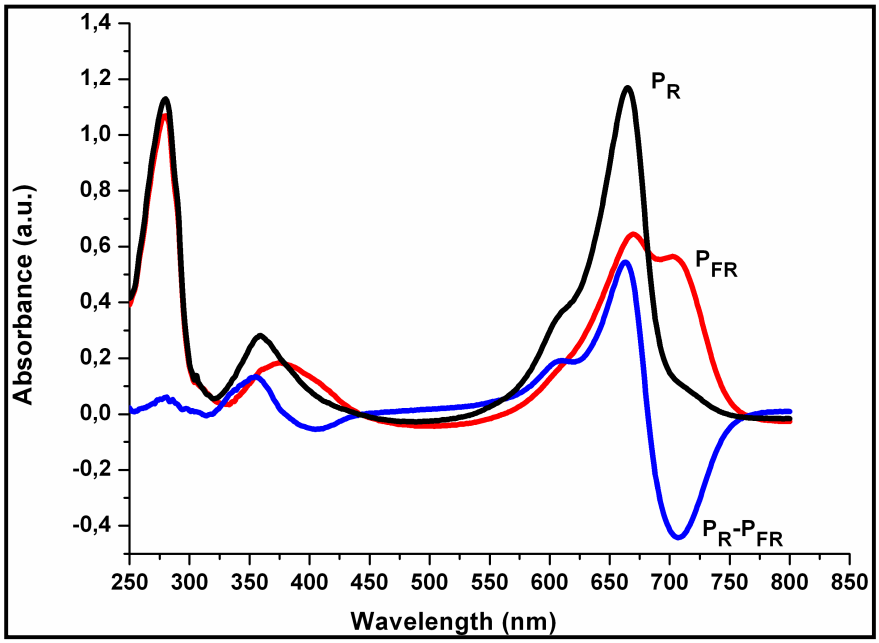

Figure 7: Absorption spectrum of CphA of *Calothrix* PCC 7601 in the P_R- (black line), the P_{FR}-form (red line), and as P_R-P_{FR} difference spectrum (blue line).

Recently, the three-dimensional structures of the cyanobacterial phytochrome Cph1 in the P_R state and bacteriophytochrome of *Pseudomonas aeruginosa Pa*BphP in P_{FR} state has been solved [52;53]. Based on these X-ray studies and Raman and NMR-studies reported in parallel, the geometry of the tetrapyrrole methine bridges has been shown to be *ZZZssa* and *ZZEssa* in the P_R and P_{FR} states, respectively (Figure 8).

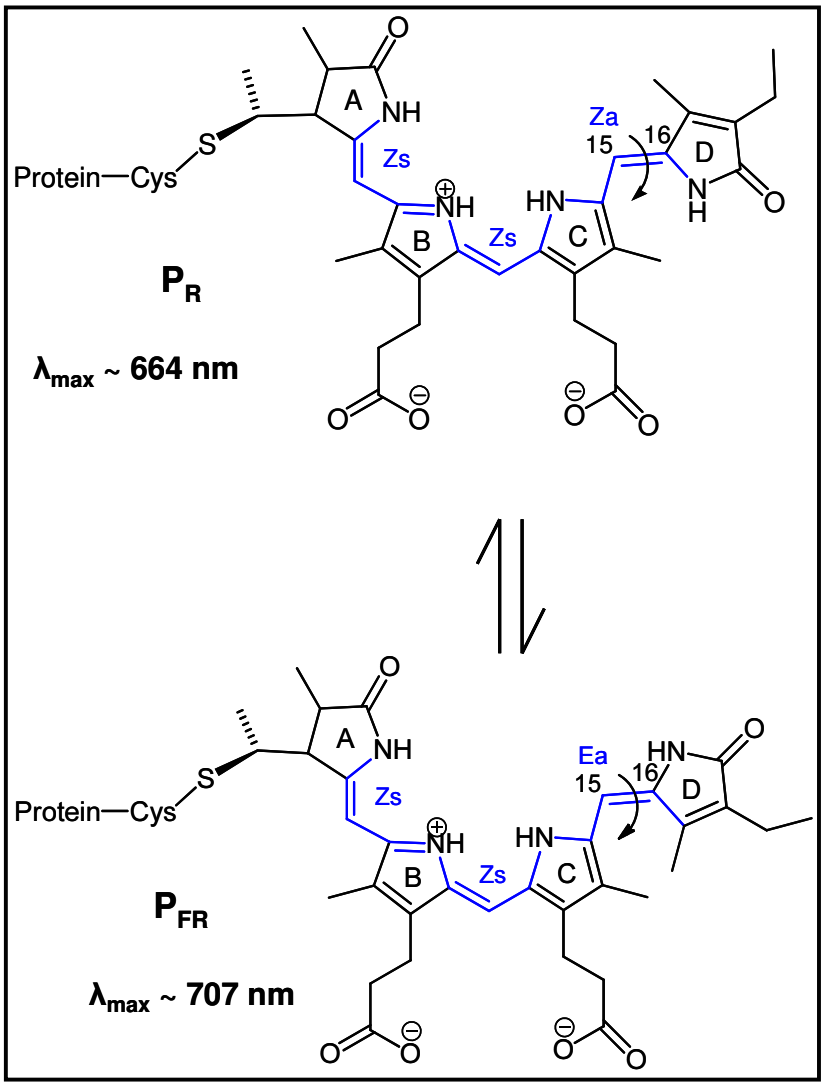

Figure 8: Photoconversion of a cyanobacterial phytochrome. The structure of the phycocyanobilin (PCB) chromophore is given as ZZZssa and ZZEssa for the P_R and P_{FR} states, respectively. The conformation change is marked in blue.

1.2.2 The biosynthetic pathway of bilins: Heme oxygenases

Heme oxygenases (HO) from mammals were the first of this family of enzymes to be identified [54]. The HO catalyzes the oxidative degradation of heme to yield biliverdin (BV) IXα, iron (Fe^{2+}), and carbon monoxide (CO). In eukaryotic HOs, NADPH and NADPH-cytochrome P450 reductase serve as the electron donor [55]. HOs fulfil a

number of biological functions: they are involved in heme catabolism, iron utilization and cellular signaling. The first bacterial gene with homologies to eukaryotic HOs was the gene *hmuO* from the pathogenic bacteria *Corynebacteriu diphtheriae* and *Corynebacterium ulcerans* [56]. In *C. diphtheriae* and *C. ulcerans* the HO reaction is utilized to release iron from heme to overcome the low concentrations of free-iron as a need for successful colonization (infection) which is the major function of HOs from pathogenic organisms. Their function in iron utilization has been shown for HOs from other pathogenic bacteria, including *Neisseria meningitidis* (HemO) and *Staphylococcus aureus* (IsdG/IsdI). Other pathogens like *Staphylococcus epidermidis*, *Listeria monocytogenes,* and *Bacillus anthracis* have homologues of IsdG and IsdI [57].

In addition to their function in iron utilization, bacterial HOs are also involved in the phytobilin biosynthesis. Phytobilins are open-chain tetrapyrrole molecules that are synthesized in plants, algae, and cyanobacteria and that are the precursors of the chromophores for the light-harvesting phycobiliproteins and the photoreceptor phytochrome [58]. In the course of bilin biosynthesis, the product of the HO reaction, BV IXα, is subsequently converted to one of the major bilins present in cyanobacteria, phycocyanobilin or phycoerythrobilin (Figure 9). Unlike plant and cyanobacterial phytochromes, bacteriophytochromes (BphPs) from prokaryotes have been shown to utilize a BV chromophore [3].

The first cyanobacterial HO that had been cloned and characterized was HO-1 from *Synechocystis* sp. PCC6803 [59]. The genome of *Synechocystis* sp. contains two genes, *ho1* and *ho2*, encoding potential HOs [59]. The recombinant HO-1 protein was shown to catalyze the conversion from heme to BV IXα but HO-2 lack of biochemical data as it is formed as an insoluble protein in recombinant expression. Genes encoding putative HO-1s and HO-2s can be found in the available genomes of other sequenced cyanobacteria, including *Anabaena* sp. PCC7120, *Thermosynechococcus elongatus*, and *Nostoc punctiforme* [58].

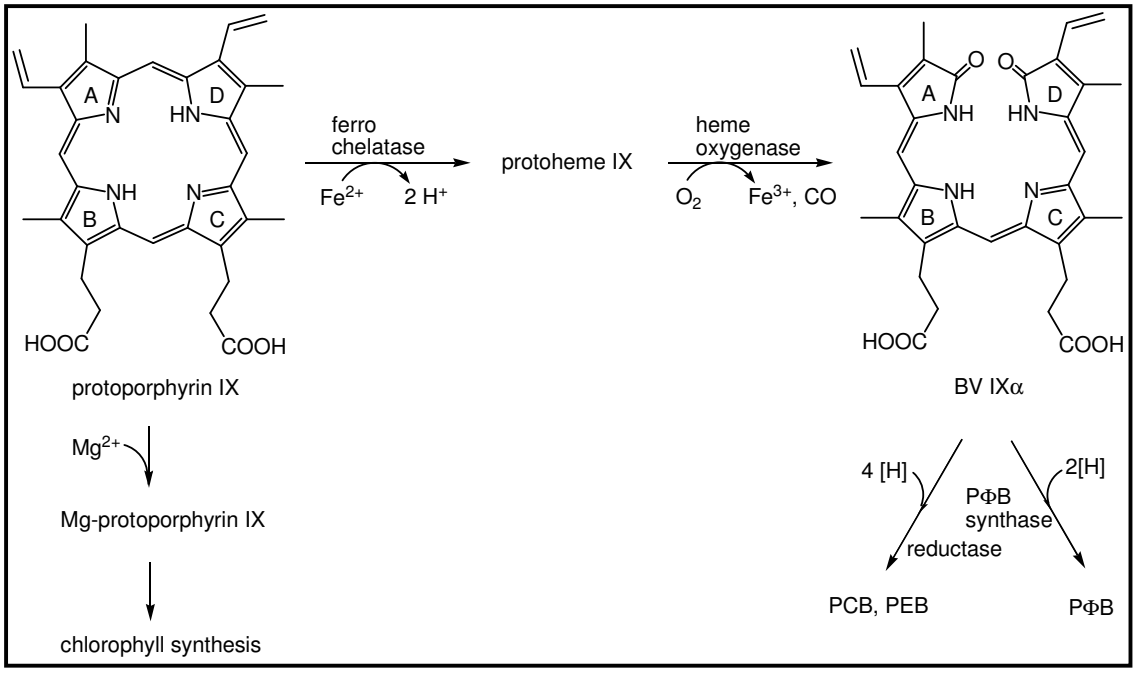

Figure 9: Pathway of the biosynthetic formation of the phytochrome chromophores. Bilins originate from porphyrin biosynthesis at the branching point to chlorophylls and heme compounds (insertion of Mg or Fe). Heme oxygenase releases the central iron atom from heme groups and opens the porphyrin compound under oxygen consumption forming a bilin (biliverdin IXα, BV). Biliverdin reductases form phytochromobilin or phycocyanobilin by performing either a two (PΦB) or a four electron reduction (PCB); this latter compound can be electronically re-organized to generate phycoerythrobilin, PEB. BV is found as a chromophore in bacteriophytochromes, PΦB is the genuine chromophore of plant phytochromes, and PCB is mostly present in the canonical cyanobacterial phytochromes, and in cyanobacteriochromes.

Besides the group of HOs involved in phytobilin biosynthesis and iron utilization from heme, other HOs have been identified in mostly nonphotosynthetic bacteria [3]. The genes coding for these HOs are usually found in operons together with a gene encoding a bacterial phytochrome and are designated as *bphO* (bacterial phytochrome heme oxygenase). The opportunistic pathogen *Pseudomonas*

aeruginosa harbors two functional HOs, bphO and pigA*,* each capable of oxidizing heme to a different BV isomers (BV IXβ and BV IXδ) [60].

1.2.3 The modular domain architecture of phytochromes

Phytochromes are large chromoproteins (comprising of up to 1100 aa in plant phytochromes and between 650 and 1300 aa in prokaryotic phytochromes). Two main domains can be identified, an N-terminal light-sensory domain and a C-terminal regulatory domain. Figure 10 shows the domain structure of various phytochrome types found in plant (Phy), cyanobacteria (Cph), other bacteria (Bph) and fungi (Fph). The N-terminal photosensory region binds the bilin cofactor and is composed of three conserved domains, termed P2 or PAS- (Per-ARNT-Sim) domain, P3 or GAF- (cGMP Phosphodiesterase/adenyl cyclase/FhlA domain), and P4 or PHY domain (uppercase letters are used to denote the Phy domain specifically). The C-terminal regulatory module contains a histidine kinase (HK) or histidine kinase-related (HKR) domain (Figure 10). Plant Phys have an additional N-terminal extension termed P1 known to stabilize the light-induced P_{FR} form [61] and two additional regulatory PAS domains (PAS1 and PAS2) located between the light-sensing and the signalling domains. These regions of the protein have been shown to be important for nuclear localization [62]. Fph proteins have distinct N-terminal extensions and additional C-terminal response regulator domains. Fused response regulator (RR) proteins are found in a minority of Bph but are common in Fph proteins. Canonical phytochromes thus consist of a PAS-GAF-PHY N-terminal photosensory module, typically combined with a C-terminal HK- or HKR module. The tandem sequence of PAS, GAF, and PHY domains attached to HK- HKR modules typifies all classes of phytochromes and phytochrome-related proteins [63;64].

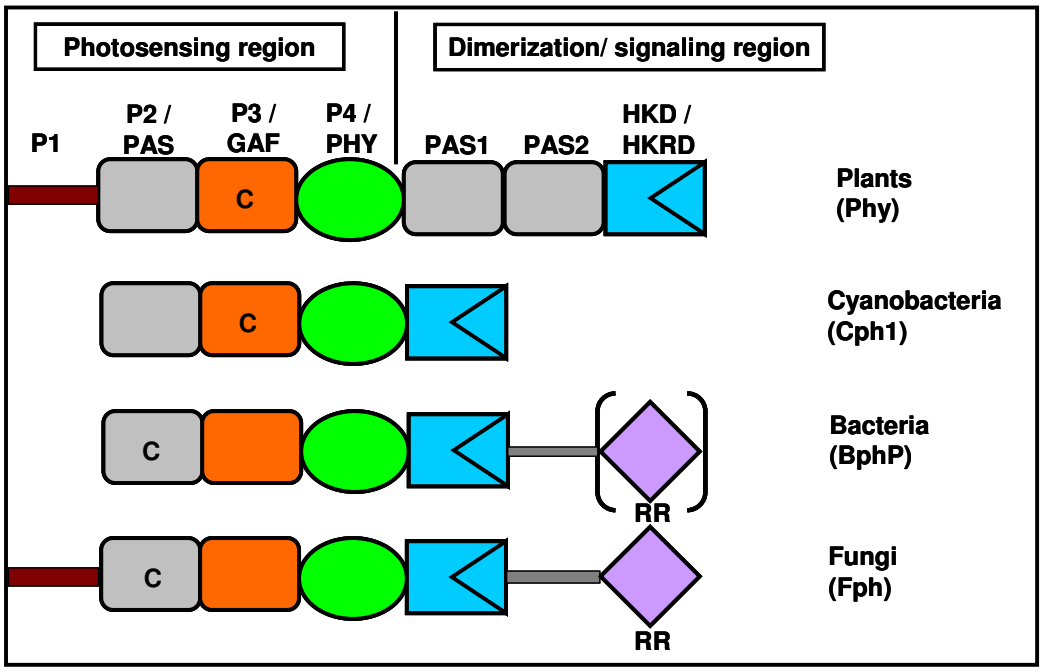

Figure 10: Domain structure of phytochromes. These photoreceptors consist of two functionally separable regions: an amino-terminal conserved PAS/GAF/PHY tri-domain photosensing core and a carboxy–terminal domain involved in dimerization of the phytochrome polypeptide chain and in generating the output signal. Conserved phytochrome domains in phytochrome form plants (Phy), cyanobacteria (Cph), Eubacteria (Bph) and Fungi (Fph) are P2/PAS, Per/Arnt/Sim domain; P3/GAF, cGMP phosphodiesterase-Adenylcyclase-FhlA; P4/Phy, Phytochrome specific domain; HK- or HKRD; Histidine-kinase (related) domain; RR, Response regulator domain. Plant phytochromes have an additional N-terminal extension termed P1, two additional PAS domains in C-terminal. BphPs and Fphs differ from plant Phy and Cph in the location of the conserved cysteine (C) residue that forms the covalent linkage to the bilin chromophore. Both plant phytochromes and Fph proteins have N-terminal extensions. In general, Fph proteins have C-terminally fused response regulator (RR) receiver domains; such domain is present in only few Bphs (in several cases a gene encoding the response regulator can be found closely located, downstream of the phytochrome gene).

The definition of a classical phytochrome includes the covalent binding of bilins PΦB or PCB via a cysteine located in the GAF domain and the red/far-red reversible photochemistry performed solely by the PAS/GAF/PHY core module such as found in plant phytochromes. Phytochromes using BV have been named bacteriophytochromes (BphPs) if found in bacteria, or called fungal phytochromes (Fphs) when identified in fungi. The BV binding site (also via a cysteine residue) is usually located in the frontal PAS domain. Moreover, cyanobacteria contain more diverse biliprotein photosensors with a minimal architecture consisting GAF/PHY or even GAF-only photosensory modules, which were named Cph2s and cyanobacteriochromes (CBCRs) [65;66]. Also the designation “cyanochrome” has recently been proposed for CBCRs [67].

1.2.4 Phylogenetic analysis of the phytochrome superfamily

1.2.4.1 Plant phytochromes (Phy)

Phytochrome was discovered and its basic photochemical properties were first described through physiological studies of light sensitive lettuce seed germination and photoperiodic effects on flowering [68]. The pigment itself was initially isolated from extracts of dark grown (etiolated) plant tissue in 1959 [1]. In most plant species, the plant phytochromes are encoded by a small gene family. There are five different genes (*phyA, phyB, phyC phyD and phyE*) in *Arabidopsis thaliana* which encode phytochromes, called phytochrome A, B, C, D and E [69;70]. The sequence homologies between these different phytochromes are about 50%. Only phytochrome B and D show a higher homology to each other of ca. 80%. In those monocotyledonous plants that were studied so far, such as corn or rice, only *phyA, phyB* and *phyC* genes have been identified [71]. Angiosperms, gymnosperms, ferns, mosses and algae usually contain three to five phytochrome genes. Phylogenetic analysis has shown that development of an ancestral phytochrome bifurcated before the divergence of seed plants [72].

The various phytochromes perform partly overlapping but distinct roles. In rice, all three phytochromes promote de-etiolation and delayed flowering in long-day (LD)

conditions, whereas in short-day (SD) conditions PhyB delays flowering and PhyA promotes flowering, especially in plants where the PhyB function is destroyed (Takano et al, 2005). In *Arabidopsis*, both PhyA and PhyB promote seed germination and de-etiolation in response to far-red (FR) and red (R) light, respectively. PhyA promotes flowering, whereas PhyB delays flowering. Similarly, PhyD and PhyE promote seedling de-etiolation and suppress shade avoidance responses [73;74].

1.2.4.2 Cyanobacterial phytochromes (Cphs)

The cyanobacterial phytochrome Cph1 from *Synechocystis* sp. PCC6803 was the pioneer member of this family. The recombinant apoprotein autocatalytically assembles with phycocyanobilin (PCB) at the canonical cysteine to generate a dimeric R/FR photochromic chromoprotein *in vitro* [2;37]. After assembly with PCB, Cph1 shows "typical" R / FR spectra, the P_R/P_{FR} absorptions maxima (654 nm and 706 nm) compared to the absorption maxima of plant phytochromes (666 nm and 730 nm) have a slight blue shift. This is most probably due to the absence of a double bond in the π-electron system of the chromophore PCB compared to PΦB (PCB carries an ethyl group at ring D instead of the vinly group in PΦB). All the members of this family, including the bacteriophytochromes, possess the PAS, GAF, PHY domains as well as the two conserved sub-domains found in the transmitter modules of two-component histidine kinases. The tryptic digestion of proteins [75;76] or the use of engineered truncated phytochrome proteins [77] has evidently shown that the PHY sub-domain is essential for full phytochrome functionality although in its absence the chromophore is still adhered to the bilin binding pocket. The crystal structure of the PAS-GAF-PHY domain of the cyanobacterial phytochrome Cph1 has given support the phy domain is required to provide strength to the bilin binding and photoreversibility [52]. The Cphs have a highly conserved histidine kinase domain at their C-terminus. Histidine kinases, together with response regulator proteins of the CheY-type, represent the prominent "two-component system" (TC) in many prokaryotic species [37;78;79]. Other important representatives of this family are CphA from *Calothrix* sp. PCC7601 [41] and AphA from *Anabaena* sp. PCC 7120

[80]. A second cyanobacterial phytochrome, Cph2, was also identified from *Synechocystis* and shown to covalently attach a bilin [81]. In contrast to Cph1, Cph2 lacks a histidine kinase domain but instead contains GGDEF and EAL output domains [63].

1.2.4.3 Bacterial phytochromes (BphPs)

The bacteriophytochromes (BphPs) are spread widely through the bacterial kingdom, with most known members are found in non-photosynthetic eubacteria and photosynthetic purple bacteria [3;38;82]. There are other potential BphP candidates in some cyanobacteria e.g. *Calothrix*, *Nostoc* and *Oscillatoria* [3;83] which are reported to contain both Cph and BphP type phytochromes [41]. BphPs bind the PΦB-/PCB precursor BV as the chromophore, while Cphs and plant phys bind (non-covalently) BV poorly or not at all. The absorption maxima of the P_R and P_{FR} froms of the chromoproteins is remarkably red-shifted (λ_{max} 700 nm and 750 nm, respectively) compared to plant phys, consistent with the addition of one double bond in the π-electron system of BV than PΦB. The BV binding is genetically well supported by the presence of a heme oxygenase gene often physically linked to the phytochrome genes in the same operon, that convert heme to BV, though no further reduction of BV to PCB or PΦB is possible due to absence of reductase activity of HO [3;58;82]. Crystal structures for some of these BV-binding phys, available from *Deinococcus radiodurans, Rhodopseudomonas palustris* and *Pseudomonas aeruginosa* [47;53;84;85], clarify the binding accounted by these phytochromes to the bilin ligand.

Bacteriophytochromes have an N-terminal PAS-like domain that contains the cysteine residue for bilin linkage instead of the canonical cysteine located in the GAF domain in plant phys and Cphs to attach bilins. A slightly different binding mechanism of the bilin has to be proposed but has not yet been proven [40;86;87]. Spectroscopic studies indicate that most BphPs function as typical Phys, with the P_R form generated during the autocatalytic attachment of the bilin. P_{FR} is created only upon light absorption and can either photoconvert back to P_R by F_R or reverts

nonphotochemically from P_{FR} back to P_R. The P_{FR} form is reported to be less stable for some of these prokaryotic phytochromes as the dark reversion process is quite fast compared to plant phys [86;88]. Bacteriophytochrome proteins function in many cases as two component histidine kinases (TC-HKs), as often a canonical HKD is found C-terminally to the photosensory core. Some species also have a response regulator (RR) domain appended to the HKD or in some cases have a new type of HKD designated as HWE-HKD (conserved histidine, tryptophan and glutamic acid residues in HKD) [88-90].

In *Agrobacterium tumefaciens*, *Bradyrhizobium*, and *Rhodopseudomonas palustris*, a novel subfamily of BphPs was identified that works in reverse, appropriately being called backwards or bathy BphPs. Bathy BphPs assemble BV to generate a P_R-like transient intermediate that rapidly converts non-photochemically to a stable P_{FR} ground state. These photoreceptors behaving opposite or different to the BphPs and the canonical Phys have absorption spectra after assembly that resemble the predicted P_{FR} spectrum without P_R contamination while P_R, generated after photoconversion with FR, is unstable and dark reverts to P_{FR} [82;88].

1.2.4.4 Fungal phytochromes (Fphs)

Also in various filamentous fungi the bilin binding sequence motifs were discovered. This finding suggested the presence of the light receptive phytochromes in the eukaryotic fungal kingdom besides plants [3]. This family of phytochromes is apparently closely related to bacteriophytochromes. Fphs contain a GAF domain with the conserved histidine preceded by a hydrophobic residue (this residue is in place of the functional cysteine residue) and an N-terminal PAS domain with the chromophore-binding cysteine similar to that in BphPs (Figure 10). The Fphs can covalently assemble with BV *in vitro* and yield photochromic proteins after irradiation with R/FR light wavelengths [44;45]. The fungal Fphs have distinct N-terminal extensions in the photosensory core and are linked to typical HKDs followed by response regulator domains (RR/REC), hence likely to function in TC-HK cascades [91].

1.2.4.5 Phy-like sequences

RcaE (Regulator of chromatic adaptation) was the first functional phytochrome-like protein identified in a prokaryotic system [92]. RcaE, which controls complementary chromatic adaptation (CCA), is required for both red and green light responsiveness in *Fremyella diplosiphon*. RcaE binds a bilin chromophore through a conserved cysteine *in vitro* and *in vivo* but the holoprotein was reported to not being photochromic [93].

Another Phytochrome-like protein CikA (Circadian input kinase A) in *S. elongatus* (*Sc*CikA) has been reported to reset the circadian clock in the cyanobacterium *Synechococcus elongatus* PCC7942 after a dark pulse [94]. However, recent studies have indicated that *Sc*CikA does not function as a photoreceptor but as a redox sensor [95]. Moreover, the Cys residue that covalently ligates the chromophore in phytochromes is not conserved in the *Sc*CikA protein. On the other hand, the CikA homolog in *Synechocystis* sp. PCC6803 (*Sy*CikA) retains this conserved Cys residue in GAF domain. The expression of *Sy*CikA in *Synechocystis* or PCB-producing *E. coli*, exhibited the identical absorption spectrum peaking at UV (~324 nm) and violet (~402 nm) [96].

Synechocystis TaxD1 has two GAF domains, one showing the canonical cysteine-histidine dipeptide in the position of chromophore binding, whereas the other one shows a proline-histidine sequence. TaxD1 is involved in the regulation of positive phototaxis in response to low-fluence R and FR [97;98].

Another Phytochromes-like protein which plays an important role in phototaxis is PixJ1 from *Synechocystis* (*Sy*PixJ1), *Thermosynechococcus elongates* (*Te*PixJ1) and *Anabaena* (Nostoc) (*An*PixJ1). *Sy*PixJ1 contains two GAFs domains but cysteine is present in second GAF. The *Sy*PixJ1-GAF2 showed a conversion between a blue light absorbing form (P_b, ~425 nm) and a green light absorbing form (P_g, ~535 nm) [99]. Dark incubation led P_g to revert to P_b, indicative of stability of the P_b form in darkness. Red or far-red light irradiation, which is effective for

photochemical conversion of the known phytochromes, produced no change in the spectra of P_b and P_g forms. The *Te*PixJ1, which carry only one GAF with Cys residue also showed the similar photoconversion and peaks of P_b and P_g as *Sy*PixJ1-GAF2 [100]. In case of *An*PixJ1, there are four GAF domains, three carry a Cys residue, but only one (GAF-2) showed a reversible and full photoconversion between a green-absorbing form (P_g, 543 nm) and a red absorbing form (P_R, 648 nm) [101].

1.2.5 The phytochrome photoconversion

The photochemical conversion processes of phytochrome have been intensively investigated. An important property of phytochromes is their photochromicity that allows the double bond isomerization to be reversed upon irradiation with light of an appropriate wavelength, thus rendering them light-driven, thermally stable systems. The immediate effect of light absorption is photoisomerization of one of the chromophore's double bonds which induces conformational changes in the protein moiety. Since P_R and P_{FR} have partially overlapping absorption spectra in most regions of the light spectrum, $P_R \rightarrow P_{FR}$ photoconversion processes lead to the formation of a photoequilibium consisting of a mixture of P_R and P_{FR} forms under saturating illumination (the long wavelength absorption of the P_{FR} state, however, allows to selectively excite this form and to study the photochemical photoconversion in the P_R form). Photoequilibrium statistics indicate that red light produces a mixture of roughly 87% P_{FR} and 13% P_R, whereas far-red light irradiation can convert >99% of phytochrome to the P_R form owing to the lack of significant P_R absorption in the far-red (FR) region of the light spectrum [65].

From time-resolved absorption measurements, low temperature trapping and vibrational spectroscopic methods, three intermediates have been identified during the $P_R \rightarrow P_{FR}$ pathway (Lumi-R, Meta-R_a, and Meta-R_c), and at least two intermediates (Lumi-F and Meta-F) during the reverse $P_{FR} \rightarrow P_R$ reaction (Figure 11). The first step of the P_R to P_{FR} conversion is the Z-to-E photoisomerization of the C15=C16 double bond which is complete after several ps [42;102;103]. The first

stable photoproduct after red light irradiation of the P_R state is called Lumi-R absorbing near 700 nm. Ultrafast Vis/Vis pump-probe spectroscopy and picosecond time-resolved fluorescence spectroscopy at room temperature have determined the time scale of the formation of Lumi-R to be in the picosecond range [104;105].

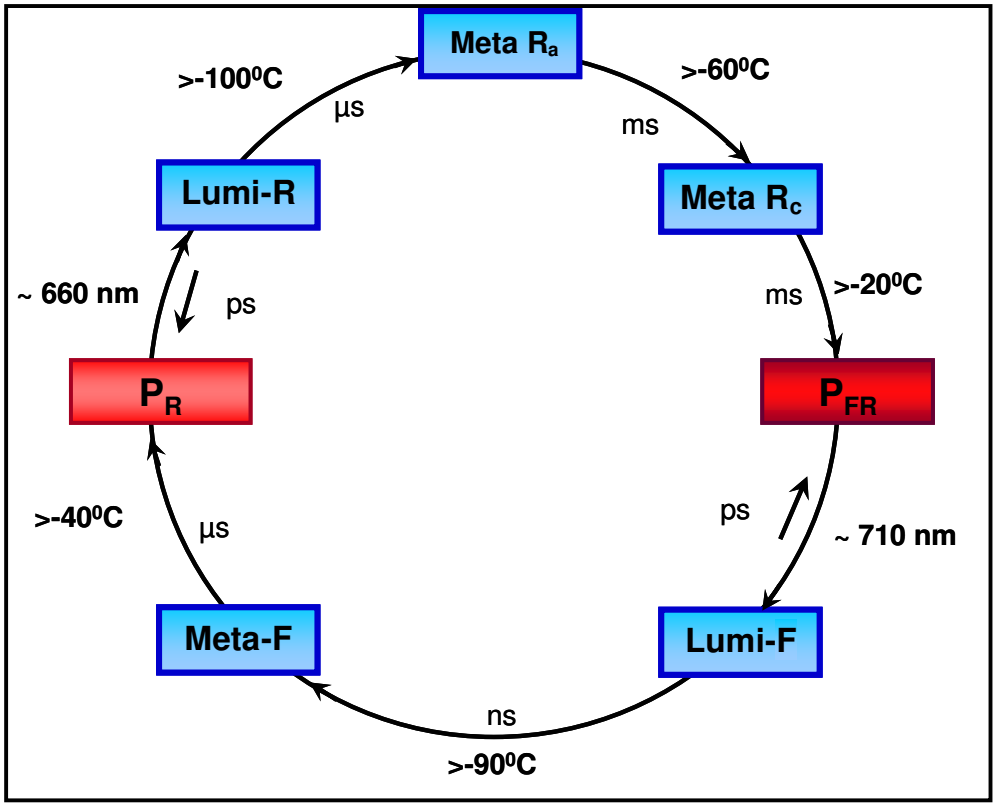

Figure 11: Phytochrome photoconversion processes. The figure shows a temperature-program dependent conversion where the initial photochemical processes occur also at very low temperatures, whereas the following intermediates are arrived through a gradual increase in temperature. The photoproducts Lumi-R and Lumi-F are photoconvertable into P_R and P_{FR} respectively in low temperature.

The extent of the photoreversible $P_R \rightarrow P_{FR}$ phototransformation upon red light illumination was determined to be about 0.75 for Cphs [2] and about 0.87 for plant Phys [106]. In both cases, the quantum yield Φ of 0.15 is relatively low. The subsequent reaction steps occur on the microsecond to millisecond time scale.

Intermediate states of the photocycle of different Phys have been addressed by Fourier transform infrared and resonance Raman spectroscopy using low-temperature trapping techniques [104;107;108]. At room temperature, the Lumi-R (~688 nm) decay occurs in microseconds to Meta-R_a (~663 nm), followed by its conversion into Meta-R_c (~725 nm) in milliseconds that ultimately yields P_{FR} [104;107;109] (Figure 11). The Meta-R_c formation is characterized by a significant red shift of the first absorption maximum and is the key step of the P_{FR} formation in milliseconds. Recently, however, Ulijasz and coworkers reported the unexpected isomerization of the C4=C5 double bond from NMR analysis of a GAF domain in the R/FR sensor Cph2 from the thermophilic cyanobacterium *Synechococcus* sp. OS B' [110].

The P_{FR} to P_R conversion has been investigated less intensely. Until now, two intermediates have been identified, Lumi-F and Meta-F. While the P_R photoreaction occurs in 40-200 ps, the P_{FR} photoreaction is much faster and occurs on the time scale of a few picoseconds [105;111-113]. The femtosecond kinetics of $P_{FR} \rightarrow P_R$ photoconversion of phyA carrying native (PΦB) and modified (PCB) chromophore showed an ultrafast excited-state relaxation within ~150 fs. Following, the chromophore returns to the first ground state intermediate ($I_{FR\ 750}$) in 400-800 fs followed by two additional ground states ($I_{FR\ 675}$ and pseudo-P_R) which are formed with lifetimes of 2-3 ps and ~400 ps [105]. The intermediates Lumi-F and Meta-F have been shown in cyanobacterium phytochrome CphA to absorb at 635 and 640 nm at low temperature, respectively [114].

Recently, Matysik and coworkers have presented investigations on the photoconversion $P_{FR} \rightarrow P_R$ of Cph1 by characterizing P_{FR}, Lumi-F, Meta-F and P_R states using Magic-Angle Spinning NMR. First, the double bond photoisomerization forming Lumi-F occurs which is transformed to Meta-F by the release of mechanical tension. Only this second reaction step leads to a disruption of the hydrogen bond of the ring D nitrogen to Asp207 and triggers signaling (Figure 12). In the P_R state, there is reformation of hydrogen bond to water [115].

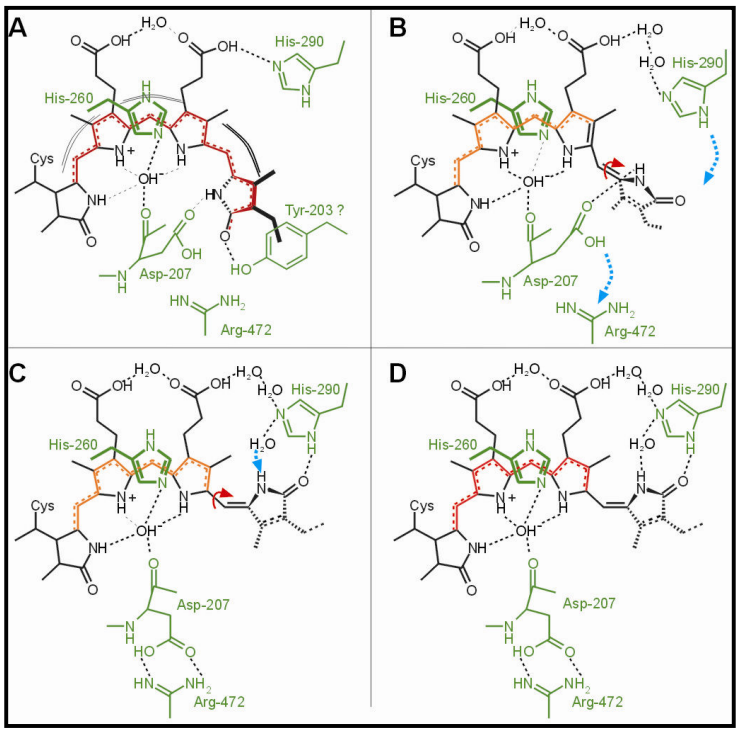

Figure 12: Structure of the chromophore and binding pocket in the P_{FR} (A), Lumi-F (B), Meta-F (C) and P_R states (D). The conjugated system is depicted in red and protein residues are in green [115].

Compared to the forward reaction, the order of events is changed, probably caused by the different properties of the hydrogen bonding partners of N24, leading to the directionality of the photocycle. Despite intensive and extensive investigations with vibrational and optical spectroscopy [104;107;108;115;116] the molecular and mechanical characteristics of these intermediates remain to be discovered.

1.2.6 Three dimensional structures of phytochromes

Until 2005, the study of the structural interactions of phytochrome protein and chromophore was possible only indirectly by their spectroscopic properties and via comparison with theoretical calculations, or it was limited to methods such as amino acid mutation. In the recent few years, three phytochrome crystal structures have been reported in the P_R state [47;52;84;85] and one in P_{FR} state [53].

The first three-dimensional structural data were obtained for the 35 kDa PAS-GAF bi-domain fragment of bacteriophytochrome from *Deinococcus radiodurans*, *Dr*BphP and provided an important insight into the 3D molecular structure. The structure clearly revealed the covalent attachment of BV at its $C3^2$ position, an extended, still slightly bent chromophore conformation, and strong interactions between the propionate side chains and amino acid side chains. The nitrogen atoms of pyrrole rings A, B, and C are all hydrogen bound and immobilized, leaving only ring D loosely stabilized and ready for photoisomerization (Figure 13). The structure reveals strong interactions between rings A, B, and C, but does not provide a mechanism to explain how the photoisomerizing ring D might be fixed in either of its conformations, P_R or P_{FR}. A later presented crystal structure from *Rhodopseudomonas palustris* (*Rh*BphP3) also revealed a similar structure as *Dr*BphP rendering most of the three dimensional facts true for bacteriophytochromes [85]. The *Rp*BphP3 - CBD crystal structure determined in the P_R state enhanced the appreciation of the structural basis of reversible P_R/P_{FR} photoconversion and the factors bestowing an unusual photoconversion behavior of *Rp*BphP3.

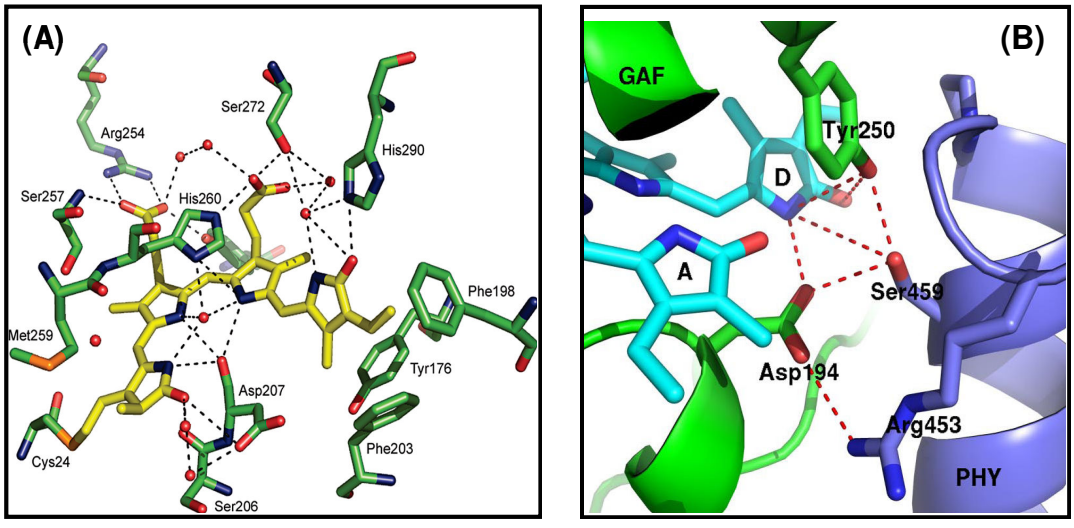

Figure 13: Three-dimensional structure of phytochrome (A) In *Dr*BphP, the PAS-GAF domains of this phytochrome shows the dense network of hydrogen bonds between several important amino acids of the protein and the BV chromophore (in yellow) in its P_R state (PDB code number 209c) [84]; (B) In *Pa*BphP, at the interface between the

GAF and PHY domains in *Pa*BphP-PCD, conserved residues Tyr250, Asp194, Ser459, and Arg453 and the chromophore form extensive hydrogen bond interactions to stabilize ring D in the 15*E*a (P_{FR}) configuration (PDB code number 3C2W) [53].

However, the chromophore pocket was clearly incomplete in these fragments. These crystal structures are all from truncated phytochromes void of the PHY domain, which has been shown to be required for P_{FR} stability [49;77;81], and they do not undergo a full photoconversion between the P_R and P_{FR} states.

The X-ray structure of the complete sensory module (PAS-GAF-PHY tri-domain) of the N-terminal part of the cyanobacterial phytochrome 1 (residues 1-514, Cph1Δ2) from *Synechocystis* sp.6803 in the P_R state has been resolved in 2008 [52]. This protein, although truncated to exclude the HK domain, behaves similar to the full length protein in photochemical measurements [75]. Thus, it would give the complete picture of a photochemically active phytochrome and the protein-chromophore modifications during photoconversion between the two types, P_R and P_{FR}. In all cases, the P_R chromophore adopts a (5Z)-syn, (10Z)-syn, (15Z)-anti configuration. The structure indicates close packing around chromophore rings A, B and C, especially around the C10 atom connecting rings B and C.

Later also the crystal structure of the *Pa*BphP-PCD BphP from *Pseudomonas aeruginosa* with an intact, fully photoactive photosensory core (comprising all three domains) in its dark-adapted P_{FR} state has been determined in 2008 [53]. The *Pa*BphP structures, which include the entire PAS-GAF-PHY core, reveal a (5Z)-syn, (10Z)-syn, (15E)-anti configuration for the P_{FR} chromophore (Figure 13B). As speculated at the interface between the GAF and PHY domains in *Pa*BphP-PCD, conserved residues Tyr250, Asp194, Ser459, and Arg453 and the chromophore form extensive hydrogen bond interactions to stabilize ring D in the 15*E*a (P_{FR}) configuration.

The unique feature of the Cph1 and *Pa*BphP structure is a long, tongue-like protrusion from the PHY domain that seals the chromophore pocket, giving an explanation for the role of the PHY domain to accomplish an efficient photochemistry

[64] (Figure 14). In the tertiary structure of these four proteins (*Dr*BphP, *Rp*BphP3, *Pa*BphP and Cph1Δ2), the PAS domain penetrates the GAF domain to form a knot in which the N-terminal extension passes through the large insert in the GAF domain.

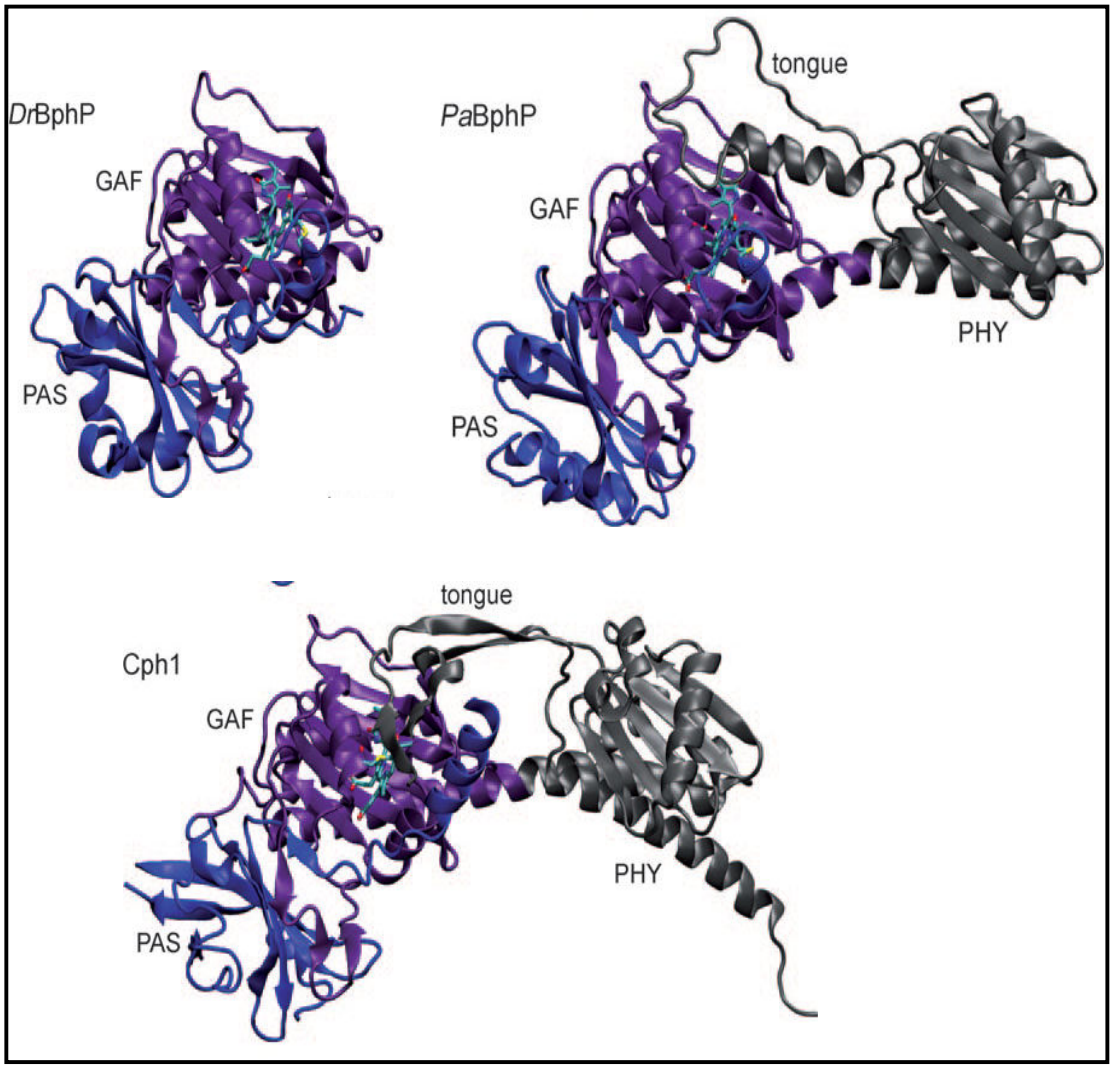

Figure 14: Structures of photosensory regions of various phytochromes. Top left, PAS-GAF fragment of *Dr*BphP in the P_R state (PDB accession 2O9C); top right, PAS-GAF-PHY fragment of *Pa*BphP in the P_{FR} state (PDB accession 3C2W) and (bottom) PAS-GAF-PHY module of Cph1 in P_R state (PDB accession 2VEA). The PAS domain is shown in blue, GAF in purple and PHY in silver. *Pa*BphP and Cph1Δ2 showed a conserved, flexible tongue from PHY domain interacting with the chromophore

binding pocket in GAF domain. The figure is adapted from Rockwell and Lagarias 2010 [64].

1.2.7 Physiological role of Phytochromes

The absorption spectra of P_R and P_{FR} overlap to some extend, and under ambient light conditions, equilibrium between P_R and P_{FR} is established. This equilibrium responds rapidly to changes in the ratio of red to far-red light, making phytochromes useful sensors of critical changes in light quality. The varied structural and spectral properties of the phytochrome proteins accredit them to be involved in a diverse array of photosensory processes. The plant phytochromes, in combination with other photoreceptors, regulate photomorphogenetic processes such as seed germination, etiolation, growth inhibition, leaf development, phototropism, shade avoidance, induction of flowering, and regulation of the circadian clock [7;74].

The physiological functions of phytochromes in microbes are conceptually analogous to functions of plant Phys i.e. phytochromes regulate the metabolic response of the organism to its light environment, however, much less detailed information on the physiological importance is available for the prokaryotes. Phytochromes are involved in physiological functions in various organisms under conditions where light is attenuated. Cyanobacterial phytochrome-like proteins embracing a weak GAF domain homology have been assigned to a number of light effects such as phototaxis [66], control of circadian clock [117], chromatic adaptation [92], and adaptation to blue light conditions [118;119], while the biological function of prototypical phytochrome is known for only a few bacteria. Cph1 from *Synechocystis* sp. PCC 6803 has been identified for its role in adaptation to strong light conditions [120] and regulation of several genes, e.g. *gif*A that encodes the glutamine synthase regulator [121].

Distinct effects controlled by bacterial phytochromes have been determined for *Bradyrhizobium* spp., a photosynthetic plant symbiont, and the purple bacterium *Rhodopseudomonas palustris*. The BphPs from these two species are involved in alleviation effects from high light fluences as well as damaging UV irradiation by

regulating the biosynthesis of the photoprotective pigments such as carotenoid pigments, but they are also involved in regulation of the photosynthetic apparatus and bacteriochlorophyll biosynthesis [82]. It is not known why phytochrome proteins are retained in non-photosynthetic bacteria. One should also keep in mind that many observable light-dependent processes in cyanobacteria are rather controlled by Phy-like proteins RcaE, PlpA, CikA or PixJ [92;99;117;118] that have no direct plant homologs. In the non-photosynthetic bacterium *Deinococcus radiodurans*, BphPs control the regulation of carotenoid biosynthesis [38], and for the phytochromes from the filamentous fungus *Aspergillus nidulans* (Fph) the regulation of the sexual development and secondary metabolism by phytochromes has been demonstrated [45].

Two component signal transduction systems are involved in several responses of bacteria, allowing an adaptation to changes in their environment. These systems generally contain two protein components - a sensor consisting of an input domain and a transmitter module, and a response regulator consisting of a receiver module and an output domain. The phytochromes, in case they carry a histidine kinase activity, are light regulated TC systems, which form a signalling transduction cascade with a second protein known as response regulator (RR). After detection of an external stimulus, i.e., light in case of the photoreceptors, the HK is phosphorylated. The phosphate group is then –upon a protein-protein contact- transferred to a conserved aspartate residue of the RR, a phenomenon biochemically demonstrated in various Cphs and BphPs [3;37;78;88]. The cyanobacterial phys have light regulated histidine kinase activity [37], while plants have been shown to contain Ser/Thr protein kinase activity (McMichael and Lagarias, 1990). The autophosphorylation of oat phyA and the resultant transphosphorylation of a phy-interacting factor, PKS1, have been proven experimentally [122]. Studies have shown that the protein kinase activities of both Cph1 and eukaryotic phytochromes are bilin and light-regulated [37;122]. The holoprotein dimer formation is stimulated by the binding of the bilin chromophore as a result of activation of the histidine kinase dimerization domain [50;81], as the

"auto"phosphorylation is considered to take place in *trans*. However, the precise biologically significant activities related to this phosphorelay mechanism of signaling are still not clear, as some reports suggest that the C-terminal domain responsible for kinase activity is not necessary for phy activity in vivo, at least in plants [123].

1.3 Aim and scope of this thesis

Phytochromes are photoreceptors that utilize the red/far red light as a source of information for controlling numerous biological processes [7;74]. They were initially identified in plants [1], aned were later reported for cyanobacteria [2], other bacteria and fungi. The photophysical and photochemical properties of biological photoreceptors have drawn attention of the researchers for their potential application in biomedical and biotechnological applications [124;125]. Recent genome sequence data of the model plant pathogen *Pseudomonas syringae* pv tomato DC3000 has revealed the presence of one blue light-sensing LOV-domain photoreceptor and two red/far red sensing putative phytochrome photoreceptors, but their function in prokaryotes and in particular in *P. syringae* is still obscure. The LOV domain containing blue light photoreceptor protein of this bacterium has been shown to be a light-driven two-component signal transduction system mediated by LOV-histidine kinase [126]. The biological functions of such TC-HK relays in phytochromes are still enigmatic though initial findings are supportive for the mechanism of gene regulation controlled by light activation of such proteins.

In this background this study is aiming to perform genomic and proteomic studies using different techniques. For this purpose, *Pseudomonas syringae* pv tomato DC 3000 and the cyanobacterium *Calothrix PCC*7601 are used in the present study. The objectives of this dissertation are followings:

- To perform and improve heterologous expression of the phytochrome genes from *Pseudomonas syringae* pv tomato DC3000 into *E. coli*, purification and characterization.
- To create a phytochrome gene-deletion mutant strain of *Pseudomonas syringae* pv. tomato DC3000 and to perform in vivo analysis.
- To create a LOV domain coding gene-deletion mutant strain of *Pseudomonas syringae* pv tomato DC3000 and to perform in vivo analysis.
- To perform phenotypic characterization of the blue and/or red light photoreceptor mutant strains of *Pseudomonas syringae* pv. tomato DC3000.

- To investigate the essential length of the protein moiety required to maintain the spectral integrity in cyanobacterial phytochromes, using CphA and CphB from *Calothrix PCC*7601 as model systems.
- To re-design the receptor sensor LOV-kinase module of *Pseudomonas syringae* pv. tomato DC 3000 by replacing its histidine-kinase with the histidine-kinase form CphA (phytochrome from cyanobacteria *Calothrix PCC* 7601) and to characterize the obtained hybrid protein.

2. Materials and methods

2.1 Bacterial strains

Host bacterial strains used in this work are presented in Table 1.

Table 1: Bacterial strains used in this study

Strains	Relevant genotype and Source
E. coli strains	
BL21(DE3) RIL:	*E. coli* B F^- *ompT hsdS*(r_B^- m_B^-) *dcm*+ Tet^r *gal*λ (DE3) *endA* Hte [*argU ileY leuW* Cam^r] (Stratagene, USA)
ER2566 :	F- λ- fhuA2 [lon] ompT, lacZ : T7 gene 1 gal sulA1Δ (mcrC-mrr) 114::IS10 R(mcr-73::mini Tn10-TetS)2 R(zgb-210::Tn10)(TetS) endA1 [dcm] (NEB, USA)
S17-1:	*recA thi pro hsdRM*$^+$ RP4-2 Tc^r::Mu Km::Tn*7* [127]
XL1-Blue:	*rec*A1, *thi*-1, hsdR1, supE44, relA1, *lacF*, *proAB*,*laclq*, *ac*ZΔ*M*15 Tn10 (Tc) [128]
Calothrix PCC7601 :	Cyanobacteria (Pasteur Culture Collection, Institute Pasteur, Paris)

Pseudomonas syringae pv. tomato DC3000 strains

Wild type :	Plant pathogen (TIGR)
bphP1Δ:	DC3000 psptp1902::Spc^r (This study)
bphP2Δ :	DC3000 pspto 2652::Gm^r (This study)
LOVΔ:	DC3000 pspto2896::Km^r (This study)
bphPOΔ :	DC3000 pspto1901::Km^r (This study)
bphP1Δ bphP2Δ:	DC3000 psptp1902::Spc^r, 2652::Gm^r (This study)

Abbreviations: ampicillin resistance (Ap^r); gentamicin resistance (Gm^r); kanamycin resistance (Km^r); spectinomycin resistance (Sp^r); streptomycin resistance (Sm^r).

2.2 Plasmids

The vectors used for cloning and protein expression are listed in Table 2.

Table 2: Plasmids used in this study

Plasmid	**Description and Source**
pUC18:	Ap^r, lacZ, cloning vector (Fermentas)
pJET1.2:	*eco47IR*, Amp^r, MCS, blunt end cloning vector (Fermentas)
pET14:	His-tag, T7 tag, lacI, Ap^r (Novagen)
pET28:	His-tag, T7 tag, lacI, Km^r (Novagen)
pET30:	His-tag, S tag, lacI, Km^r (Novagen)
pET52 3C/LIC:	His-tag, Strep tag, *lacI*, Amp^r, ligation independent cloning (Novagen)
pET28CphA-PAS-GAF-PHY:	PAS-GAF-PHY domain of *CphA* from *Calothrix* in pET28; Km^r (This study)

pET28CphA-PAS-GAF:

PAS-GAF domain of *CphA* from *Calothrix* in pET28; Km^r (This study)

pET28CphB-PAS-GAF-PHY:

PAS-GAF-PHY domain of *CphB* from *Calothrix* in pET28; Km^r (This study)

pET28CphB-PAS- GAF:

PAS-GAF domain of *CphB* from *Calothrix* in pET28; Km^r (This study)

pET28PstbphP1: pspto1902 in pET28; Km^r (This study)

pET52PstbphP1: pspto1902 in pET52b; Ap^r (This study)

pET28PstbphP2: pspto2652 in pET28; Km^r (This study)

pET52PstbphP2: pspto2652 in pET52; Ap^r (This study)

pET30PstbphO: pspto1901 in pET30; Km^r (This study)

pET14PstbphO: pspto1901 in pET14; Ap^r (This study)

pET52PstbphO- bphP1: operon of pspto1901 and pspto1902 in pET52; Ap^r (This study)

pET52PstbphO-bphP2: Fusion of pspto1901 and pspto2652 in pET52; Ap^r (This study)

pET52PstbphO-bphP2 C/S: Fusion of pspto1901 and pspto2652 in pET52; 2^{nd} and 3^{rd} cysteine mutated to Serine; Ap^r (This study)

pHP45-Ω: Ω cassette source ; Sp^r/Sm^r [129]

pWKR202: Gm^r cassette source; Cm^r Km^r Gm^r [130]

pBSL15 : Km^r cassette source; Km^r [131]

pSUP202 : Suicide plasmid; Tc^r Cm^r [127]

pUCbphP1: pspto1902 fragment in pUC18; Ap^r (This study)

pUCbphP1::Ω-spc^r: Ω cassette inserted into *Eco*RV site of pspto1902 (This study)

pSUPbphP1::Ω-spc^r: bphP1::Ω-spc^r inserted into EcoRI site of pSUP202 (This study)

pUCbphP2: pspto2652 fragment in pUC18; Ap^r (This study)

pUCbphP2::Gm^r: Gm^r cassette inserted into *Bgl*II siteof pspto2652 (This study)

pJETLOV: pspto2896 fragment in pJET; Ap^r (This study)

pJETLOV::Km^r: Km^r cassette inserted into *Bstz*17I site of pspto2896 (This study)

pETHO: pspto1901 fragment in pET14; Ap^r (This study)

pETHO::Km^r: Km^r cassette inserted into *Stu*I site of pspto1901 (This study)

Abbreviations: ampicillin resistance (Ap^r); gentamicin resistance (Gm^r); kanamycin resistance (Km^r); spectinomycin resistance (Sp^r); streptomycin resistance (Sm^r).

2.3 Oligonucleotide primers

Oligonucleotide primers used for PCR amplification and sequencing reactions are given in table 3, 4, 5 and 6. Restriction sites used for cloning are underlined.

Oligonucleotide primers used for study of phytochrome from *Calothrix* PCC7601 are listed in Table 3.

Table 3: Primers used on study of phytochrome from *Calothrix* PCC7601

Name	Sequence (5'---3')
CphAPas For	TCCGGTCCATGGTGAATAGCTTAAAAGAAGCA
CphAPhy Rev	AAACTCGAGCGCATTCGAGCGTTCTAAGTC
CphAGaf Rev	AACTCGAGAGCCGCACCTTGAGCGCTAGT
CphAHisKi For	TACTTTGCCATGGTCAGCCAAACAGAAGGA
CphAHisKi Rev	ATTTAGCTCGAGTCCTCGACCAAAAAGTGT
CphBmPas For	TATACCATGGGCTTAAGTCCTGAAAATTCTCCAG
CphBmPhy Rev	AAACTCGAGATCGTTGCTGCGCTGCAGTTC
CphBmGaf Rev	AAACTCGAGAACAGCCGCGAATGTAGCATT
CphBmHisKi For	TACTTTCCATGGCAGGAAATCCTCATAAGCCT
CphBmHisKi Rrev	ATTTAGCTCGAGTTTGACCTCCTGCTGCAAAGT

Oligonucleotide primers used for the study of heterologous expression of phytochrome from *Pseudomonas syringae* pv. tomato DC3000 are listed in Table 4.

Table 4: Oligonucleotide primers used for the study of phytochromes from *P. syringae pv tomato* DC3000

Name	Sequence (5'---3')
745NdeIFor	TTGGACATATGAGCCAACTCGACAAGGAC
745EcoRIRev	TATGGAATTCTCAATGTGCGATCGGCACC
993NdeIFor	TTGGAACATATGATCGAGCACACACTGG
993EcoRI28Rev	TAGCGAATTCTCATAGACTGCTTTCCGGCTT
993EcoRI30Rev	TATGGAATTCTGTAGACTGCTTTCCGGCTT
757EcoRI28Rev	TAGCGAATTCTCACAGCGTGAAGGAAAACACA
757EcoRI30Rev	TATGGAATTCTGCAGCGTGAAGGAAAACAC
9933clicfor	CAGGGACCCGGTATGATCGAGCACACACTG
9933clicrev	GGCACCAGAGCGTTTAGACTGCTTTCCGGCTT
7573clicrev	GGCACCAGAGCGTTCAGCGTGAAGGAAAACAC
993IBAEcoRI3cFor	TTGGACGAATTCATGATCGAGCACACACTGGA
993IBAKpnI3cRev	TAGCTCGGTACCTAGACTGCTTTCCGGCTT
757IBAKpnI3cRev	TAGCTCGGTACCCAGCGTGAAGGAAAACACA
993IBAEcoRI45For	TTGGACGAATTCAATGATCGAGCACACACTGGA
993IBAKpnI45Rev	TAGCTCGGTACCTGTAGACTGCTTTCCGGCTT
757IBAKpnI45Rev	TAGCTCGGTACCTACAGCGTGAAGGAAAACAC
Phy2C2toSFor	GTCGCAGGTGATCCGCTTTCCATTGAACAGGTCAGCG
Phy2C2toSrev	CGCTGACCTGTTCAATGGAAAGCGGATCACCTGCGAC
Phy2C3toSFor	GAACAGGTCAGCGCCAATTCCGCGAAGAGTCTTGGC
Phy2C3toSrev	GCCAAGACTCTTCGCGGAATTGGCGCTGACCTGTTC
Phy2Q185Efor	GCAAGGTCGTTGCCGAGGCACTTACCGGCC
Phy2Q185Erev	GGCCGGTAAGTGCCTCGGCAACGACCTTGC
BphONdeIFor	TTGGAACATATGCCGGCAAGTTTTTCACCTGTCA
BphOBamHI14Rev	TATTGGATCCTCATAGCAGTACCTCTTGACCGT
BphOSalI30Rev	TATTAGTCGACTAGCAGTACCTCTTGACCGT
HOP1coexpFor	CAGGGACCCGGTATGCCGGCAAGTTTTTCACC
HOP1coexpRev	GGCACCAGAGCGTTATGTGCGATCGGCACCGTGAA
HOP2coexpFor	CAGGGACCCGGTATGCCGGCAAGTTTTTCACC
HOP2coexpRev	GGCACCAGAGCGTTTAGACTGCTTTCCGGCTT

Oligonucleotide primers used for the construction of knock-out mutations in *P. syringae* pv tomato DC3000 are listed in Table 5.

Table 5: Oligonucleotide primers used for the construction of knockout mutations of *P.syringae pv tomato* DC3000

Name	**Sequence (5'---3')**
PhP1	ATCAAGACGTGTGTGCTGGTGAA
PhP2	CGGAATTCCGGTGCCACAGTCGAGTATTACC
Phy1C_SFor	GTCCTCCTGGCCAATTCTGCGGATGAGCCCATTC
Phy1C_SRev	GAATGGGCTCATCCGCAGAATTGGCCAGGAGGAC
Uh1	GTATGTCCGAACATGACATCAGAC
Uh2	ATGCTGTTCAGGCTTGAGTCTTCAAC
P2pUCF	ATGAATTCGGCTGACGAAAACCTCTCCAAAT
P2pUCR	CAAAACTGCAGTGCTCACACGTTG
Phy2C1_SFor	GAAGCAGCGCTTGCTGAATCTGCACGTGAGCCGATC
Phy2C1_SRev	GATCGGCTCACGTGCAGATTCAGCAAGCGCTGCTTC
Phy2C2_SFor	GTCGCAGGTGATCCGCTTTCCATTGAACAGGTCAGCG
Phy2C2_SRev	CGCTGACCTGTTCAATGGAAAGCGGATCACCTGCGAC
Phy2C3_SFor	GAACAGGTCAGCGCCAATTCCGCGAAGAGTCTTGGC
Phy2C3_SRev	GCCAAGACTCTTCGCGGAATTGGCGCTGACCTGTTC
P2F	TTGGACGAATTCATGATCGAGCACACACTGGA
P2R	TATTCTCGAGTCACACGTTGAGCAACTCGCT
LP1	AACTGCAGCTACGCCTTCTTCGGTATAG
LP2	GAGGGGCAGAGCGTACCTTTCTAT
LOVdel_CFor	CCCCTGAAGAAACCGATTGGTGCCAAGGATTTC
LOVdel_CRev	GAAATCCTTGGCACCAATGGCCGGTTTCTTCAGGGG
LOVH_Lfor	CAGGTTGTTGAAATCGAGAGCAATGCCACCGGTG
LOVH_Lrev	GCTCACCGGTGGCATTGCTCTCGATTTCAACAACCTG
Pspto2896_for	GTGTCGGAAAACAAGACCCGTGTCGA
Pspto2896_rev	TCAGGCAATGCCGTTGGGACCATCC
LOVa	CCAATCGTCCGGACAATCCGATCA
LOVb	CGCTGCACGTCAATGACCGGTTT

HO1	TTGGAACATATGCCGGCAAGTTTTTCACCTGTCA
HO2	TATTGGATCCTCATAGCAGTACCTCTTGACCGT
HOU1	ATGCCGGCAAGTTTTTCACCT
HOU2	TTGAGCGTGAACAACAGACC

Oligonucleotide primers used for domain swapping in *Calothrix* PCC7601 (phytochrome) and *Pseudomonas syringae* pv tomato DC3000 (LOV) are listed in Table 6.

Table 6: Primers used for domain swapping

Name	Sequence (5'---3')
PstLOVNdeIfor	TCCAGTACATATGTCGGAAAACAAGACCCGTGT
CphAXhoIrev	TACGGTCTCGAGTTATCCTCGACCAAAAAGATC
LOV142ACphA516for	AGTCGCCGCAAAGACGCTGATGAACTAGCGCAGTTAG
LOV142ACphA516Arev	CTAACTGCGCTAGTTCATCAGCGTCTTTGCGGCGACT
LOV155ACphA533Afor	CAGAAGATGGAAGCGCTGAAAAAGTTTGCTTATGTCGCC
LOV155ACphA533Arev	GGCGACATAAGCAAACTTTTTCAGCGCTTCCATCTTCTG

2.4 Chemicals, consumables and enzymes

All chemicals used were of analytical grade. The chemicals were obtained from Merck (Darmstadt), Sigma (Deisenhofen), Serva (Heidelberg), DIFCO (Detroit, USA), Gibco/BRL (Eggenstein), Biomol (Hamburg), Pharmacia (Freiburg), ICN Biomedicals (Aurora, USA) and BioRad (München). Restriction enzymes and DNA-modifying enzymes used in this work were purchased from Fermentas (St. Leon Rot, Germany). Oligonucleotides used as PCR and sequencing primers were synthesized by Metabion International AG (Martinsried). Ni^{2+} IDA Metal Affinity Resin and disposable columns from Clontech (Palo Alto, USA) were used for the purification of the His-tagged proteins. The anti-penta His antibodies were from Qiagen (Hilden) and the secondary antibodies (AP conjugates) were from Dako (Hamburg, Germany).

2.5 Microbiological techniques

2.5.1 Media and supplements

Liquid media were prepared in the required volume in tri-distilled water and autoclaved at 121℃ (Systec, Germany). Threefold-distilled water was used for the preparation of media and buffers. Solid media were prepared with the addition of 15 g/L bacteriological agar (Serva, Germany) before autoclaving. When required, heat labile components e.g., antibiotics, IPTG, X-Gal were filtered through 0.22 µm filter and added to the autoclaved media.

Media

LB:	10 g/l NaCl, 5 g/l yeast extract, 10 g/l tryptone
LB-agar:	10 g/l NaCl, 5 g/l yeast extract, 10 g/l tryptone, 15 g/l agar
TBY:	16 g/l tryptone, 10 g/l yeast extract, 5 g/l NaCl
TBY-agar:	16 g/l tryptone, 10 g/l yeast extract, 5 g/l NaCl, 15 g/l agar
KB:	20 g/l tryptone, 1.5 g/l $MgSO_4$, 1.5 g/l K_2HPO_4, glycerol 10 ml
KB:	20 g/l tryptone, 1.5 g/l $MgSO_4$, 1.5 g/l K_2HPO_4, glycerol 10 ml, 15 g/l agar.

Antibiotics and supplement stock solutions

Ampicillin:	100 mg/ml in tdH_2O
Chloramphenicol:	25 mg/ml in 50% ethanol
Gentamycin:	5 mg/ml in tdH_2O
Kanamycin:	50 mg/ml in tdH_2O
Nalidixic acid:	5 mg/ml in tdH_2O
Spectinomycin:	100 mg/ml in tdH_2O
IPTG:	100 mg/ml in tdH_2O
X-Gal:	50 mg/ml in DMSO

Antibiotic solutions, IPTG and X-Gal were stored at -20℃. The tubes containing the stock solution of X-gal were wrapped with aluminum foil to protect the substances from light. Media supplements were added to the sterile media after cooling below 50℃.

2.5.2 Growth conditions

All *E. coli* strains except for pre-cultures (see below) were grown at 37℃. The incubation period varied depending on the following application for the cells as mentioned in the related topics. *E. coli* cells were grown overnight on LB agar plates or in liquid LB media in test tubes or Erlenmeyer flasks. A single colony or an aliquot from a glycerol culture stock was used to inoculate the culture medium. 1% (v/v) of a pre-culture was used to inoculate the large volume liquid cultures. Pre-cultures (starter cultures) were prepared by overnight incubation of the cells at 30 ℃. *Pseudomonas* strains were grown at 30 ^{o}C on KB agar plates or KB liquid medium.

2.5.3 Culture maintenance

Frequently required strains were maintained on LB or KB agar plates for short term storage. The agar plates were sealed with paraffin sheet and stored at 4℃ for 4-6 weeks. In order to preserve cells for long term, glycerol stocks were prepared by mixing of an overnight grown liquid culture (60 vol %) with 40 vol % of sterile glycerol (99.6%) in sterile vials. The glycerol stock cultures were kept in -80℃ for long term preservation.

2.5.4 Cell harvesting

Cells from liquid cultures of up to a volume of 5 ml were sedimented using a tabletop centrifuge (Hettich, Germany), at room temperature for 2-5 minutes at 6,000 to 13,000 rpm. Larger volumes of cells were pelleted using a rotor centrifuge (Beckman Coultor, USA) with JA-10 or JLA-16250 rotors at 4℃ at 6,000 rpm 10 to 20 minutes.

2.5.5 Measurement of cell growth using optical density

The growth of unicellular organisms could be rapidly determined by measuring the turbidity related to cell density. As microbial cell numbers increase, the light intensity passing through the culture decreases, the output is often expressed as absorbance or optical density at a given wavelength which is a logarithmic expression of the amount of light that passes through the culture, thus allowing the measurement of cell density.

Cell density was determined by observing the optical density using spectrophotometer taking the pure medium as blank. Cells in specified solution or culture medium were observed in cuvettes with a pathlength of 1 cm at a wavelength of 600 nanometer (nm).

2.5.6 DNA manipulation

2.5.6.1 General techniques

All heat stable solutions and devices were autoclaved in order to inactivate nuclease activity and to reduce contamination. Solutions were autoclaved at 121 °C for 20 minutes and instruments were autoclaved at the same temperature for 15 minutes. Devices that could not be autoclaved were rinsed with 70% ethanol and flamed to evaporate ethanol. Heat sensitive chemicals and solutions were filter-sterilized using 0.2 µm sterile filters.

2.5.6.2 Genomic DNA isolation

Genomic DNA was isolated using the "DNeasy Blood and Tissue kit" from Qiagen (Hilden, Germany). Overnight grown cells (2-3 ml, containing maximally 2 x 10^9 cells) were lysed using proteinase K. The lysate was loaded on to spin columns which contain a silica-based gel matrix. Remaining contaminations and enzyme inhibitors are removed by washing the spin column (matrix). DNA was eluted in

tdH_2O; the quality of recovered DNA is usually appropriate for PCR. The required buffers are provided by manufacturer.

2.5.6.3 DNA extraction from pure cultures using chloroform/isoamyl alcohol

The cells are lysed with anionic detergents in the presence of a DNA stabilizer and peptide bonds are hydrolyzed to free the DNA from associated proteins. A bacterial culture (1.5 ml) was centrifuged in an E-cup and re-suspended/washed in 1 ml of 0.9% NaCl using vortexing; it was centrifuged again to sediment the cells. The supernatant was discarded. The pellet was re-suspended in 564 µl 1XTE buffer (10 mM Tris-HCl, 1 mM EDTA pH 8.0). 30 µl of 10% SDS was added and the solution was mixed gently. 6 µl of proteinase K (20 mg/ml) was added and again mixed gently. The mixture was then incubated for 1 hour at 37°C. 100 µl 5 M NaCl was added, mixed gently, and 80 µl of a prewarmed (65°C) CTAB/NaCl solution (NaCl 4.19 g, CTAB 10 g, tdH_2O 100 ml, filter sterilized) was added. The solution was again mixed gently and incubated for 10 minutes at 65°C.

The chloroform/isoamyl alcohol (24:1 v/v) extraction was performed as a stand-alone DNA purification step. Extraction using chloroform removes protein contaminations from the DNA samples, using the different behaviour of proteins in comparison to DNA with organic solvents. While the proteins are denatured by the organic solvent and are localized after phase separation as a thin layer between the two phases, the DNA remains in soluble form and can be recovered from the aqueous phase. The DNA-containing solutions (bacterial extracts, restriction reactions mixture) were mixed with an equal volume of chloroform/isoamyl alcohol and mixed vigorously. The mixture was centrifuged at 4°C at 13000 rpm for 15-20 minutes. The upper aqueous phase was carefully transferred into a new tube. The clear nucleic acid phase obtained after chloroform/isoamyl alcohol extraction was precipitated using isopropanol or ethanol. 0.6 volume of ice-cold isopropanol or 2-3 volume of ice-cold absolute ethanol was added to the aqueous phase containing DNA and mixed carefully. The mixture was incubated at -80°C for 10-20 minutes. Precipitated DNA was obtained after centrifugation at 13,000 rpm at 4°C for 20-30

minutes. The DNA pellet was washed with 100 to 200 µl 70% ethanol and centrifuged again at 4°C for 5-10 minutes. The DNA pellet was then dried, resuspended in tdH_2O and stored at 4°C.

2.5.6.4 Plasmid-DNA isolation using the "QIAprep Spin Miniprep Kit"

"QIAprep Spin Miniprep Kit" from Qiagen (Hilden, Germany) was used to obtain pure DNA. The bacteria are lysed by SDS in presence of NaOH in the cold reaction mixture. The reaction leads to denaturation of RNA, DNA and proteins. Following the neutralization reaction, chromosomal DNA and proteins co-precipitate, whereas plasmid DNA remains in solution and can be collected by adsorption of the negatively charged DNA at a Silica gel matrix in presence of high salt concentrations. About 25 µg highly pure plasmid DNA (high copy number vectors) could be obtained from 3-5 ml of an *E. coli* culture. The quality of DNA after elution with tdH_2O allows sequencing and other activities that require high quality DNA.

2.5.6.5 Rapid plasmid isolation from *E. coli* by "Cracking"

This method allows rapid isolation of plasmid DNA from a single colony or a pellet obtained by centrifugation of a liquid culture, for, e.g., the size determination of plasmids. This method bypasses the need to prepare overnight liquid cultures. This method does not allow further manipulation of plasmid DNA, for, e.g., cloning or sequencing.

A single colony is lifted from an agar plate and placed into an E-cup containing 25 µl of 10 mM EDTA (pH 8.0). 25 µl of fresh cracking buffer (100 µl of 2N NaOH; 50 µl of 10% SDS; 0.2 g sucrose; td H_2O 850 µl) was added to the suspension, mixed well with a pipette, incubated for 5 minutes at 70°C, and then placed on ice. 2 µl of cracking stain (1.5 µl of 4M KCl; 0.5 µl of 0.4% Bromophenol) is added, mixed well with a micro pipette and the mixture is incubated in ice for 5 minutes. The solution is then centrifuged at 4°C at 13,000 rpm for 10 minutes. 15-20 µl of supernatant are directly poured into the agarose gel slot and the gel is run for 1 hour at 100V.

2.5.6.6 Agarose gel electrophoresis

Agarose gel electrophoresis is a method used to separate DNA strands by size in a porous agarose gel by application of an electric field. The electric field is applied to drag the negatively charged DNA molecules through a gel matrix, where the shorter DNA molecules move faster than the longer ones. The rate of migration is affected by a number of factors that are concentration of agarose, voltage applied and conformation of DNA.

Agarose gels were made from 0.8% to 1% agarose in TAE buffer (40 mM Tris-acetate, 1 mM EDTA pH 8) as required. The DNA is then mixed with 0.2 volumes loading dye (Glycerol 30% (v/v); EDTA 50 mM; Bromophenol blue 0.25% (w/v)) in order to visualize and sediment it in the gel pocket. When the SYBR Green staining method is followed, the DNA is stained before loading to the gel by adding SYBR Green in a ratio of 1:5000. The gels are then run at 5 V/cm until optimal separation is achieved. For ethidium bromide-based staining the gels are exposed to 0.1 µg ethidium bromide/ml (in td H_2O or 1XTAE buffer) for about 10 to 15 minutes and de-stained for about 2-10 minutes in a water bath in order to reduce the background. The stained DNA (after SYBR Green or ethidium bromide staining) can be visualized under UV light. For size determination, the Gene Ruler^{TM} 1 kb Ladder Plus (Fermentas) can be used as a marker as required.

2.5.6.7 DNA extraction from agarose gel

DNA fragments are recovered from an agarose gel using “QIAquick gel extraction kit” (Qiagen, Hilden) following the manufacturer’s protocol. By this method, selection and recovery of a particular fragment of DNA from the gel is possible. The required reagents and DNA adsorption columns used are supplied with the kit.

2.5.6.8 Restriction digestion

This method is based on type II restriction enzymes isolated from prokaryotes which are highly specific and act on recognition sites of double stranded and in most cases palindromic DNA. The enzymes hydrolyze the phosphodiester bond between two bases in defined places of the double strand making two incisions, one through each of the phosphate backbones of the double strand without damaging the bases. This method produces over-hangs (sticky) or smooths (blunt) ends.

For cloning of DNA into a circular plasmid vector, the vector DNA is first linearized using appropriate restriction enzymes. PCR products or DNA to be cloned is also digested using the same or appropriate restriction enzymes to produce complementary overhangs or blunt ends for cloning into the linear vector. There are two protocols in use, depending of whether conventional or rapid hydrolyzing restriction enzymes are used.

Analytical digestion reaction using conventional restriction enzyme

DNA	7 µl (~0.5 µg)
10X Buffer	1.5 µl
Enzyme	0.3 µl
H_2O	to 15 µl

The reaction is incubated at the temperature recommended by the manufacturer for 3 to 16 hours.

Analytical digestion reaction using fast digest enzyme

DNA	7 µl (~0.6 µg)
10X Buffer	1.5 µl
Enzyme	1 µl
H2O	to 15 µl

In this case, the digestion reaction is incubated for 10 to 30 minutes at the temperature recommended by the manufacturer.

2.5.6.9 Dephosphorylation

In order to avoid re-ligation of empty plasmid vectors during the ligation reaction, the 5' phosphate residues at the end of linearized vectors are removed by alkaline phosphatase treatment. Dephosphorylation of digested vector DNA is performed by incubation with 1 µl (1 unit per pmol 5' ends) shrimp alkaline phosphatase (SAP) (Fermentas, Germany), and 10x dephosphorylation buffer (10% of the total reaction volume) for 45 minutes at 37°C. The volume is adjusted with H_2O. To finish the reaction, the phosphatase enzyme is inactivated by incubation for 10 minutes at 65°C. The DNA can then be purified using the Qiaquick PCR purification kit (Qiagen, Germany).

2.5.6.10 Ligation

DNA ligation involves creating a phosphodiester bond between the 3' hydroxyl end of one nucleotide and the 5' phosphate end of another. Cloning of DNA into plasmid vector is accomplished by ligating the complementary ends produced by the digestion of appropriate restriction enzymes with the linear vector prepared by the same or a similar restriction enzyme that produces complementary overhangs or blunt ends.

Ligation reaction

DNA	~8 µl (~ 0.5 µg)
Vector DNA	~ 5 µl (~0.2 µg)
10X T4 buffer	2 µl
T4 ligase	0.5 µl
Sterile H2O	to 20 µl

The ligation reaction is incubated overnight at 16℃.

For cloning into the ligation-independent pET52 3C/LIC vector, primers are designed to introduce a 12 bp 5’ extension into the sense and a 14 bp 5’ extension into the antisense strand to generate vector-specific complementary ends. The PCR product is then cloned into a linearized pET52 3C/LIC vector using the 3C/LIC cloning kit (Novagen) according to manufacturer’s protocol.

2.5.7 Polymerase chain reaction

PCR is performed in 0.2 ml plastic tubes in a reaction volume of 50 µl. For several or many parallel PCR reactions, a reaction master mix can be prepared.

PCR reaction using *Pfu/Taq* polymerase:

Template DNA (max. 0.1 µg/µl)	1 µl
10X polymerase buffer	5 µl
dNTP mix (10 mM each)	1 µl
Forward primer (25 pmol/ µl)	2 µl
Reverse primer (25 pmol/ µl)	2 µl
Pfu/Taq polymerase	0.5 µl
ddH2O	38.5 µl

PCR reaction using Hot start master mix

The mi-Hot *Taq* mix (Metabion) is used to carry out analytical PCR when several PCR are being performed in parallel. The pre-mix saves time for pipetting of different components and reduce the risk of errors in preparation of PCR components. Moreover, the antibodies present in the hot start mix prevent the polymerase activity in room temperature.

Template DNA (max. 0.1 µg/µl)	1 µl
Forward primer (25 pmol/ µl)	2 µl
Reverse primer (25 pmol/ µl)	2 µl
Hot taq master mix	25 µl
ddH2O	20 µl

Thermal conditions used for *Taq polymerase*:

Initial denaturation	95°C	5 min.
1. Denaturation	95°C	1 min
2. Annealing	58°C-62°C	45 sec
3. Elongation	72°C	1 min/ kb.

Number of cycles 30

Final elongation 72 °C 20 min

Thermal conditions used for *Pfu polymerase*:

Initial denaturation	95°C	3 min.
1. Denaturation	95°C	1 min
2. Annealing	55°C-58°C	45 sec
3. Elongation	72°C	2 min/ kb.

Number of cycles 30

Final elongation 72 °C 20 min

The obtained PCR products are analyzed by agarose gel electrophoresis. For the thermal cycling of the reaction Master cycler from Eppendorf (Eppendorf, Germany) was used.

2.5.8 Colony PCR

Colony PCR can be performed to quickly screen plasmid inserts directly from *E. coli* colonies or for the detection of genes from bacterial DNA: a colony of *E. coli* or *Pseudomonas syringae* pv tomato DC3000 was mixed in 25 µl of 1XTE buffer, boiled for 5 minutes, vortexed and centrifuged for 5 minutes at 13000 rpm. 2 µl were removed from the supernatant and used as template for PCR using Hot *Taq* PCR protocol as mentioned above.

2.5.9 Site directed mutagenesis (point mutation)

Site directed mutation is a method to insert aimed point mutations into a stretch of DNA. The point mutation for plasmid cloned DNA is based on the principle of two complementary primers, which contain the desired mutation as a mismatch [132]. The mutation primers should contain approx. 30 correct base matches with the template. A PCR is accomplished using the *Pfu* polymerase, which possesses an extremely low error rate and multiplies the entire plasmid. The PCR product is treated with restriction enzyme *Dpn*I to digest the original DNA and 5-10 µl of these PCR product is transformed in *E. coli*. The desired mutation is confirmed by sequencing.

2.5.10 RT-PCR ("reverse-transcriptase")

Overnight grown cultures of *P. syringae* DC3000 wild type and mutant cells (at OD_{600} about 0.7 to 1.0) were harvested by centrifugation for 2 minutes at 12000 rpm. The total RNA was isolated using the total-RNeasy mini kit (Qiagen). The DNA-free total RNA was reverse-transcribed into cDNA using the First strand complementary DNA synthesis kit (Fermentas) with the help of gene specific primers. A 2 µl aliquot of the reaction was used as template in the amplification reaction.

2.5.11 Bacterial cell transformation

2.5.11.1 Transformation by heat shock method

2.5.11.1.1 Preparation of competent *E. coli* cells

Competent *E. coli* cells were prepared in the presence of $CaCl_2$ following the method developed by [133]. 250 ml LB medium was inoculated with 1% (v/v) overnight culture of *E. coli* and grown at 37°C in rotary shaker up to OD_{600}= 0.4. The culture was kept on ice for 10 minutes. The cells were then centrifuged at 4,000 rpm at 4°C for 7 minutes. The cell pellets were re-suspended in 25 ml ice-cold 100 mM $CaCl_2$ solution and centrifuged again at 4,000 rpm at 4°C for 5 minutes. The pellets were re-suspended in 2 ml ice-cold 100 mM $CaCl_2$ solution. Glycerol was added to the

cells to a final concentration of 20% and the cell suspension was divided into different precooled E-cups with 100 µl aliquots in each. The competent cells prepared in this way were stored in -80°C.

2.5.11.1.2 Transformation using the heat shock method

Competent *E. coli* cells were transformed using the heat shock method [134]. 200 µl competent cells (from -70°C) were kept on ice for 10 minutes to thaw. 4 µl of ligation (10 - 150 ng DNA) mixture was added and incubated for 30 minutes in ice. A heat shock (42°C) was applied for 90 seconds enabling the cells to take up DNA. The cells were then incubated on ice for 3 minutes, after which 800 µl LB broth was added. The mixture was then incubated at 37°C for 1 hour by gentle shaking. 50 to 100 µl of the transformation mix was poured on LB agar plates with appropriate antibiotics, spread with a sterile spatula and incubated overnight at 37°C.

2.5.11.2 Transformation by electroporation

2.5.11.2.1 Preparation of electro-competent cells

About 200 ml of cells were grown at 30 ^{o}C with shaking at 180 rpm to OD_{600} of 0.5-0.6. The cells were cooled on ice for 15 minutes and centrifuged at 5000 rpm at 4 ^{o}C. The pellet was washed with ice-cold distilled water for 3-4 times with intermittent centrifugation at 4000 rpm at 4 ^{o}C. After the final wash, cells were resuspended in 2 ml of 10% glycerol (td H_2O) resulting in a total volume of about 3-4 ml; the cells are frozen and stored at -80 ^{o}C.

2.5.11.2.2 Electroporation

The competent cells stored in -80 ^{o}C were thawed on ice for about 15 minutes. About 100 ng (5-10 µl) of plasmid or linear DNA was added to about 100 µl of competent host cells and kept on ice for about 2-5 minutes. The mixture of cells and added DNA was transferred to an electroporation cuvette (0.1 cm) (Biorad), pre-chilled on ice. The cells were pulsed at 25 mF, 2.4 kV and 200 ohm (5 milliseconds) using the GenePulser (Biorad). Immediately after electroporation 1 ml of chilled LB

media was added to the cuvette and all the content was transferred to 2 ml Eppendorf tubes. The tubes were incubated at 30 °C for 1 ½ hours by gentle shaking. The content was spread immediately after incubation on LB plates containing appropriate antibiotics. The electroporation method is also used to construct the gene inactivation (knock-out mutant strains) of *P. syringae tomato*.

2.5.12 Selection of recombinant clones (blue/white screening)

The X-Gal-plate-test is used for the selection of *E. coli* clones that contain recombinant plasmid DNA inserted into a cloning site of the plasmid within the *lac*Z gene. This method is based on the induction by IPTG (Isopropyl-β-thiogalacto-pyranoside) that induces formation of β-galactosidase by the *lac*Z gene which converts the indicator X-Gal (5-bromo-4-chloro-3-indolyl-ß-D-galactoside) (included in the agar) into blue product. The inactivation of *lac*Z site by insertion inhibits the synthesis of this enzyme and the colony remains white. In this way the selection of one or several colonies harboring recombinant DNA was possible from the entire mixture of a transformation experiment. This test represents a further selection marker apart from the plasmid-coded antibiotic resistance. It should be kept in mind that the *E. coli* XL1Blue and DH5α strains used for transformations already carry a deletion of the *lac*Z gene and are therefore not applicable for this assay. The cloning sites of the pDRIVE PCR cloning vector, on the other hand, are located in the *lac*Z gene which codes for

2.5.13 Conjugation

Genes encoding phytochromes, LOV-kinase or heme oxygenase in the genome of *P. syringae pv. tomato* DC3000 were inactivated by conjugation. Plasmids containing each of these genes, interrupted by an antibiotic resistance cassette, were introduced into the *E. coli* strain S17-1. The resulting strains were used in a conjugation experiment with *P. syringae pv. tomato* DC3000, such that the *E. coli* cells containing the respective plasmids and *P. syringae pv. tomato* DC3000 cells were mixed in a ratio of 1:2, plated on KB agar, and grown for 18 to 24 hours. The

mixed colonies were scraped from the plate, resuspended in 1 ml of 10 mM $MgSO_4$, and plated on KB medium containing nalidixic acid (5 µg/ml) and antibiotic. Exconjugants were streaked for isolation on the same medium and subsequently characterized for the proper insertion by PCR amplification.

2.6 Protein chemical techniques

2.6.1 Heterologous protein expression

One liter of TBY medium containing the appropriate antibiotic was inoculated with 10 ml of an overnight grown *E. coli* culture transformed with the recombinant gene-containing plasmid in a baffled flask and grown at 30^0C and 180 rpm. At OD_{600} between 0.5 and 1, 0.5 mM (final concentration) IPTG was added to the culture medium. After induction, cells were grown overnight at room temperature and harvested by centrifugation at 4 ^{o}C for 10 to 12 minutes at 6000 rpm. Growth, induction and expression conditions were modified as required. After determining the weight of the pellets, they were stored at -20 ^{o}C or directly used for the isolation of the expressed protein.

2.6.2 Extraction of heterologous protein

Cell pellets were thawed on ice and resuspended in lysis buffer (100 mM Tris, 600 mM NaCl, 10% Glycerol, pH 8.0). The lysis buffer contained also ß-mercaptoethanol as a reducing agent (final concentration of 0.1%) and Pefabloc (final concentration 200 mM) to prevent protease activation. The suspension was dropwise added to liquid nitrogen and was broken by an ULTRA TURRAX (Milian, Geneva, Switzerland) under these conditions. After evaporation of the liquid nitrogen, the homogenate was centrifuged for 30 minutes at 4 ^{o}C and 20,000 rpm. The resulting supernatant was cleared by ultracentrifugation for 1 hour at 4 ^{o}C and 50,000 rpm.

2.6.3 Reconstitution of phytochrome with chromophore

The biliverdin chromophore was obtained by the method described by Mcdonagh et al,1980 [135] and PCB was isolated from the cyanobacterium *Spirulina platensis*

according to the method of Kufer and Scheer [136]. The apophytochrome was reconstituted in the dark with about a ten-fold molar excess of chromophore (dissolved in few µl of DMSO). After a few minutes of irradiation with far-red light > 715/750 nm, depending on the chromophore used, the P_R absorption spectrum was measured. After a few minutes of irradiation with red light (655 nm interference filter), the P_{FR} absorption spectrum was measured. Subtraction of the P_{FR} spectrum from the P_R spectrum resulted in the difference spectrum. If the concentration of apoprotein was unknown, PCB/BV was added stepwise, until no further increase in the difference spectrum was observed.

2.6.4 Ammonium sulfate precipitation of phytochrome

One volume of 3.3 M $(NH_4)_2SO_4$, 50 mM Tris, pH 8.0, 100 mM NaCl was added gradually during 1 hour to the protein solution on ice. The precipitate was pelleted by centrifugation for 30 min at 39,000 x *g* and 4°C. The pellet was dissolved in an appropriate volume of lysis buffer. Subsequently, the solution was cleared by centrifugation for 20 min at 16,000 x *g* and 4°C.

2.6.5 His-tag purification

The attachment of a tag of six or ten histidine residues at the N- or C-terminus of recombinant proteins enables affinity purification via Immobilized Metal Affinity Chromatography (IMAC). This method is based on the interaction between divalent metal ions (like Co^{2+}, Ni^{2+}, Cu^{2+} and Zn^{2+}) and the unprotonated imidazole ring of histidine. These metal ions have six coordination sites available for interaction with electron rich ligands. Ni-metal chelate affinity resin 26 (Serva) was used for purification of recombinant protein fused with His-tag, which has tetradentate chelators that bind the metal ions to the chromatographic substrate, leaving two sites available for interaction with histidine residues. After application of the protein mixture from the cell lysis onto the column and washing to remove the non-His proteins allows then the His-tag fusion protein to be eluted by lowering the pH,

resulting in the protonation of the imidazole ring of the histidines, which is then repelled by the metal ions.

Alternatively, the recombinant protein can be eluted using imidazole that competes for the Ni-sites on the resin. In this case, the resin was washed 2-3 times with water and further 2 times with wash buffer (50 mM Tris, 150 mM NaCl, 5% Glycerol, pH 8.0). The crude lysate solution was added to the resin and bound by incubation for about 1 hour by gentle shaking. The resin was transferred to a gravity column and allowed to settle. The column was then washed 10 times with wash buffer (50 mM Tris, 150 mM NaCl, 5% Glycerol, pH 8.0, 0.1% ß-mercaptoethanol (final amount), 200 mM Pefabloc (final concentration), and containing increasing concentrations of imidazole (10 to 40 mM). Finally, the His tagged protein was eluted with 2 ml of elution buffer (wash buffer with 250 mM imidazole).

2.6.6 Strep-tag purification

Strep-tag purification was performed using a streptactin sepharose drip column with a column volume of 5 ml. The column was equilibrated by washing with 5 column volumes of buffer W (20 mM Tri-HCL, 20 mM NaCl, pH 8.0). Crude lysate was poured in column and washed with 5 column volumes of buffer W. The washing step was repeated for 5 times. Elution of the fusion protein was carried out with 5 column volumes of buffer E (20 mM Tri-HCL, 20 mM NaCl, 2.5 mM desthiobiotin, pH 8.0).

2.6.7 Gel purification

For protein purification, an Ächta^{TM}basic system 10/100 from Amersham Pharmacia Biotech (GE Healthcare) was used. Ächta^{TM}basic is an automated liquid chromatography system and consists of a compact separation unit and a personal computer running the UNICORN^{TM} control system version 3.0. His-tag purified protein was further gel purified by this system using a Tricorn^{TM} Superdex^{TM}75 column that was washed and run at a flow rate of 1ml/minute with wash buffer (25 mM Tris-HCl, containing 10 mM NaCl, pH 8.0).

2.6.8 Dialysis

Purified (=eluted) proteins containing high amounts of imidazole or any other salt were subjected to dialysis. Appropriate molecular size exclusion cut-off dialysis membranes were used for this purpose. The concentrated protein solutions were dialyzed against 400-600 volumes of buffer with a minimum salt concentration at 4 °C. Routinely, apo-proteins were dialyzed, although sometimes holoproteins were also subjected to dialysis to remove high salt concentrations.

2.6.9 Protein concentration determination

The purified protein obtained by the His tag affinity chromatography was concentrated using a Centricon device using phosphate buffer (10 mM NaCl, 10 mM Na_2PO_4, 10 mM NaH_2PO_4, pH 8.0) or Tris buffer (20 mM Tris, 20 mM NaCl, pH 8.0) before their biochemical characterization. Concentration was performed via the ultrafiltration method with Ultrafree 15 Biomax 10K, 30K or 50K (Milipore, Bedford, MA, USA) filter devices. The procedure was perfomed by centrifuging at 4 °C and 4000 rpm as per the manufacturer‘s instructions.

2.6.10 SDS-polyacrylamide gel electrophoresis (PAGE)

Purified protein preparations were separated and analyzed by standard SDS-PAGE (Laemmli, 1970), for which NuPAGE minigels (Invitrogen) were used. The precasted gels are 4-12% acrylamide/bis-acrylamide gradient gels. Protein samples were mixed with 0.2 volume of Laemmli-buffer (100 mM Tris (pH 6.8), 200 mM DTT, 4% SDS (w/v), 0.2% bromophenol blue (w/v), 20% glycerol), and heat-denatured (95 °C, 5 min). Gel electrophoresis was performed in the Minigel Electrophoresis Unit (GE Healthcare) with 1XSDS buffer at 130 to 180 V, until the tracking dye reached the bottom of the gel. Prestained Protein Marker (Invitrogen Sea Blue 2) was used as the molecular weight marker. Proteins were visualized by staining with Coomassie staining solution (0. 2 % Coomassie-blue, 20% ethanol and 10 % acetic acid (final concentration) in water) for 20 minutes. The gel was then placed in destaining solution (40% ethanol, 10% acetic acid in water) for 20 minutes. To prevent cracking

of the gel during drying, the gel was washed for 5 min in 10% glycerol and rinsed in water, before allowing it to air-dry.

2.6.11 Western blot

For a Western blot analysis, proteins on the gel were blotted onto a PVDF membrane via a semi-dry electrophoretic transfer. The transfer sandwich was assembled under transfer buffer (25 mM Tris, 150 mM Glycin, 20% methanol, pH 8.0) in the following way: starting from the cathode, stacking was in the following order: 2 pieces of soaking pads, 1 piece of filter paper (of same size as gel and membrane), gel, membrane, filter paper and soaking pads. Prior to use, the membrane was immersed in methanol until it did not float any more, and was then kept in transfer buffer until use for blotting. All air bubbles were carefully removed from both sides of the gel. This sandwich was placed into a transfer cassette, which was then inserted into the buffer tank, and filled with transfer buffer. The proteins were transferred at a constant current of 25 V for 80-90 minutes. A pre-stained marker was used to control the completion of transfer. 3 % (w/v) BSA in TBS buffer (10 mM tris HCl (pH 7.5), 150 mM NaCl) was used to block the membrane. After washing two times for 10 minutes in TBST (20 mM Tris HCl (pH 7.5), 500 mM NaCl, 0.05 % (v/v) tween-20), and one time for 10 minutes in TBS, the membrane was incubated with the primary antibody (1:1000 diluted in blocking buffer) for one hour at RT. Any unspecifically bound antibody was removed by washing the blot two times for 10 minutes in TBST, and one time for 10 minutes in TBS. It was then incubated with the secondary antibody (1:1000 diluted in blocking buffer) for one hour at RT. Before developing the blot it was again washed four times for 10 minutes with TBST. To develop the blot, it was stained in freshly prepared 10 ml (100 mM Tris-HCl, 100 mM NaCl, pH9.5) with NBT/BCIP, and the color was allowed to develop in the dark. The chromogenic reaction was stopped by washing twice in water.

2.6.12 Tryptic digestion

Protein bands were excised manually from the electrophoresis gels after SDS PAGE separation. The gel plugs with specific protein bands were placed into polypropylene 96-well plates. Automated in-gel digest and sample preparation for MALDI-TOF MS was performed using the robotic liquid handling system FREEDOM EVO-150 Base (Tecan) and process as described by Jahn et al, [137] with some modification as shown in Table 7.

Table 7: Steps used by automated in-gel digest

Step	Reagent	Volume (µl)	Time (min)	Temp (^{0}C)
1. Destaining	50 mM ABC/30% ACN	100	10	45
2. Dehydration	100% ACN	100	12	RT
3. Drying			12	50
4. Reduction	5 mM DTT in 50mM ABC/30% ACN	20	30	45
5. Alkylation	22.5 mM IAA in 50 mM ABC/30% ACN	20	30	RT
6. Wash	50 mM ABC/30% ACN	100	2	RT
7. Dehydration	100% ACN	100	10	RT
8. Drying			10	50
9. Cooling			10	RT
10.Trypsin	25 ng/µl Trypsin in 5mMTris pH8.0/0.1% OGP/5 mM $Cacl_2$	6	15	RT
11.Digest buffer	5 mM tris pH8/0.1% OGP	15		RT
12.Digest			120	45
13.Extraction	0.5% TFA/0.1% OGP	25	60	RT

ABC, ammonium bicarbonate; ACN, acetonitrile; DTT, dithiothreitol; IAA, iodoacetamide; Tris, tris(hydroxymethyl) aminomethane; OGP, n-octyl-β-glucopyranoside; TFA, trifluoroacetic acid; RT, room temperature.

2.6.13 MALDI-TOF MS molecular weight analysis

MALDI-TOF MS (Matrix Assisted Laser Desorption Ionization-Time Of Flight Mass Spectrometry) is used to identify the subunit composition and the molecular mass of a purified protein. MALDI-TOF MS is performed by embedding the analyte into a solid, crystalline matrix, which absorbs the energy generated by a LASER beam. This energy absorption, which can be up to the order of 10^6 W/cm², leads to intense heating and generation of a plume of ejected material that rapidly expands and undergoes cooling. Since this process takes place within the high vacuum of the

mass spectrometer, the protein is gradually stripped from matrix and solvent molecules, and can then be separated according to its apparent mass to charge ratio.

For the experiments conducted, a Voyager-DE PRO Workstation and a Voyager-DETM PRO Biospectrometry Workstation from Applied Biosystems (USA) was used. The matrices used here were α-cyano-4-hydroxycinnamic acid (CHCA)(M1), 2,5-dihydroxybenzoic acid (2,5- DHB)(M2), Sinapinic acid and a mixture of 2,5-dihydroxybenzoic acid and 5-methoxysalicyclic acid (DHBs).

2.7 Ultraviolet/Visible (UV/VIS) spectrometry

UV-VIS spectroscopy is the measurement of wavelength and intensity of absorption in the near-ultraviolet and visible light region for a given sample. The concentration of an analyte in solution can be determined by measuring the absorbance at certain wavelengths and applying the Lambert-Beer law,

$$A = \varepsilon \times c \times d$$

where A is the measured absorbance, ε is a wavelength-dependent absorption coefficient, c is the concentration of the solution, and d is the path length. All the measurements were done with Shimadzu (UV-2401PC) spectrophotometers. The buffer or the eluent solution used to prepare the dilution of the sample was applied as a reference solution.

UV-Vis spectra from 200 - 900 nm were recorded with a Shimadzu spectrophotometer (UV- 2401PC). For recording P_R to P_{FR} conversion and the reverse reaction, the samples were repeatedly irradiated for 1 - 2 min with red light (650 ± 7 nm interference filter) and far-red light (> 715/750 nm cut-off filter), respectively, followed by recording of the P_R or P_{FR} spectrum after each irradiation. Difference spectra were formed by subtracting the P_{FR} spectrum from the P_R spectrum.

2.7.1 Assembly kinetics

To determine the chromophore assembly kinetics, the rise in absorption at the λ_{max} of the P_R form was followed at 10^0C directly after addition of the chromophore. To allow for correction for possible changes in scattering or a shift of the absorption maximum, spectra were recorded from 600 - 750 nm at regular time intervals. A detection-interval of 2 nm was used instead of the normally used interval of 0.5 nm, enabling recording of a spectrum with high scanning speed every 20 s. The chromophore (about ten-fold molar excess to the apophytochrome) was pre-dissolved in DMSO at a high concentration and diluted to 30 µl in buffer. The cuvette with apoprotein (470 µl) was placed into the spectrophotometer and cooled to 10^0C. The chromophore was added and mixed by "pipetting" up and down a few times. By this way it was possible to start recording the first spectrum within 15 s after the addition of the chromophore.

2.7.2 P_{FR} dark reversion

To determine the thermal stability of the P_{FR} form, the samples were exhaustively converted to P_{FR} by 5 min of irradiation with red light (655 nm interference filter). Directly after irradiation, spectral changes were recorded by measuring spectra from 450 – 850 nm at room temperature (20 ^{0}C) at regular time intervals. Alternatively, the absorbance change at a given, fixed wavelength could be followed. The increase of absorption in the P_R-maximum (or the decrease of the P_{FR} absorbance itself) was used to determine the P_{FR} dark reversion. At the beginning and at the end of the experiment, difference spectra were recorded to determine an eventual decrease of the absorption due to degradation of the protein.

2.8 Bioinformatics

2.8.1 DNA sequencing

DNA sequencing was performed at the Automatic DNA Isolation and Sequencing (ADIS) company at the Max Planck Institute for Plant Breeding Research, Cologne. Plasmid clones were sequenced using standard primers.

2.8.2 Analysis of sequence data

The evaluation of the sequence data was accomplished by the nucleotide-blast program (BLASTN), and/or translated query vs. protein database (BLASTX) service offered by National Center for Biotechnology Information (http://www.ncbi.nlm.nih.gov).

2.8.3 Sequence alignment and editing

Alignment of two sequences was performed with the specialized BLAST-bl2seq service of NCBI. Multiple sequence alignment was performed using the clustalW2 web-based server at http://www.ebi.ac.uk/ [138].

2.8.4 Protein domain scan

Protein domains were determined with ScanPro [139] at http://www.expasy.org and SMART v5 [140] at http://smart.embl-heidelberg.de/, using both as complementary tools.

2.8.5 Primer design

Most of the cloning primers were designed manually. However, few web-based tools were used to design primers to target specific regions in certain DNA molecules for PCR-based detection and mutagenesis. Primer-3 [141], a web-based primer design tool was used to find specific primer sequences to amplify a target region of a DNA. Primers for site directed mutagenesis were designed using the QuickChange® Primer Design Program (Stratagene).

2.8.6 Other resources

The determination of protein molecular weight and the identification of peptides from trypsin digested proteins were performed using the TrEMBL software available online. The 3D structures of proteins were taken from the Brookhaven protein data base (PDB) (http://www.rcsb.org/pdb/cgi/).

For secondary structure prediction, the PSIPRED method [142] was applied.

3. Results and discussion

Phytochromes are red-/far-red light sensitive photoreceptors, ubiquitous in plants and in many prokaryotic species [7]. They regulate a broad variety of photomorphogenetic responses, based on the photochemical properties of their covalently bound chromophore. As introduced in the previous chapters, different phytochrome families use different chromophores. This present thesis will try to broaden our understanding about the bacterial phytochromes from the cyanobacterium *Calothrix* PCC7601 and the pathogenic bacterium *Pseudomonas syringae pv tomato* DC3000.

Section 3.1 will focus on the essential length of the protein moiety required to maintain the spectral integrity in CphA and CphB phytochromes from *Calothrix*. Calothrix is the only cyanobacteria which carry two phytochromes, CphA and CphB, with different chromophore PCB and BV, respectively.

Section 3.2 will present results on construction of a fusion protein generated from the PAS domain of a blue light photoreceptor and the HK domain of a red/far red light-sensing photoreceptor. This reprogrammed fusion protein is recombinantly produced and biochemically studied.

Section 3.3 will describe the red and far-red light-sensing photoreceptors present in the pathogen *P. syringae tomato*. This bacterium carries two bacterial phytochromes, *Pst*BphP1 and *Pst*BphP2. The proteins were expressed in vitro and studied biochemically. The heme oxygenase, which is responsible for the production of the bilin chromophore of these phytochromes is expressed individually and co-expressed with phytochromes to study its role for chromophore production.

Although much is known about the molecular biology of *P. syringae tomato*, very little is known about the role of blue and red/far-red light photoreceptors and the effect of light on *P. syringae tomato*. To identify the photoreceptor involved in the light dependent regulation of motility, the insertion knockout mutants, defective of one or both phytochromes and of *LOVΔ* which encodes the blue light photoreceptor

(LOV) were generated and used to test for the effect of light on the bacterial motility and plant-mutant interaction. This result will be discussed in Section 3.4.

Section 3.1

3.1 Domain interaction in cyanobacterial phytochromes CphA/CphB from *Calothrix* PCC7601

Two phytochromes, CphA and CphB, from the cyanobacterium *Calothrix* PCC7601 were investigated for the essential length of their protein moiety required to maintain the spectral integrity.

3.1.1 The cyanobacterial phytochromes CphA and CphB

The cyanobacterial phytochromes, CphA and CphB, from the cyanobacterium *Calothrix* PCC7601, with similar size (767 and 765 amino acids) and domain structure (Figure 15), were investigated for their spectral properties. The full length CphA and CphB are 88 kDa and 87 kDa proteins, which had been cloned previously in the group [41;143], to study the biochemical characteristics of these photoreceptors.

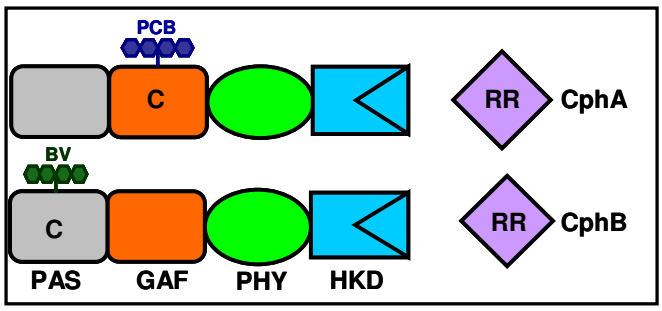

Figure 15: Graphical representation of the domain structure for the cyanobacterial phytochromes CphA and CphB from *Calothrix* PCC7601 with their cognate response regulators. Genes encoding these response regulators are on the same operon as the phytochrome genes.

Despite their high simialrity in molecular weight and in large part of their sequences, both phytochromes show significant functional differences: CphA is a canonical phytochrome, binding PCB in its GAF domain. It is highly homologous to plant

phytochromes and to classical cyanobacterial phytochromes such as Cph1 (748aa) of *Synechocystis* PCC6803 and AphA (755 aa) of *Anabaena* PCC7120, possessing the cysteine residue within a conserved amino-acid sequence motif of the GAF domain, to which phycocyanobilin (PCB) binds covalently as a chromophore [41;50;80]. *Calothrix* CphB is homologous to AphB of *Anabaena* PCC7120 and most of other bacteriophytochromes (BphPs) with a leucine instead of a cysteine residue in the chromophore binding domain unlike plant phytochromes. In this phytochrome, here coined CphBm, which is similar to other BphPs and lacks the canonical cysteine residue, an N-terminally located cysteine (Cys 24) was found as an alternative binding site for biliverdin (BV) that in this case serves as chromophore [143]. A comparison of the absorption maxima of a homologously expressed CphB with the heterologously generated apoprotein, assembled with phycocyanobilin (PCB, λ_{max} of 686 nm and 734 nm, Pr and Pfr maxima, respectively) or with biliverdin (BV) (λ_{max} of 700 nm and 750 ±2 nm) proved that BV works as the genuine chromophore [144]

3.1.2 Heterologous expression and purification of full length CphA and CphB

The phytochrome-encoding ORFs *cphA* and *cphB* were cloned in the pMEX8 and pET28a expression vectors behind the tac /T7 promoter. The heterologous expression of *Calothrix* CphA (full length) and CphB (full length) was successfully performed in expression cells BL21 (DE3) RIL. Both proteins carried a His_6-tag at their C-terminal end. The expression was induced at various temperatures ranging between 18-30℃ by adding IPTG up to a final concentration of 400 µM to the culture, after which growth was continued for 10-16 hrs. 1 litre of the culture resulted in up to 20 g of cell pellet. The crude lysate of phytochrome was precipitated by ammonium sulfate and His tagged affinity purification was performed after resolving the precipitated protein. Bis-Tris gels (4 -12%) were used for the identification of specific proteins and for the analysis of the purity of the proteins. Besides following the affinity purification by protein gel electrophoresis, also Western blotting was employed for the recognition of specific proteins in a mixture of expressed proteins in the host cells. For the phytochromes from *Calothrix*, the western blot was done

with the antibodies against the C-terminally located His tag. *Calothrix* CphA and CphBm showed the expected molecular weight of ca. 88 and 87 KDa (Figure 16, molecular weight prediction was done with the pI/MW calculator).

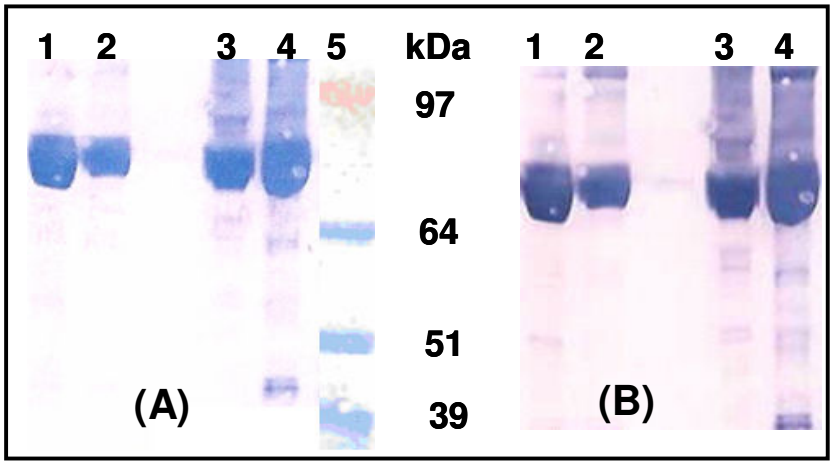

Figure 16: (A) SDS-PAGE and (B) Western blot analysis of *Calothrix* CphA and CphB expression in *E. coli*. Lane 1: 200 mM Imidazole eluate, lane 2: 300 mM Imidazole eluate of *Calothrix* CphBm, Lane 3: 200 mM eluate and lane 4: 300 mM eluate of *Calothrix* CphA. Lane 5: molecular weight marker; the sizes (in kDa) are indicated on the right side.

3.1.3 Truncation of CphA and CphB phytochromes

On the molecular level, the CphA and CphB proteins are composed of different domains which collectively form the fully functional phytochrome. Definition of these domains is based on the high similarity alignment of the amino acid composition of the phytochromes. Thus, the purpose of this part of the thesis was designed for a deeper understanding into the inter-domain interaction of the constitutive domains of the phytochromes as well as to detect the essential length of their protein moiety required to maintain the spectral integrity. The two phytochromes, CphA and CphB, fold into PAS, GAF, PHY, and Histidine-kinase (HK) domains. CphA autocatalytically binds a phycocyanobilin chromphore at a canonical cysteine within the GAF domain,

identically as in plant phytochromes, whereas CphB binds biliverdin IX at a cysteine positioned in the N-terminal PAS domain. The contribution of the various domains for maintaining the spectral properties was probed by generating C-terminally truncated CphA- and CphB-phytochromes. The details and graphical representation of the constructs are given in figure17.

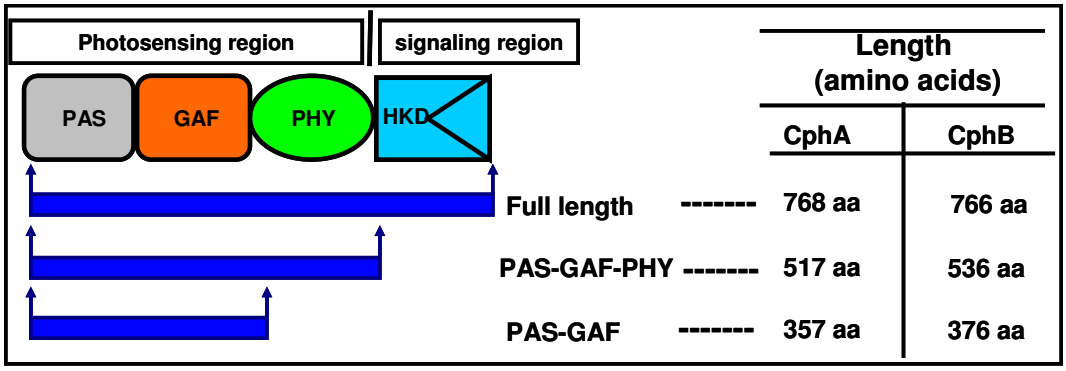

Figure 17: Molecular organization of the functional entities in cyanobacterial phytochromes from *Calothrix* PCC 7601. The N-terminal halves of the proteins contain a PAS (Per/Arndt/Sim) domain, the photosensor GAF (Guanylate/Adenosine/FhlA) domain and the phytochrome-specific PHY domain. The C-terminal half harbors a histidine kinase domain (HK) with an ATPase activity. The expression constructs are indicated by the abbreviated notations as PAS/GAF/PHY (PGP) domains and PAS/GAF (PG) domains. The size of these constructs (number of amino acids) is also given.

For designing meaningful trucation sites, the CphA and CphB protein secondary structure was predicted using program PSIPRED. The predicted structures were examined for secondary structure elements, allowing a primer design that would not intersect the continuity of the secondary structure motif. This step was done with greatest precaution aiming at not affecting the soluble expression of the truncated domains. The respective domains generated from the coding sequence of the full length phytochrome proteins, CphA and CphB, were cloned into pET28a between the *Nco*I and *Xho*I restrictions sites for expression in *E. coli*. The PCR primers were

designed to include the C-terminal His_6 tag provided with the vector, to ensure isolation only of full-length constructs.

Stepwise, the full length CphA and CphB were truncated after the PHY domain, excluding the histidine-kinase (HK) domain (constructs CphA-PAS-GAF-PHY, named CphA-PGP, and CphB-PAS-GAF-PHY, named CphB-PGP, respectively). These construct were further truncated to yield CphA-PAS-GAF (CphA-PG) and CphB-PAS-GAF (CphB-PG), by introducing a stop codon after the GAF domain excluding the PHY domain.

3.1.4 Expression of truncated CphA and CphB

The heterologous expression of the truncated phytochromes CphA and CphB from *Calothrix* PCC7601 was accomplished in *E. coli* strains BL21 (DE3) RIL. The various constructs of truncated CphA and CphB had lengths of 517 (PAS–GAF–PHY), and 357 amino acids (PAS–GAF) in case of CphA, and 536 (PAS–GAF–PHY), and 376 amino acids (PAS–GAF) in case of CphB. The genes for these proteins were designed to include C-terminal poly-histidine tags for affinity purification. From one litre of bacterial culture, a total of approximately 20-30 g wet cell mass was obtained. The truncated CphA constructs, CphA-PGP and CphA-PG expressed poorly and the majority of this recombinant protein was found in insoluble form in inclusion bodies. The CphB constructs, CphB-PGP and CphB-PG, in contrast, were found as well soluble proteins with a higher expression yield. Despite the problems with the CphA-constructs, sufficient amounts of all recombinant proteins could be accumulated and purified for the spectral analysis.The yields for CphA-PGP and CphB-PGP per litre were about 1 mg and 8 mg, respectively.

After the His-tag purification of the apoproteins, the molecular weight of all truncated CphA and CphB was determined via SDS-PAGE (Figure 18A). Single bands migrating at approx. 61 kDa and 62 kDa were obtained on SDS-PAGE, which correlate with the predicted molecular mass calculated from amino-acid composition of CphA-PGP and CphB-PGP, respectively. The molecular weight of the CphA-PG

protein was found as 42 kDa, while that of CphB-PG was 43.5 kDa, as predicted by EXPASY Server and confirmed via SDS-PAGE and western blot (Figure18B).

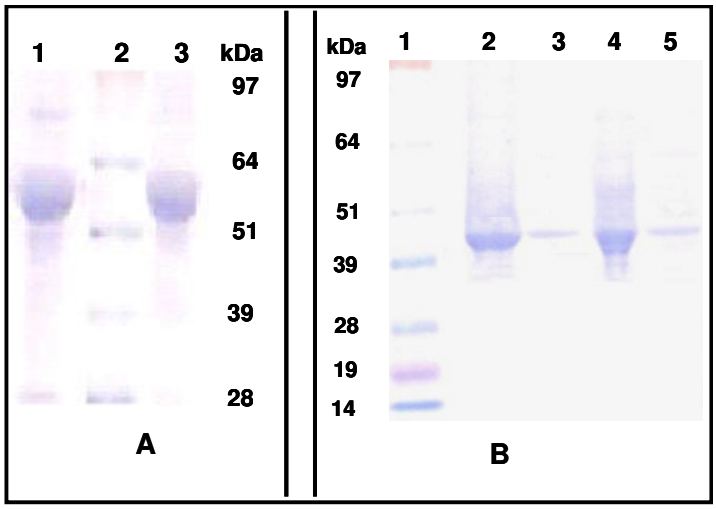

Figure 18: SDS-PAGE analysis of *Calothrix* CphA-PGP/CphB-PGP and CphA-PG/CphB-PG expressed in *E. coli and* purified using the His tag, after sample concentration. (A) Lanes 1 and 3 are CphA-PGP and CphB-PGP, respectively. Lane 2: the protein molecular weight marker, sizes (in kDa) is indicated on the right side. (B) Lane 1: Protein molecular weight marker. Lane 2: CphA-PG, eluted by 125 mM imidazole; lane 3: CphA-PG, eluted with 150 mM imidazole; lane 4: CphBm-PG, eluted with 125 mM imidazole; lane 5: CphBm-PG, eluted with 150 mM imidazole.

The reconstitution of the domain proteins was done with PCB for CphA (full length and its truncated domain construct) and BV for CphB (full length and its truncated constructs) apo-proteins. The reconstitution with the desired chromophore (PCB or BV) was either done in the clarified cell lysate or after purification. Purified receptor domain proteins were tested by UV/VIS spectroscopic analysis in order to assess the absorption profiles and photoreversibility of the photochromous proteins.

The full-length CphA, assembled with PCB, absorbs at 663 nm and 707 nm in its P_R and P_{FR} forms, respectively (Figure 19A). CphB, binding BV, shows bathochromically shifted absorbance maxima with respect to those from CphA at

704 and 750 nm (P_R and P_{FR}) (Table 8 and Figure 19B). The expression in *E. coli* resulted in amounts of reconstitutable phytochrome of about 2 mg/l and 6 mg/l for CphA and CphB, respectively. The amount of the reconstituted phytochrome was determined by using the extinction coefficient of the recombinant *Synechocystis* phytochrome Cph1, ε_{max} of 80,000 $M^{-1}cm^{-1}$ [50].

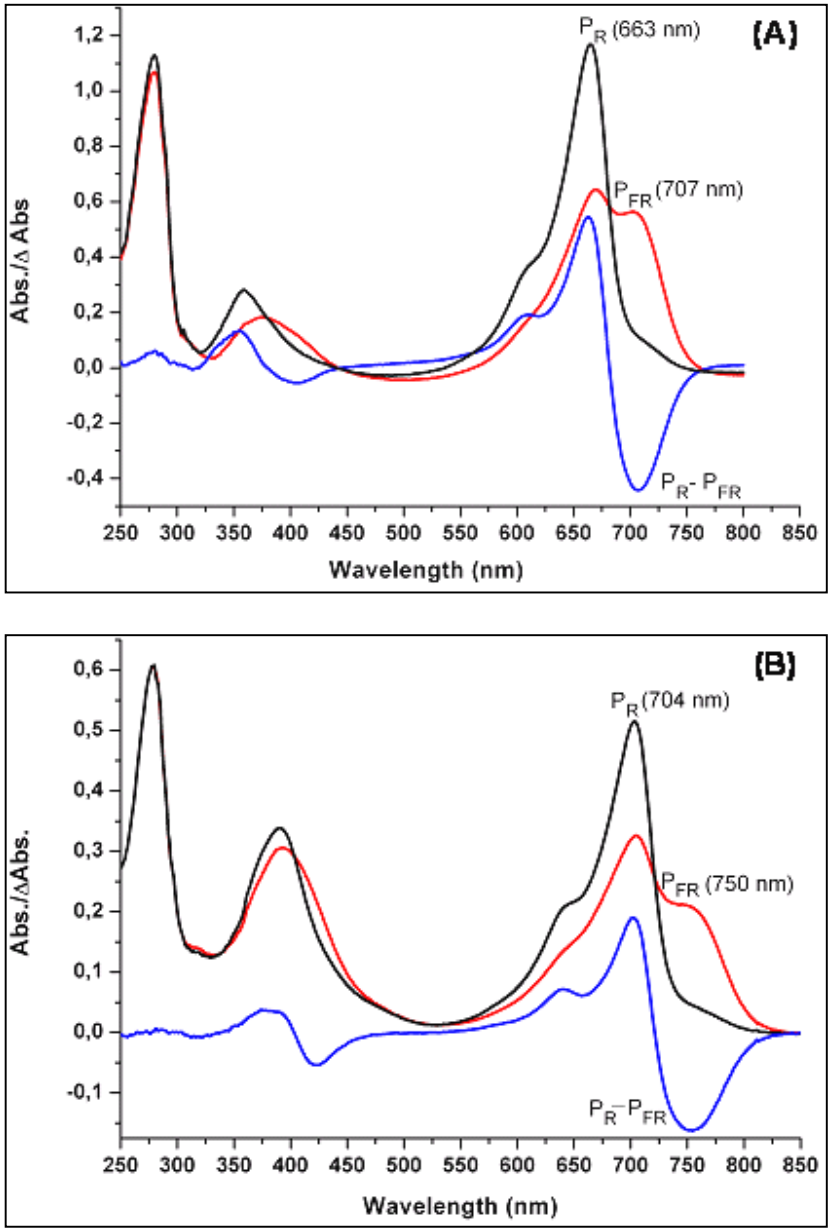

Figure 19: UV/VIS absorption spectra of full-length CphA and CphB: Typical UV/VIS spectra of (A) CphA and (B) CphB expressed in *E. coli* and reconstituted with PCB/BV, after His tag affinity purification and sample concentration. Both proteins exhibit the characteristic absorption band at 663/704 nm (P_R-form, black spectrum) and the photoinducible bathochromic shift (λmax = 707/750 nm) after illumination with red light, indicating the formation of the P_{FR} form (red spectrum). The difference spectra (blue spectrum) were used to determine the protein concentration by

calculating between the P_R and P_{FR} absorption maxima. The spectra were recorded in quartz cuvettes after irradiation for 1 min for CphA and at least 2 min for CphB, which yields maximal photoconversion with the respective light quality.

Table 8: The P_R and P_{FR} absorbance maxima of full length- and truncated CphA/CphB constructs from *Calothrix*.

	CphA		CphB	
Constructs	**P_R λ_{max}** (nm)	**P_{FR} λ_{max}** (nm)	**P_R λ_{max}** (nm)	**P_{FR} λ_{max}** (nm)
Full length	663	707	704	750
PAS-GAF-PHY	663	707	704	750
PAS-GAF	658	698	702	746

After the reconstitution with PCB, A-PGP showed photoreversibility with a P_R maximum of 663 nm and a P_{FR} maximum of 707 nm (Figure 20A). Similarly, reconstitution of B-PGP with BV showed P_R maximum of 704 nm (in accordance to the Table) and P_{FR} of 750 nm (Figure 20B). The difference spectrum was used to calculate the amount of protein which was found to be ca. 1-2 mg per liter culture of CphA-PGP and 6-10 mg for CphB-PGP. Removal of the signaling HK domain from CphA and CphB had virtually no effect on the absorbance maxima and the relative intensity of the P_R and the P_{FR} forms. It can thus be concluded that a construct comprising the PAS, GAF and PHY domains is sufficient to preserve the spectral properties of bacterial phytochromes. This finding is quite in accordance to the finding for plant phytochromes, and it has been demonstrated for other cyanobacterial phytochromes: Hughes and coworkers reported that C-terminally truncated Cph1Δ2 (amino-acids 1 to 514) from the cyanobacterial *Synechocystis* PCC6803 showed spectral parameters very similar to full-length Cph1 with similar λ_{max} values of 655/707 nm [49]. Also, C-terminally truncated AphA (1-490) from the cyanobacterium *Anabaena* sp PCC7120 was reported to have characteristics in the visible and near UV regions similar as the full-length [80]. In plant phytochrome

PhyA of oat, the removal of the C-terminal half yields a phytochrome fragment with spectral (and kinetic) properties virtually identical to those of the full-length protein, whereas any removal of amino acids form the N-terminal part of a plant phytochrome results in a pronounced hypsochromic shift of the P_{FR} absorption maximum [145;146].

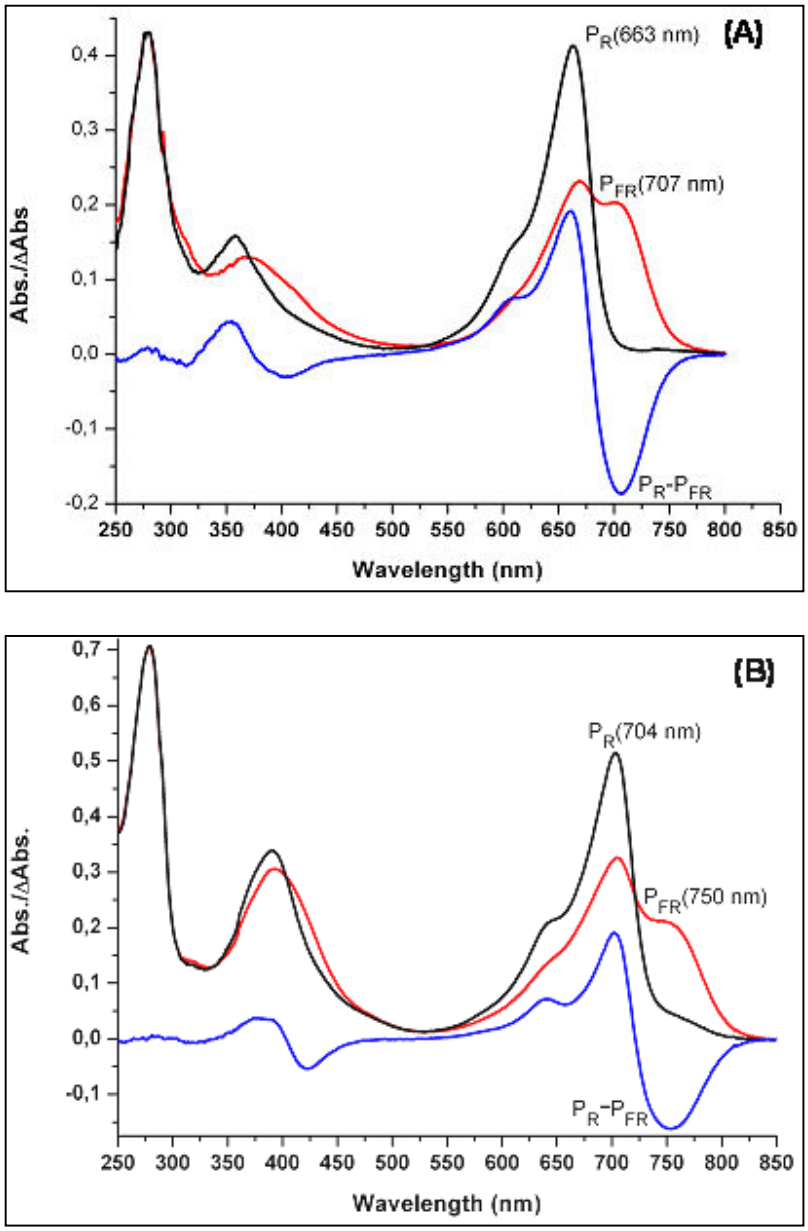

Figure 20: UV/VIS absorption spectra of (A) CphA-PGP and (B) CphB-PGP expressed in *E. coli* and reconstituted with PCB and BV, respectively. Both proteins exhibit the P_R form at 663/704 nm (black spectrum) and the P_{FR} form with bathochromic shift (λ_{max} = 707/750 nm) after illumination with red light (red spectrum); the difference spectra (ΔP_R-P_{FR}) is given in blue.

After extensive irradiation with red light to obtain a maximal formation of P_{FR}, dark reversion was checked at room temperature (20°C) by measuring spectra at regular time intervals. In these truncated proteins, even after 14 days no clear P_{FR} to P_R dark reversion was detected, but the percentage of degradation of CphA-PGP and CphB-PGP were found to be ca. 4.3% and 2%, respectively (Table 9). In case of full length CphA, Jorissen (2001) reported a degradation of 18% after 14 days [147].

Table 9: Percentage of degradation of CphA-PGP and CphB-PGP

	ΔAbs (t = 0)	ΔAbs (t = 14 days)	Degradation
CphA-PGP	0.092	0.088	4.34%
CphB-PGP	0.311	0.305	2%

CphB-PGP had shown 0.155 A after 30 days of incubation which is a degradation of 50%. The degradation was assumed to be due to the precipitation of the purified protein.

The removal of the HK and in addition also of the PHY-domain from either CphA or CphB causes significant changes in the absorption properties of these truncated proteins. The reconstitution with chromophore using both crude and purified proteins of CphA-PG and CphB-PG was very slow in comparison with PAS-GAF-PHY partners or full length proteins. The crude lysate obtained for these domains was incubated with their respective chromophores overnight for maximal assembly (the chromophores were always added in 4-10-fold molar excess). There was an increase in the amount of reconstitutable proteins with increasing time of incubation. The spectrum was measured at different time intervals to assess the binding, which is shown in Figures 21 and 22 of CphA-PG with PCB and CphB-PG with BV, respectively. This slow assembly maybe a result of the truncation of the PHY domain that was formerly shown to stabilize the chromophore in its binding cleft [52].

The deletion of the PHY domains caused a blue-shift of the P_R and P_{FR} absorption of CphA (λ_{max}= 658 and 698 nm for P_R and P_{FR}, respectively), but the photoreversibility was fully maintained (Figure 21). In case of CphB-PG, the P_R form of this

chromopeptide remained nearly unchanged (λ_{max} = 702 nm), when compared to the extended PAS–GAF–PHY protein (λ_{max} = 704 nm). The P_{FR} absorbance was slightly hypsochromic (λ_{max} = 746 nm), but has lost practically all its intensity (Figure 22). This finding clearly indicates a different interaction between domains in the typical phycocyanobilin-binding and the biliverdin-binding phytochromes. Similar difference spectra can be obtained in plant phytochromes, where the 39-kDa fragment recombinant chromoprotein shows an only slightly modified P_R peak, but a very broad, unstructured P_{FR} form with a reduced thermal stability and a rapid thermal reversion into the P_R form upon the removal of C-terminal [145]. Karniol and group [40] have reported that the PHY-domain is important for stabilizing the functional form (P_{FR}) of phytochrome. Also for the C-terminally (PHY) truncated *Agrobacterium tumefaciens* bacteriophytochrome-*At*BphP1 (N320, N-terminal 320 aa) a normal P_R form was reported, but saturated red irradiation created only a "P_{FR} like" bleached state that rapidly reverted to P_R form. A similar effect was reported in AtBphP2 (N314, N-terminal 314 aa) upon removal of the PHY-domain. This construct failed to assume the P_{FR} ground state upon BV binding [88]. The PHY-domain, although not essential for bilin binding, is important for stabilizing the functional form and proper photochromicity [40].

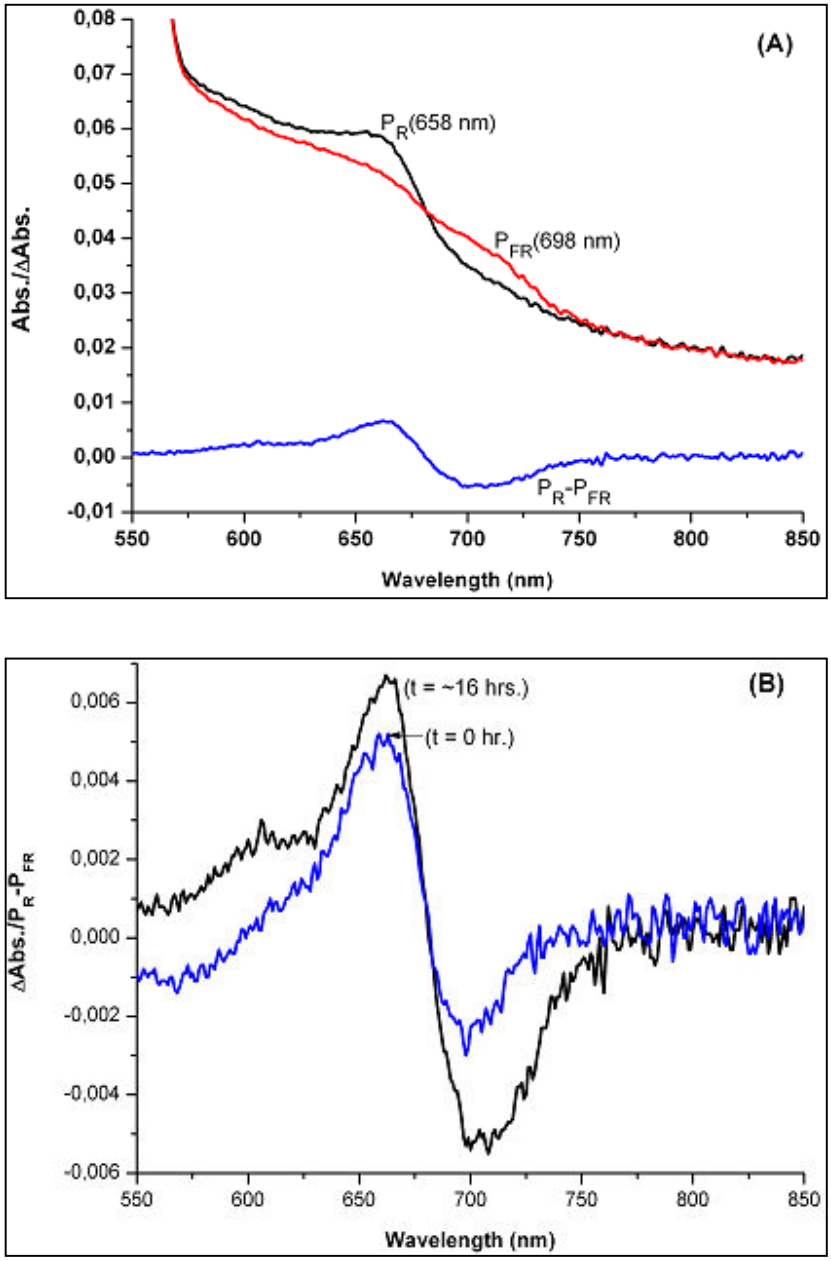

Figure 21: UV/VIS absorption spectra of *Calothrix* CphA-PG. (A) P_R, P_{FR} and ΔP_R - P_{FR} (difference spectrum) of CphA-PG, expressed in *E. coli* and reconstituted with PCB. (B) Difference Spectrum (ΔP_R - P_{FR}) of CphA-PG at different incubation times with PCB at 0 hr (blue spectrum) and after overnight incubation (~ 16 hrs) with PCB (black spectrum); no further chromophore incorporation was observed after that time period.

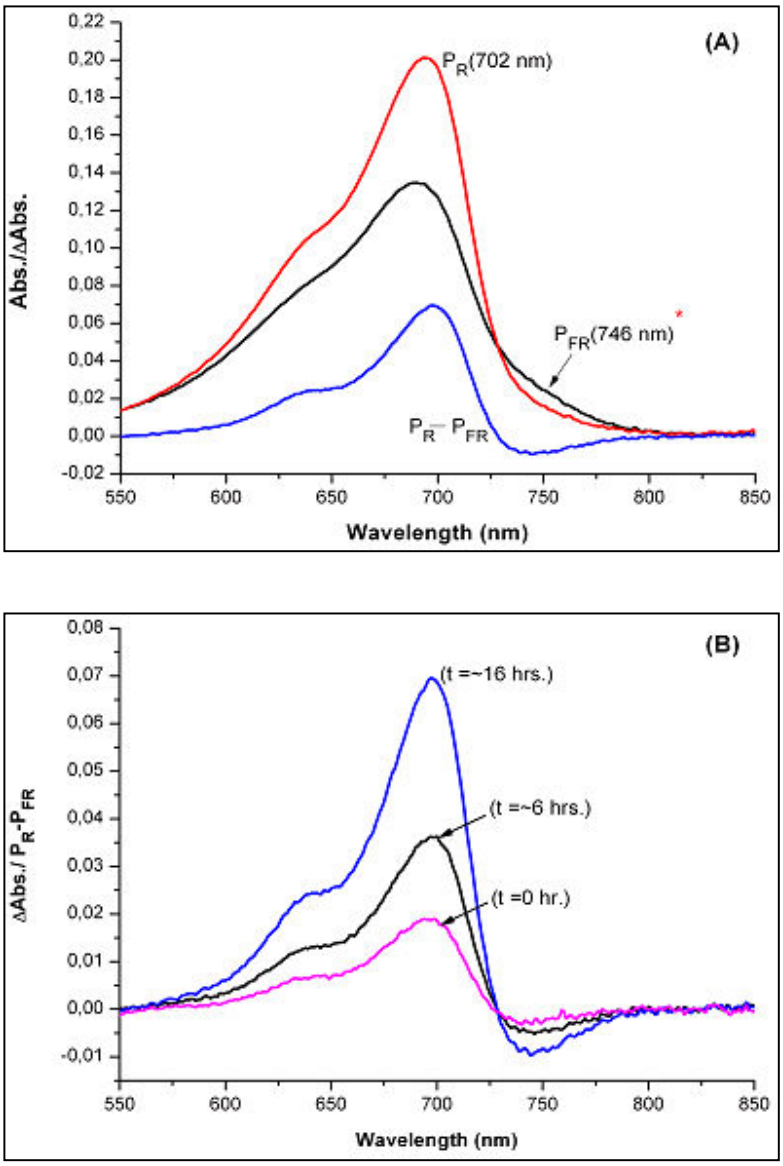

Figure 22: UV/VIS absorption spectra of *Calothrix* CphB-PG. (A) P_R, P_{FR} and ΔP_R - P_{FR} (difference spectrum) of CphB-PG expressed in *E. coli* and reconstituted with BV. (B) Difference Spectrum (ΔP_R - P_{FR}) of CphB-PG at different incubation times with BV at 0 hour (magenta spectrum), 6 hours (black spectrum) and after overnight incubation (~ 16 hrs) (blue spectrum); no further chromophore incorpration was observed after this time period.

The phytochromes CphA and CphB bind different chromophores (PCB; CphA, BV: CphB) at different positions (PCB in GAF and BV in PAS). After irradiation with red/far-red light, CphB-type phytochromes exhibit bathochromic shift of roughly 50 nm for both (P_R and P_{FR}) forms in comparison to PCB-binding CphAs. It raises the question whether it is meaningful at all to compare these two proteins. The inspection of the BV-binding bacteriophytochrome structure, e.g., the 35 kDa PAS-GAF bi-domain fragment from *Deinococcus radiodurans*, *Dr*BphP reveals as chromophore-binding amino acid Cys-24 in the PAS domain [84]. The three dimensional structure of the PCB-binding cyanobacterial phytochrome Cph1 (PAS-GAF-PHY) shows the ring A of PCB chromophore attached through a thioether link to Cys-259 in the GAF domain. The chromophore adopts a ZZZssa conformation in P_R state of both phytochromes.

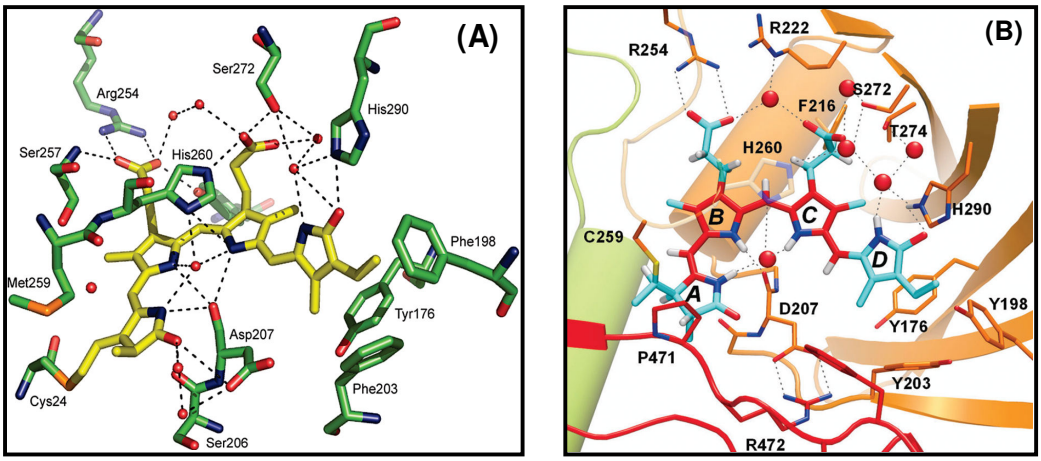

Figure 23: Three-dimensional structures of phytochromes. (A) The PAS-GAF domains of phytochrome from *Deinococcus radiodurans* in its P_R state (PDB code number 209c), showing the dense network of hydrogen bonds between several important amino acids of the protein and the BV chromophore (in yellow) [84]. (B) The chromophore binding pocket of Cph1 (PAS-GAF-PHY) in P_R state. (PDB code number 2VEA) [52].

The binding site of the crystallized *Deinococcus radiodurans* phytochrome PAS-GAF domains reveals strong interactions between rings A, B, and C, but does not yield a mechanism to explain how the photoisomerizing ring D might be fixed in its conformation in P_R and in P_{FR}.

The *Dr*BphP structures indicate the nitrogen atoms of pyrrole rings A, B and C being well hydrogen bonded and immobilized, especially around the C10 atom connecting rings B and C (Figure 23). Also, in case of the bacteriophytochrome *Dr*BphP, there is space for ring D to undergo a Z–to-E photoisomerization of the C15=C16 double bond.

The chromophore pocket of crystallized *Dr*BphP was clearly incomplete in working only with the PAS-GAF fragment, and omitting the PHY domain. In fact, it turned out that the PAS-GAF portion of a BV-binding phytochrome shows a modified photochemistry. The P_R form of CphB-PG (PAS-GAF) construct remained unchanged (λ_{max} ~ 702 nm) but the P_{FR} is hypsochromic (λ_{max} ~ 746 nm) and has lost practically all its intensity. Therefore, the protein from PAS-GAF domain is considered as dysfunctional upon irradiation; the P_R ground state is spectrally similar to the native protein but a stable P_{FR} does not arise after photon absorption.

The structure of Cph1 on the other hand, which has a fully functional photosensory domain (PAS-GAF-PHY) reveals a unique feature of the phytochrome structure: a long, tongue-like protrusion from the PHY domain seals the chromophore pocket and stabilizes the photo activated far-red-absorbing state (P_{FR}). The tongue carries a conserved PRxSF motif, from which an arginine finger (Arg-472 in Cph1) points into the chromophore pocket close to ring D forming a salt bridge with a conserved aspartate (Asp-207) residue. The main-chain oxygen of Asp-207 is hydrogen-bonded to the protonated nitrogens of chromophore rings A, B and C (Figure 23B). Apparently, this construction is important in P_{FR} function: mutations (D207A and D207N with E196G) which disturb the salt bridge bleach in red light without forming the typical P_{FR} peak [49]. The recently published work by Matysik et al. has characterized the course of back reaction, $P_{FR} \rightarrow P_R$ of Cph1 by characterizing P_{FR},

Lumi-F, Meta-F and P_R states [115]. First, the double bond photoisomerization forming Lumi-F occurs which is transformed to Meta-F by the release of mechanical tension. Only during this process the hydrogen bond between the ring D nitrogen (N24) and Asp207 is broken. It is assumed that this event triggers signaling. The release of Asp-207 would allow for the formation of the Asp-207/Arg-472 salt bridge connecting the PHY domain tongue to the chromophore region.

Section 3.2

3.2 *In vitro* study of a novel hybrid kinase protein (fusion of blue and red light photo-sensor domains)

For each organism, the key to adapt itself to the surrounding environment is to efficiently recognize the changing stimuli and to rapidly regulate gene expression of the cell to fit the new situations. In most cases, proteins involved in signal transduction are constructed in a modular fashion from individual domains which are input or sensor domains and output or effector domains. The input or sensory domains are sensitive to various signals such as absorption of light or binding of a chemical ligand, and output or effector domains are involved in biological activity such as catalytic or DNA binding activity [148]. A mechanism commonly found in bacteria for signal transduction pathways to sense the cellular external environment and regulate cellular functions in response to environmental signals is the two component system (TCS).

The TCS can be divided into two different types according to their sensor domains: the cytoplasmic systems and the transmembrane periplasmic systems. TCS genes are typically located within the same operon encoding two signaling proteins: a transmembrane sensor histidine kinase (HK) and a cytoplasmic response regulator (RR) [79]. The mechanism of signal transduction by TCS proteins is based on phosphotransfer reactions between histidine (H) and aspartate (D) residues in highly conserved signalling domains of the HKs and their cognate RRs. TCS proteins have a modular organization, which may give rise to highly complex structures, but the core structures and activities are maintained [149].

Recently, analysis of the *Pseudomonas syringae tomato* DC3000 genome yielded the identification of 69 HKs and 95 RRs [150]. The pathogenic *P. syringae tomato* DC3000 requires a complex array of TCS proteins to cope with diverse plant hosts, host responses, and environmental conditions.

One of the sensor proteins identified in *P. syringae tomato* is pspto_2896. This protein contains an N-terminal LOV (light, oxygen, or voltage) domain and is blue-light-activated [126;151]. Blue light perception has been demonstrated for some other bacterial species to be associated with pathogenicity [151], cellular attachement [152], and up-regulation of a general stress response [153]. Signaling proteins containing PAS domains occur in all kingdoms of life and the majority of prokaryotic PAS domains function as the sensor modules of two-component systems (TCS) [154].

3.2.1 A blue light inducible two component signal transduction system in pseudomonas syringae pv tomato DC3000.

The ORF *pspto_2896* from the genome of *P. syringae pv. tomato* DC3000 encodes a LOV protein (blue-light photoreceptor) of 534 amino acids. The *Pst*LOV protein is composed of input domains (PAS) ready to detect a broad variety of incoming stimuli, thereby activating its HK domain, which in turn activates a signal-transducing RR protein. This identifies *Pst*LOV as a two component system which is well known and precisely characterized in many other prokaryotic organisms [89]. In prokaryotes, the hybrid kinases that contain also response regulators are rare, but in eukaryotes hybrids (i.e., fused constructs) of kinase and response regulator are the common pattern.

The phosphorylation reaction with *Pst*LOV resulted in a phosphorylated full-length protein (Figure 24) [126]. To understand the different steps of phosphorylation, *Pst*LOV truncated constructs - LOV-HK protein (46 kDa) and the RR domain (16 kDa) separate – were generated and subjected to light-dependent phosphorylation assays. In both full-length and C-terminally truncated *Pst*LOV, radioactive phosphate is incorporated, but in a much higher yield upon blue light irradiation than under dark conditions. The reaction reaches a plateau for both constructs within 10 min, indicating that apparently the residual amount of illuminated sample is fully phosphorylated and the removal of the RR domain does not hinder the phosphorylation of the histidine residue in the HK domain. Addition of the RR to the

fully phosphorylated LOV-HK fragment resulted in a practically instantaneous phosphate transfer to the RR (Figure 24B).

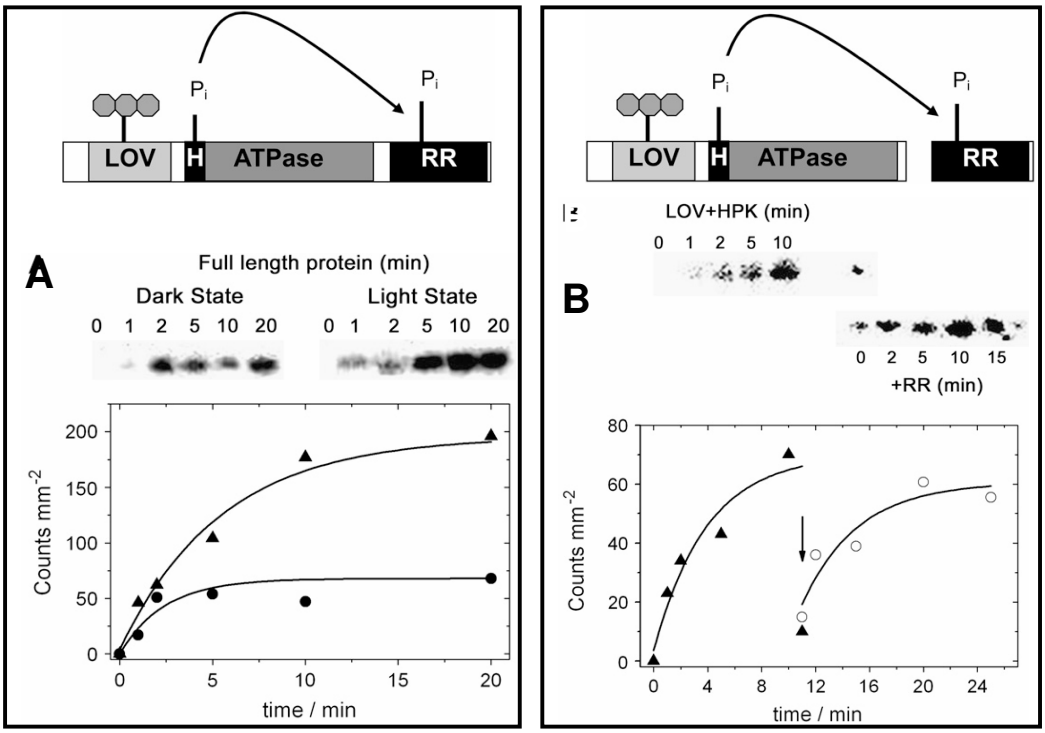

Figure 24: Phosphorylation assay of *Pst*LOV. (A) Blue light-mediated phosphorylation of the kinase domain from *P. syringae* pv. *tomato* LOV was demonstrated. Irradiation results in upregulation of the two component signal transduction system consisting of a LOV-HK-RR module full-length protein. The time course (0–20 min) indicates ^{32}P-phosphate incorporation under blue light irradiation and in the dark with preferential activity under irradiation. (B) A C-terminally truncated fragment containing solely the LOV and the HK domains. After incorporation of (radioactive) phosphate, the reaction undergoes phosphate transfer to the RR after addition to the reaction mixture. Addition of RR is indicated by an arrow during the time course of phosphate incorporation (and phosphate transfer) [126].

3.2.2 Swapping of the HK domain of a blue-light photo receptor with the HK domain of a red/Far light photoreceptor

The sequence alignment of *Pst*LOV reveals a domain architecture with a typical LOV domain (aa 33–136) containing a PAS motif which contains all signatures to bind a flavin-mononucleotide (FMN) chromophore, which is followed by a HK motif and an ATP binding domain (aa 154–389). The final part of *Pst*LOV is built as an RR domain (aa 409–534). The question is how this module adapts, when the conserved HK of a blue light photoreceptor like that of *Pst*LOV is replaced by HK of other prokaryotes or with red/far red light photoreceptor? As an approach to answer this question, the N-terminal 136 aa of the LOV protein (LOV domain) from *Pseudomonas syringae* have been fused with the HK domain of the cyanobacterial phytochrome CphA from *Calothrix* PCC7601.

3.2.3 Cloning of a fusion gene for hybrid photoreceptor expression

The N-terminal domain of *Pst*LOV which consists of a PAS motif was fused to the HK of the cyanobacterial phytochrome CphA from *Calothrix* PCC7601 as shown in Figure 25. For this purpose, the region of 426 bp of N-terminal *Pst*LOV was amplified by *Pst*LOV*Nde*Ifor and LOV142ACphA516Arev, and the 765 bp region of CphA-HK was amplified using primers LOV142ACphA516for and CphA*Xho*Irev. The Primers LOV142ACphA516for and LOV142ACphA516Arev shared a common alanine residue (Ala-142 of LOV and Ala-516 of CphA). These PCR products were taken as template for the next PCR, using primers *Pst*LOV*Nde*Ifor and CphA*Xho*Irev. This PCR product was purified and blunt-end cloned into the vector pJET1.2. The insert DNA was excised from the vector pJET1.2 by digestion with *Nde*I and *Xho*I restriction enzymes, and the linear fusion DNA was gel -purified and extracted, before ligating into the pET28a expression vector to generate the *Pst*LOVphyHK construct for expression in *E. coli* (Figure 25). The PCR primers were designed such that the N-terminal His_6 tag provided with the vector is included in the construct.

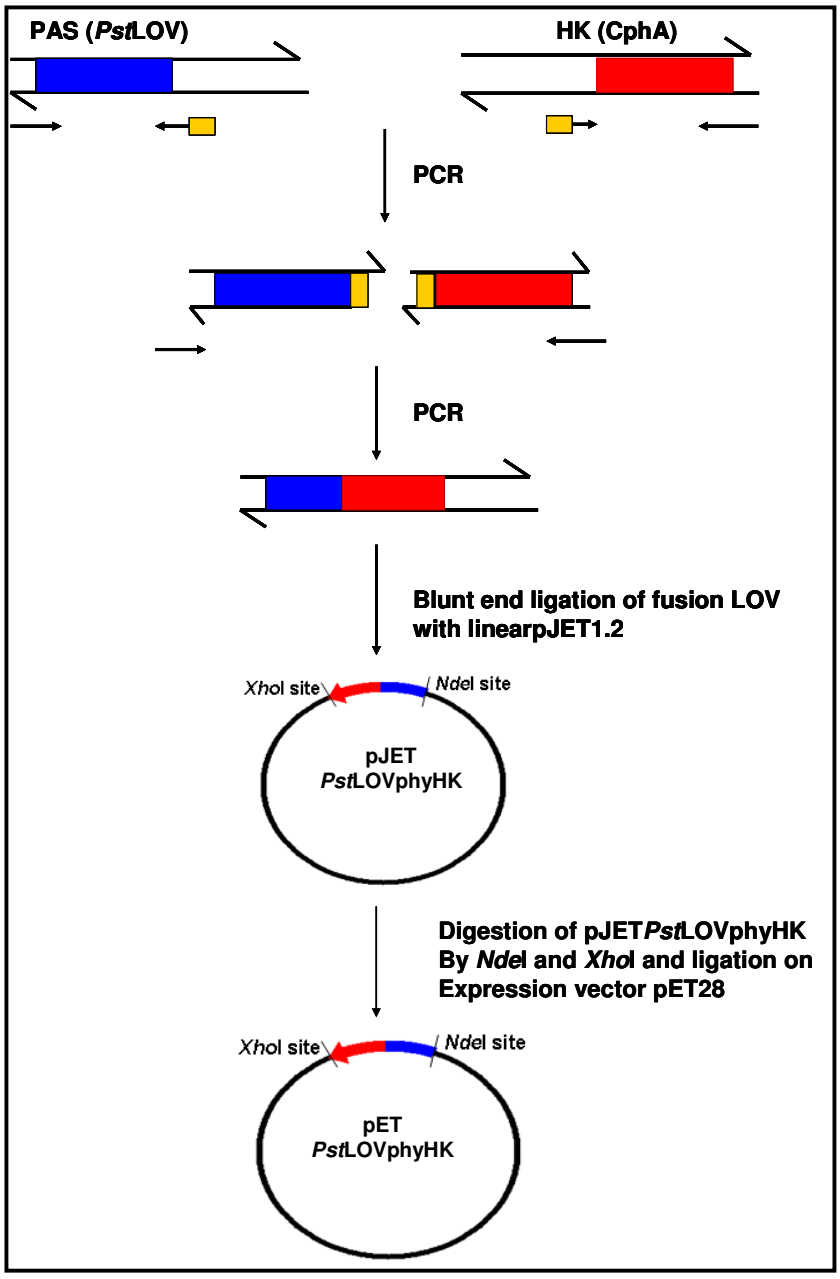

Figure 25: Schematic outline of the gene fusion using the N-terminal LOV (PAS motif) of *P. syringae tomato* DC3000 and the C-terminal part of the HK from cyanobacterial phytochrome CphA. Two genes are fused with one amino-acid in common (three base-pairs), shown as orange blocks. The fused gene was first blunt-end cloned into pJET1.2 which was confirmed by sequence determination. This clone was then digested with *Nde*I and *Xho*I, separated from the agarose gel and ligated into pET28a.

3.2.4 Expression of the hybrid protein *Pst*LOV-phyHK

The fused protein *Pst*LOVphyHK was expressed heterologously in *E. coli* BL21 DE3. The predicted molecular weight of the recombinant *Pst*LOVphyHK protein with His_6 tag at N-terminal was 46 kDa; this was confirmed by analysis of the His-tag mediated purification (Figure 26).

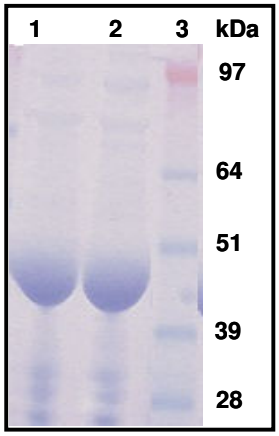

Figure 26: SDS-PAGE analysis of the fusion protein *Pst*LOV-phyHK, expressed in *E. coli* and affinity-purified, using the His tag. Lane 1: eluted material using 125 mM imidazole; lane 2: elution with 150 mM imidazole; lane 3: protein molecular weight marker, sizes (in kDa) is indicated on the right side.

The photochemical properties of the purified recombinant protein were determined with UV/VIS absorption spectroscopy. The heterologously expressed *Pst*LOV-phyHK showed a fine-structured absorption spectrum with λ_{max} = 447 nm under dark conditions, characteristic in form and position for an FMN-binding LOV domain. Blue light irradiation produced photobleaching of the absorption band in the visible region, concomitant with the formation of a short-wavelength maximum around 390 nm, indicative for the generation of a photoproduct (Figure 27A). In the dark, the photoadduct slowly reverts to the dark state, as can be followed by recording the recovery of absorbance at 447 nm. The kinetic trace can best be fitted with a single

exponential decay function, yielding an average life time (γ_{rec}) of 5503 sec (Figure 27B) which is slightly faster in comparison to native full-length *Pst*LOV (6210 sec).

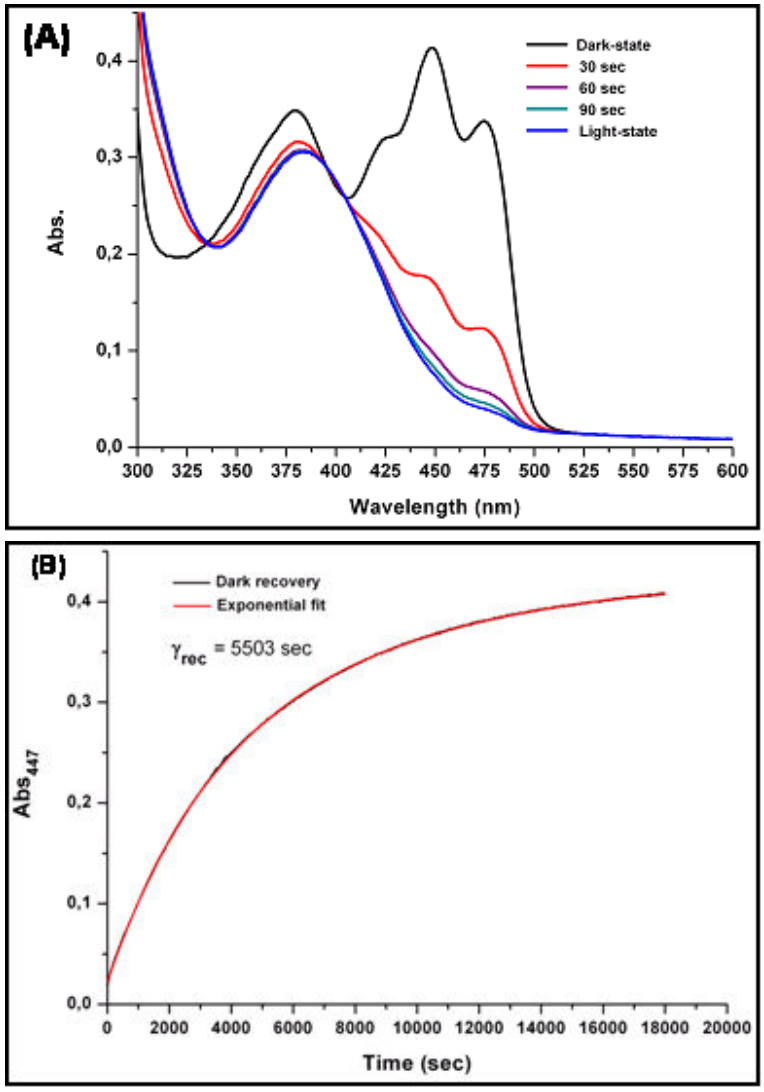

Figure 27: Photochemistry of recombinant *Pst*LOVphyHK; (A) Absorption spectra of the dark-light state; the dark state (λ_{max} = 447 nm, black spectrum) shows the characteristic three-peaked absorption band of an oxidized, protein-bound flavin. Blue spectrum: maximal generation of lit state by continuous blue light irradiation (for about 2 minutes); red, magneta and green spectra are after 30, 60 and 90 sec irradiation respectively (T = 20 ^{0}C). (B) Dark recovery kinetics of *Pst*LOVphyHK (20 ^{0}C), obtained by measuring the absorbance at 447 nm (black trace). Experimental data were fitted by a first-exponential decay function (red curve).

The results indicate that even after the domain-swapping of the HK motif of *Pst*LOV *P. syringae* pv *tomato* DC3000 vs. the HK from CphA, the protein retained the typical photochemical properties of *Pst*LOV.

Photoreceptor proteins that utilize the information "light" to elicit a physiological response are signaling photoreceptors, i.e., they induce a change in biological activity. The remarkable properties of photoreceptors to control the activity of target proteins allow their utilization even in living cells of other organisms; in case this property can stably by inserted into the genome of the host organism (or cell culture) this has been termed "optogenetics" [155]. The scope of optogenetics has recently been expanded beyond the use of naturally occurring photoreceptors by the biologically-inspired design of engineered (or synthetic) photoreceptors. There are several examples reported in the literature where light-regulated enzyme activity has been accomplished: an early application of engineered photoreceptor was the development of a light-switchable promoter using the light dependent interaction of plant phytochromes PhyA and PhyB with phytochrome interaction factor 3 (PIF3) [156]. In another approach, the bacterial phytochrome was used to furnish a red-light dependent gene-expression system by connecting the phytochrome sensor module of histidine kinase Cph1 to the histidine kinase of *E. coli* EnvZ via a common coiled-coil linker [157]. Lee *et al* [158] used a different approach to design a photoactivatable *E. coli* dihydrofolate reductase. Insertion of LOV2 into sites statistically identified to be allosterically important was used to achieve a roughly 2-fold reversible increase in dihydrofolate reductase activity upon illumination. Strickland *et al* [159] had fused together the LOV domain and TrpR (Trp repressor) domains through a shared helix. The rigidity of the helix allowed the transmission of structural changes from one domain to another. Möglich and Moffat fused the histidine kinase of *Bradirhizobium japonicum* with the LOV sensor domain of YtvA of *B. subtilis*. The fused, reprogrammed YF1 protein changes the signal specificity of the FixL protein that originally senses oxygen, to blue-light sensitivity, while retaining its catalytic efficiency [160].

Such “hybrid” photoreceptors are obtained by fusion of one or more light-absorbing sensor domains with an output or effector domain displaying the selected activity to be controlled. Two photosensor classes which are currently most widely used in fusion-based design are LOV domains and phytochromes.

Although quite recently introduced, optogenetic applications have already seen a tremendous success.

Section 3.3

3.3 Red/far red photoreceptors of *Pseudomonas syringae* pv tomato DC3000

The plant-pathogenic organism *Pseudomonas syringae* pv. *tomato* carries two genes (*pspto_1902* and *pspto_2652*) encoding putative red-/far red light sensing photoreceptors of the bacterial phytochrome type (*bphP*s) phytochromes. One of the phytochrome genes, *bphP1* (*pspto_1902*), is preceded by a heme oxygenase-encoding gene *bphO* (*pspto_1901*). Both genes overlap by four nucleotides, causing a frame shift. Heme oxygenases are involved in phytobilin biosynthesis [58]. The second phytochrome-encoding gene, *bphP*2 (*pspto_2652*), is followed by a gene encoding a canonical CheY-type RR (*pspto_2651*) (Figure 28). The *bphP2* is arranged in an operon (after 3 nucleotides) with the response regulator (*pspto_2651*). Although no obvious response regulator gene in conjunction to the phytochrom-1 could be identified, both phytochromes are clearly identified as members of the two-component system proteins.

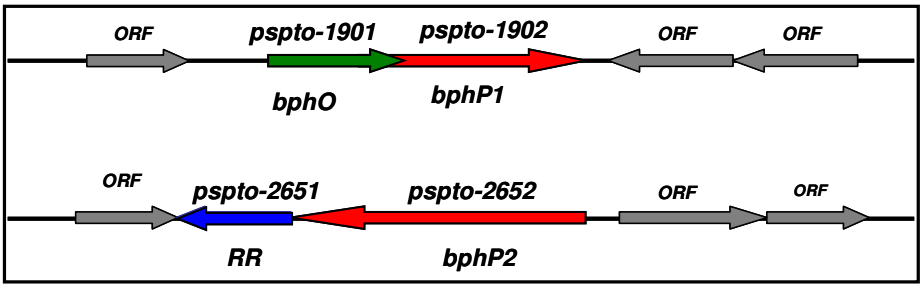

Figure 28: Operon-orientation of *P. syringae* phytochromes (*Pst*BphPs). The *PstbphP1* is preceded by *bphO* (heme oxygenase) and *PstbphP2* is followed by RR (response regulator).

Besides heme oxygenase, BphO, *in P. syringae tomato* another gene encoding a heme oxygenase, ORF *pspto_1283*, was found. This gene showed 48 % similarity with the heme oxygenase *pigA* (*Pseudomonas* iron regulating genes) of *P. aeruginosa*. The *pigA* gene, originally identified in a screen for iron-regulated genes, was shown to encode a protein with homology to the *Neisseria meningitidis* HOs

[161]. Unlike BphO, the PigA produces the unusual biliverdin isomers IXβ and IXδ (Figure 29)[60;161].

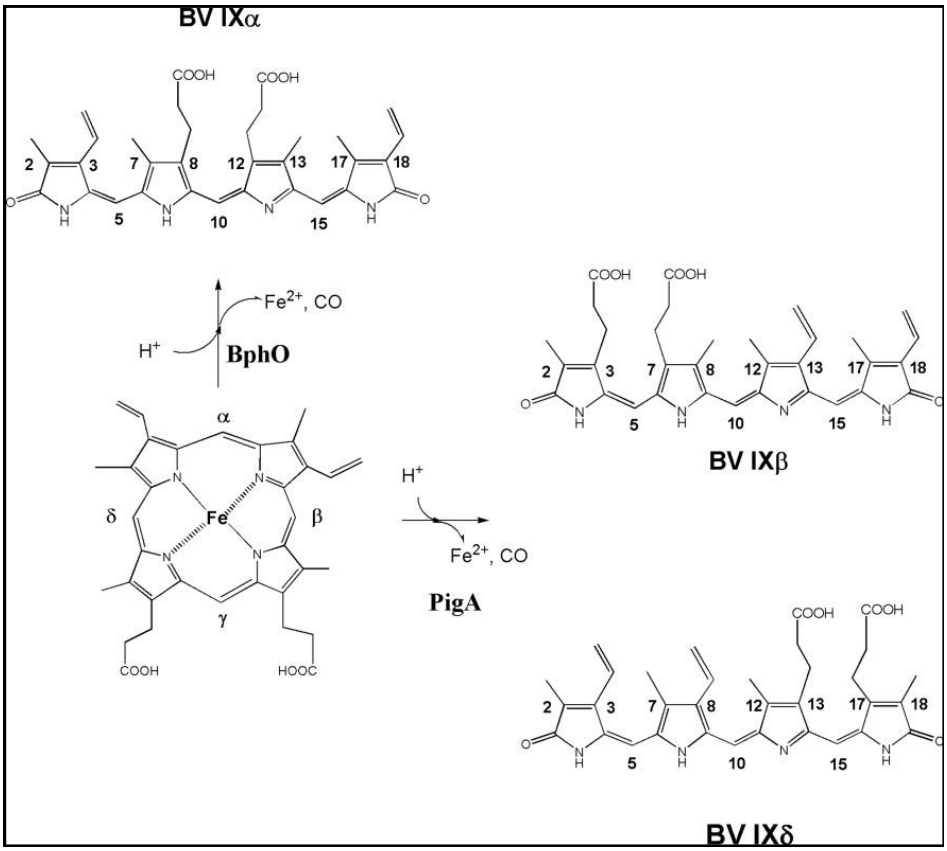

Figure 29: Reaction scheme for Heme oxygenase (HO) function. The HO cleaves the heme at the α–meso carbon position yielding BV IXa. The only HO showing a different regiospecificity is PigA from *P. aeruginosa*, which displays a β- and δ-carbon-specific HO [60].

The gene encoding *bphO* and ORF *pspto_1283* from *P. syringae tomato* were cloned and expressed to study its involvement in phytochrome in chromophore biosynthesis.

3.3.1 Cloning and heterologous expression *of PstbphO*

The full length gene *bphO* (615 bp) was amplified by PCR using oligonucleotide primers (5′-TTGGAACATATGCCGGCAAGTTTTTCACCTGTCA and (5′-TATTGGATCCTCA TAGCAGTACCTCTTGACCGT). The resulting PCR product was digested with *Nde*I and *Bam*HI and ligated into an *Nde*I- and *BamH*I digested pET14b with ampicillin resistance. For the coexpression of *Pst*bphO with phytochrome constructs, another BphO construct was generated with kanamycin resistance. *PstbphO* was cloned in pET30b between *Nde*I and *Sal*I for the Kanamycin resistance construct allowing coexpression with the phytochrome constructs. The *PstBphO* constructs in pET14 and pET30b were expressed in *E. coli* BL21 RIL (induction with 0.4 mM of IPTG at OD_{600} = 0.8 and overnight growth at room temperature). After cell-breaking and centrifugation, the soluble fraction was found to be green in color.

Purification of the heterologously expressed protein was accomplished using the His_6 tagged affinity method. The purified BphO (204 amino-acids showed one single band on SDS-PAGE, migrating at the expected molecular weight of 24 kDa. The MALD-TOF also showed the peak at the expected molecular mass (Figure 30).

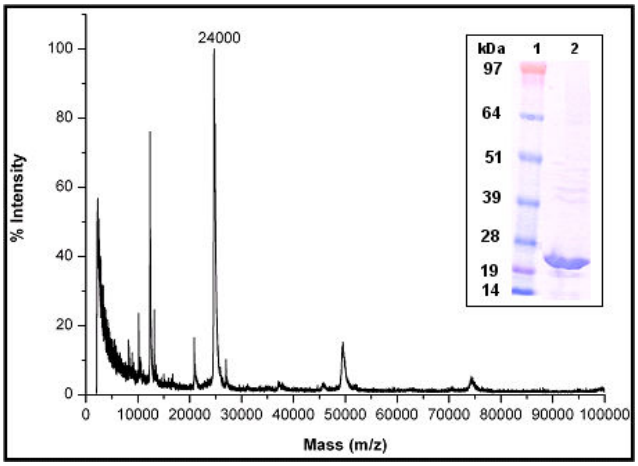

Figure 30: The MALDI-TOF MS molecular mass profile of the heme oxygenase *Pst*BphO from expression in *E. coli* after purification and concentration; inset SDS-PAGE analysis of the same protein. Both analyses confirmed the expected size of 24 kDa.

The photochemical property of the purified recombinant proteins of *Pst*BphO was determined with UV/VIS absorption spectroscopy. The spectra of purified protein of *Pst*BphO showed two peaks at 660nm and 380 nm (Figure 31).

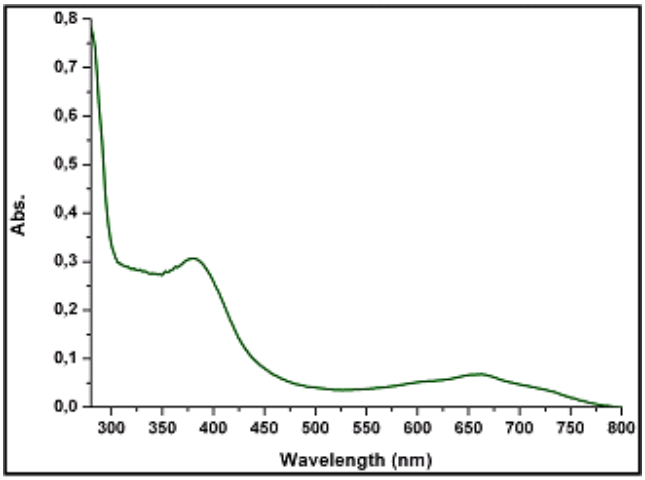

Figure 31: UV/VIS absorption spectroscopy of *Pst*BphO. The spectra showed two peaks at 660 nm and 380 nm characteristic for protein-bound biliverdin.

Heme oxygenase (HO) degrade heme molecule to yield equimolar amounts of iron, carbon monoxide (CO) and biliverdin (BV) (Figure 29).

The expression of the recombinant *Pst*BphO protein resulted in the development of green colored cells, indicating the production of BV during the recombinant expression of BphO (the absorption at 660 nm in the spectrum can be seen, Figure 30). The *Pst*BphO expressed under anaerobic conditions resulted in brown colored cells instead of the green color in aerobic culture, an indication for the requirement of oxygen for the HO reaction and the lack of BV formation. The produced BV appears to have a high affinity to the heme oxygenase, because the BphO-BV complex remained stable throughout the entire purification process at room temperature. Similar BphO-BV complexes were also produced in the expression of BphO from *Pseudomonas aeruginosa* (*Pa*BphO) which was converted to bilirubin (BR) upon addition of rat biliverdin reductase. It was reported that for this protein, *Pa*BphO, phytochrome is involved in the release of biliverdin from the BphO [60].

The 765 bp of the ORF *pspto-1283,* encode the putative heme-oxygenase PigA was cloned into pET14 and expressed it using TBY which is nutrient rich medium. Unlike BphO, it did not yield any green colored cells which indicate that the recombinant protein is not expressed.

This well characterized PigA enzyme is involved in iron re-utilization from heme under iron-limiting condition and produces the BV isomers IXβ and IXδ [161]. The unusual production of β- and δ-BV was shown to be due to a rotated setting of the heme substrate in the active site pocket of PigA in comparison to other orthodox heme oxygenases [162]. Only BV IX δ isomer was reported to bind the *Pa*BphP and yield a photoactive holo-phytochrome in *P. aeruginosa* [60].

3.3.2 Bacterial phytochromes *Pst*BphP1 and *Pst*BphP2 from *P. syringae pv tomato* DC3000

The bacterial phytochromes, *Pst*BphP1 and *Pst*BphP2, from the plant pathogen *P. syringae tomato* have the size of 745 aa and 993 aa, respectively. The two phytochromes share only 50% of identity with each other. They show the general modular architecture of a three domain-chromophore binding region (PAS-GAF-PHY) that is followed by a histidine kinase domain at the C-terminal part. The second phytochrome, *Pst*BphP2 carries an extra domain, called HWE following the signatures of conserved residues, histidine (H), tryptophan (W) and glutamic acid (E) (Figure 32A). The sequential features of both proteins identify the cysteine in the PAS domain which binds the biliverdin (BV) chromophore. In case of *Pst*BphP2, however, there are three cysteines in PAS domain (Figure 32B). The cysteine of the N-terminus of the PAS domain has been proved to be the functional position in *Agrobacterium tumefaciens* phytochrome (*Ag*BphP) [163] which is in the conserved motif.

(A)

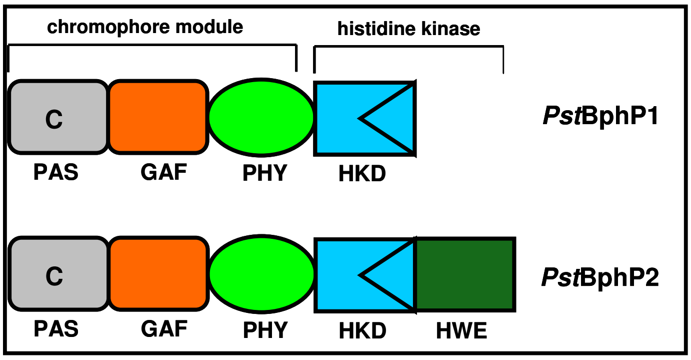

(B)

```
                                            *                       *      *
1.PstBphP1     --------MSQLDKDAFEVLLANCADEPIQFPGAIQPHGLLFTLKEPELTILQVSANVQS 52
2.PstBphP2     ---MIEHTLDANPDAALEAALAECAREPIRIPGAIQPHGVLLSVAGDPLCIEQVSANCAK 58
3.DrBphP       MSRDPLPFFPPLYLGGPEITTENCEREPIHIPGSIQPHGALLTADGHSGEVLQMSLNAAT 60
4.PaBphP         ----------MTSITPVTLANCEDEPIHVPGAIQPHGALVTLR-ADGMVLAASENIQA 47
```

Figure 32: (A) Domain structures of *Pst*BphP1 and *Pst*BphP2. Both phytochromes show a similar module organization of the chromophore-binding motif PAS-GAF-PHY

with a C-terminally positioned histidine kinase domain. *Pst*BphP2 carries also an extra HWE type of a histidine kinase. The position of the chromophore-binding cysteine is in the PAS domain. (B) The N- terminal parts (beginning of the PAS-domains) of BphPs. *Pst*BphP1 and *Pst*BphP2, phytochrome 1 and 2 from *Pseudomonas syringae tomato*; *Dr*BphP and *Pa*BphP, BphPs from *Deinococcus radiodurans* and *Pseudomonas aeruginosa*, respectively. *Pst*BphP2 has three cysteines in the PAS region (marked with *).

3.3.2.1 Cloning and heterologous expression of bacterial phytochromes *Pst*BphP1 and *Pst*BphP2

The two genes of 2235 bp and 2979 bp encoding *Pst*bphP1 and *Pst*bphP2, respectively, were amplified from genomic DNA and cloned into pET28a between the *Nde*I and *Eco*RI restriction sites. In addition, *PstbphP1* and *PstbphP2 were* also cloned in pET52b 3C/LIC vector. The *Pst*bphP1 and *Pst*bphP1 constructs in pET28 and in pET52 were then transformed into the *E. coli* strain BL21-RIL, which encodes an IPTG (isopropyl-β-D-thiogalactopyranoside) inducible copy of the RNA polymerase gene from bacteriophage T7. Transformants were grown at 37°C in TBY media and induced with 0.4 mM of IPTG at OD_{600} = 0.8. After induction the cultures were grown overnight at room temperature.

The purification of the expressed proteins again employed the N-terminal His_6 tag in pET28 constructs, whereas for the constructs cloned into pET52 3C/LIC, the C-terminal His_{10} tag was used. The purified recombinant protein *Pst*BphP1 showed the expected size of 85 kDa (Figure 33A), whereas the recombinant *Pst*BphP2 protein showed an apparent mass that was smaller than the predicted 111 kDa. The DNA sequence analysis of the plasmid encoding recombinant *Pst*BphP2 indicated clearly that the cloned gene is expected to encode a protein with 993 amino acids (Figure 33B).

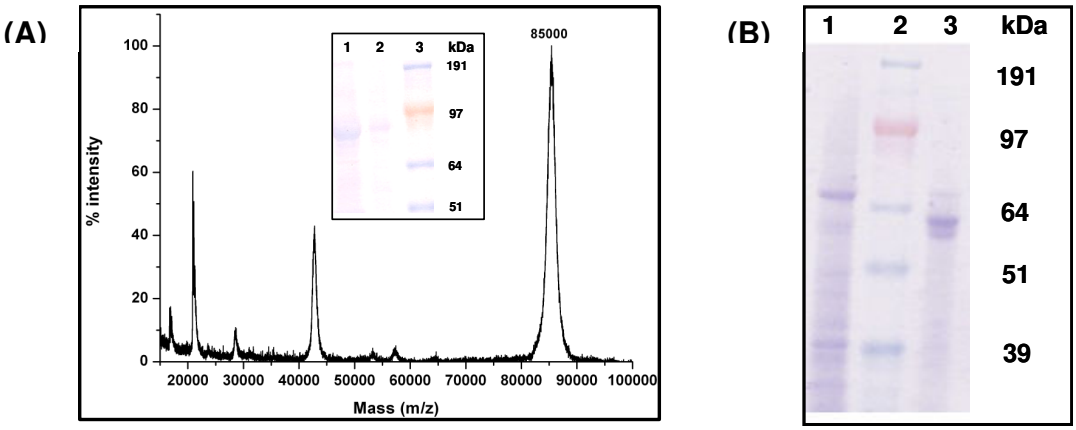

Figure 33: (A) The MALDI-TOF MS molecular weight profile of *Pst*BphP1 protein; insert: SDS-PAGE analysis. Both methods showed the expected size of 85 kDa. (B) SDS-PAGE analysis of *Pst*BphP2, indicating that the protein band migrated at a lower mass than predicted. Lane 1 and 3: *Pst*BphP2, eluted with 150 mM and 200 mM imidazole respectively; lane 2: protein molecular weight marker, sizes (in kDa) are indicated on the right side

In addition, *Pst*bphP2 was cloned into pET30b, pASK-IBA3C and pASK-IBA45 expression vectors. pASK vectors contain the *tetA* promoter/operator for a tightly regulated expression, whereas pET vectors contain a T7 promotor and T7 RNA polymerase for the induction with IPTG. The constructs in pET30b contained a His_6-tag at the C-terminal end, whereas pASK-IBA45 carries a strep-tag at the N-terminal and His_6 tag at the C-terminal end. The construct in pASK-IBA3C contained only a strep tag at the C-terminus. All constructs of *Pst*bphP2 were expressed in the *E. coli* strain BL21-RIL, by inducing with 0.4 mM of IPTG at OD_{600} = 0.8 in pET-constructs and with 0.2 µg/ml of anhydrotetracycline (AHT) in the pASK vectors at OD_{600} = 0.6. After induction the cultures were grown overnight at room temperature.

3.3.2.2 Photochemical properties of phytochromes from *P. syringae tomato*.

The photochemical properties of the purified recombinant phytochromes were determined with UV/VIS absorption spectroscopy after assembly with the chromophore, by irradiation with red and far-red light. The ground state of the proteins consisted of the red-absorbing P_R form, which upon irradiation generates a mixture of the two photoreversible forms, P_R and P_{FR}. These experiments could be performed only with *Pst*BphP1 which formed upon incubation with BV a photoactive chromoprotein with the expected P_R absorption band and also, to a lower extent, an absorption typical for the P_{FR} form. A dark incubated sample or upon with irradiation with 780 nm showed a maximal absorbance at 700 nm for the P_R form that upon irradiation with light of 655 nm could be converted into a 750 nm P_{FR} absorption band. The spectral analysis showed that only a small fraction of the protein could be converted by irradiation with red light into the P_{FR} form (Figure 34), which is probably due to a strong overlap of both forms.

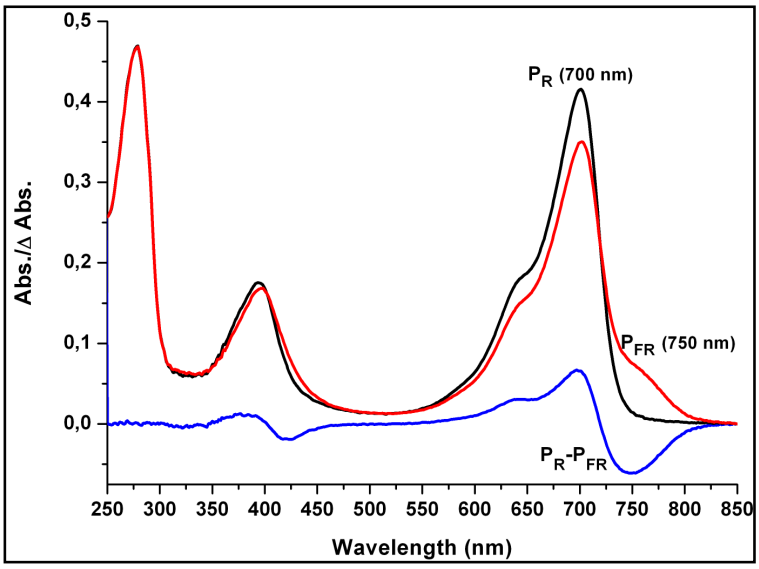

Figure 34: UV/VIS absorption spectra of *Pst*BphP1 expressed in *E. coli* and reconstituted with BV. The protein exhibits the P_R form at 700 nm (black spectrum) and a P_{FR} form with a bathochromic shift (λ_{max} = 750 nm) after illumination with red light (red spectrum); the difference spectra (ΔP_R-P_{FR}) is shown in blue.

The incubation of *Pst*BphP2 with BV yielded only minute amounts of a chromoprotein, and very little photochemistry could be initiated upon irradiation although a comparison of the primary sequences shows all essential residues for antibiotics agar plates and grown in TBY medium to an OD_{600} of 0.8. All expressions were induced at room temperature by addition of IPTG to a final concentration of 0.4 mM or 0.2 µg/ ml of anhydrotetracycline (in case of *Pst*BphP2 in pASK-IBA45) and growth was continued for 10-16 hrs. The co-expressed proteins were purified using N- or C- terminal His_6 /His_{10}-tag or strep tag chromophore binding for both proteins.

3.3.2.3 Heterologous co-expression of the bacterial phytochromes *Pst*BphP1 and *Pst*BphP2 with *Pst*BphO

PstbphP1 is a two-gene operon that encodes a heme-oxygenase (BphO) and phytochrome-1 (BphP). It was thus intended to investigate a potential interaction of both proteins upon co-expression, as the product of one protein (heme oxygenase), biliverdin, represents the substrate of the other (bacterial phytochrome). Accordingly, as well the bacterial phytochrome *Pst*BphP1 as also in a separate experiment *Pst*BphP2 were co-expressed with the heme-oxygenase (*Pst*BphO), either in a two plasmid approach or in an operon construct.

*Pst*BphP1 in pET28 and also in pET52 was co-expressed with *Pst*BphO (in pET14 and pET30, respectively). In case of *Pst*BphP2, the constructs generated in pET52 and also in pASK-IBA45 were coexpressed with *Pst*BphO in pET30. In addition, *Pst*BphP2 constructs in pET30 and pET28 were coexpressed with *Pst*BphO in pET14. Positive transformants were selected on appropriate

However, such experiments only reproduced the results from the expression of the apo-phytochromes: a photochemically active protein was obtained in case of the *Pst*BphP1 and *Pst*BphO coexpression (Figure 35A), and practically no photochemical activity was observed for the *Pst*BphP2 and *Pst*BphO (Figure 35B). Although *Pst*BphP1 was clearly identifies, the amount of photo-chemically active

phytochrome is relatively low in this two plasmids (*Pst*BphP1 and *Pst*BphO) expression experiment.

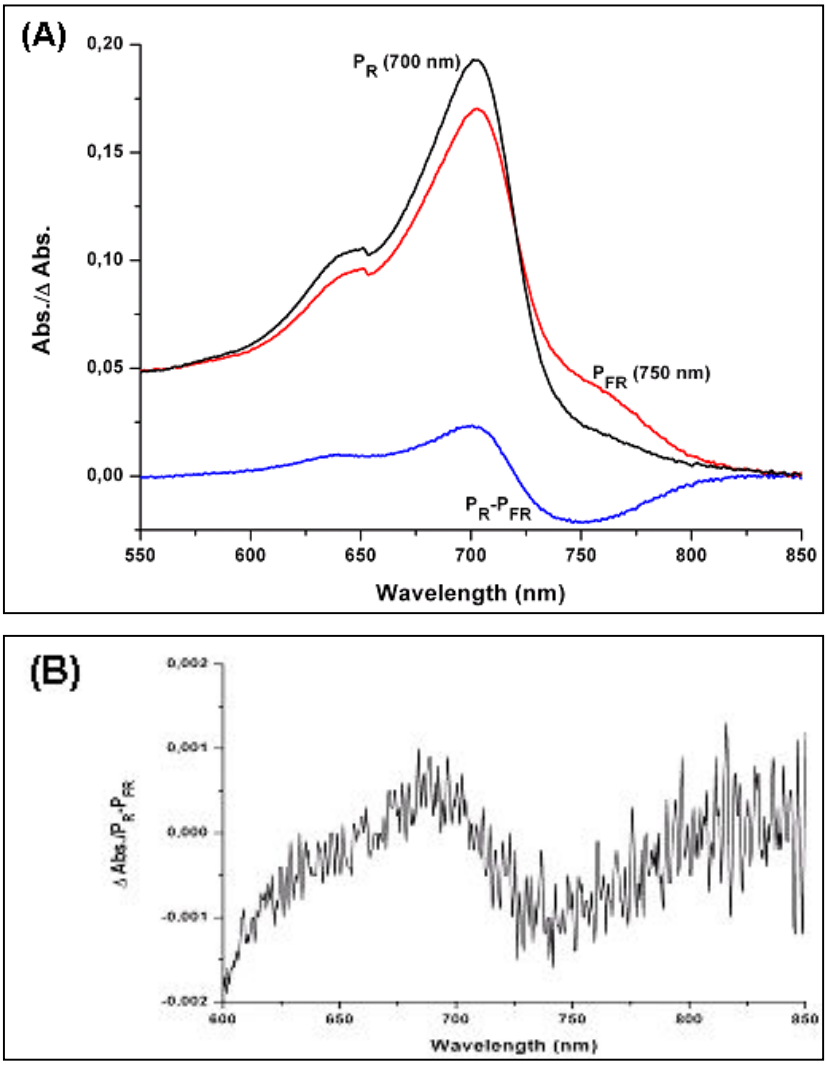

Figure 35: UV/VIS absorption spectra of *Pst*Bphp1 and *Pst*BphP2 coexpressed with *Pst*BphO in *E. coli* (using two plasmids). (A) *Pst*BphpO and *Pst*BphP1 coexpression exhibits the P_R form at 700 nm (black spectrum) and the P_{FR} form with a bathochromic shift (λ_{max} = 750 nm) after illumination with red light (red spectrum) and the difference spectra (ΔP_R-P_{FR}) in blue. (B) Difference spectra (ΔP_R-P_{FR}) of recombinant co-expressed protein of *Pst*BphpO and *Pst*BphP2.

3.3.2.4 Cloning and heterologous expression of *PstbphP1* (*PstbphO::bphP1*) operon

Following above experiments of co-expressing heme oxygenase and the bacterial phytochromes in the two-plasmid approach, it was then attempted to clone and express the existing operon of *PstbphO::bphP1*, and to generate an identical operon replacing *bphP1* by *bphP2*. The operon *Pst*bphO::bphP1 was amplified using oligonucleotides primers HOP1coexpFor and HOP1coexpRev, and cloned into an expression vector pET52 3C/LIC to get some detailed information and activity of the BphO with the phytochrome. This cloning generates an N-terminal strep-tag and a C-terminal His_{10} tag fusion protein.

The *Pst*bphO::bphP1 construct in pET52 3C/LIC was expressed in *E. coli* BL21 RIL under identical induction and growth conditions as described above. The cells collected after overnight growth showed a green color, which was also present in the soluble fraction after breaking the cells and centrifugation. Both N-terminal strep-tag and C-terminal His_{10} tag were used for purification. The SDS-PAGE analysis of the purified, co-expressed *Pst*BphO::BphP1 proteins using the N-terminal strep tag showed three bands, whereas two bands appeared for the purification using the C-terminal His_{10} tag (Figure 39; this gel will be discussed later in 3.3.2.7).

3.3.2.5 Photochemical properties of *Pst*BphO::BphP1

The photochemical property of the purified recombinant PstBphO::BphP1 protein was determined with UV/VIS absorption spectroscopy. The BphP1 protein from this operon expression showed a much more pronounced conversion of P_R to P_{FR} in comparison to the in vitro BV-assembled apo-*Pst*BphP1.

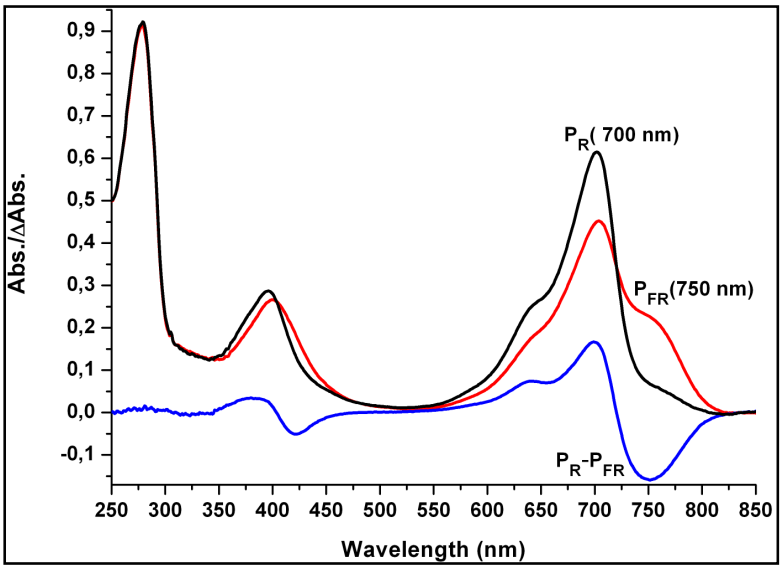

Figure 36: UV/VIS absorption spectra of operon *PstbphO::bphP1* expressed in *E. coli*, after His-tag affinity protein purification and concentration. Both forms, P_R and P_{FR}, showed the expected absorption bands at 700 nm and 750 nm, respectively.

The operon-arranged genes of *PstbphO* and *PstbphP1* overlap by four nucleotides. No strong promoter was detected in the oxygenase gene that might regulate the expression of the *Pst*BphP1 phytochrome. It was thus assumed that both genes are co-transcribed and expressed simultaneously. The expression of the operon indeed yielded both proteins, the BV-loaded heme oxygenase and the BV-assembled *Pst*BphP1 phytochrome (Figure 36). It is interesting to note that heme oxygenases usually can not be used for a production of biliverdin in significant amounts. Apparently, the reaction partner, in our case the apo-phytochrome, has to be present to release BV from the enzyme's binding site. Under these conditions, i.e., performing the operon-based expression a higher percentage of chromophore-bearing and photoreactive protein was obtained.

3.3.2.6 Cloning and heterologous expression of fused protein of *PstbphO::bphP2*

Encouraged by the improved expression of the *Pst*BphP1 from its native operon structure and also aiming to understanding the function of *Pst*Bphp2 and its capacity to bind biliverdin generated by a heme oxygenase, an attempt to create a similar fusion model protein was performed, for which several different constructs were generated (Figure 37).

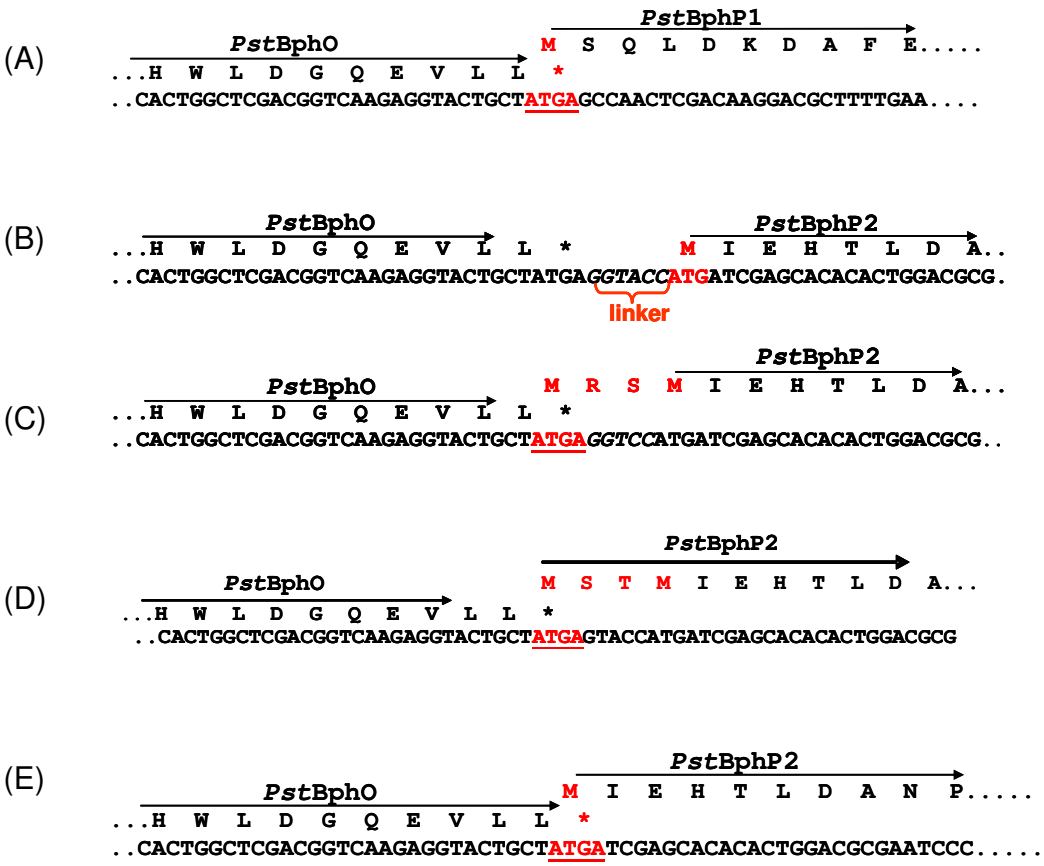

Figure 37: (A) *PstbphO* and *PstbphP1* in a native operon are arranged with an overlapping of both ORFs by four nucleotides (underlined). B, C, D, and E are different constructs for fusions of *Pst*BphO::*Pst*BphP2. (B) Construct made by fusion of the 3' *Kpn*I site (linker) of *bphO* with 5' *Kpn*I site (linker) of *bphP2*. Arrows denote the open reading frames in the construct. Both reading frames are separated by 6

nucleotides and have their own start and stop codon. (C,D) Constructs made by deletion of one nucleotide in the *Kpn*I site (linker) of BphO with 5' *Kpn*I site (linker) of BphP2. This step changes the reading frames of both BphO and BphP2. The linker has a start codon fused with the BphO stop codon, giving a similar fusion as in the original BphO::BphP1 arrangement; the actual start codon of BphP2, however, is shifted by six nucleotides to the 3'-direction (after linker). (E) Construct made by fusion of BphO::BphP2 exactly as in the case of the native BphO::BphP1 arrangement in the *P. syringae* DC3000 chromosome.

All the generated constructs were expressed in *E. coli* strain BL21-RIL under conditions described above. The collected cell-pellets (of overnight grown cultures) and the crude lysate after breaking the cells showed a bright green color in constructs B, C, and D, and a light green color in construct E which is constructed in the native operon-identical (*Pstb*phO::bphP1) manner. The crude lysate of all constructs were analysed in absorption spectroscopy before the purification, as the native operon of *Pstb*phO::*b*phP1 construct has always given two reversible forms (P_R and P_{FR}) for the holo-phytochrome even in the crude lysate. In no case of the *Pst*BphO::BphP2 operon constructs, a remarkable detection of holo-phytochrome was found. The green color of cells and crude lysate of constructs B, C, and D are evidence for a successful expression of BphO which was then also proven by absorption spectroscopy.

After the purification, the *Pst*BphO::BphP2 construct (original in arrangement to the native operon), showed a minimal amount of chromophore-bound functional holo-*Pst*BphP2 (Figure 38).

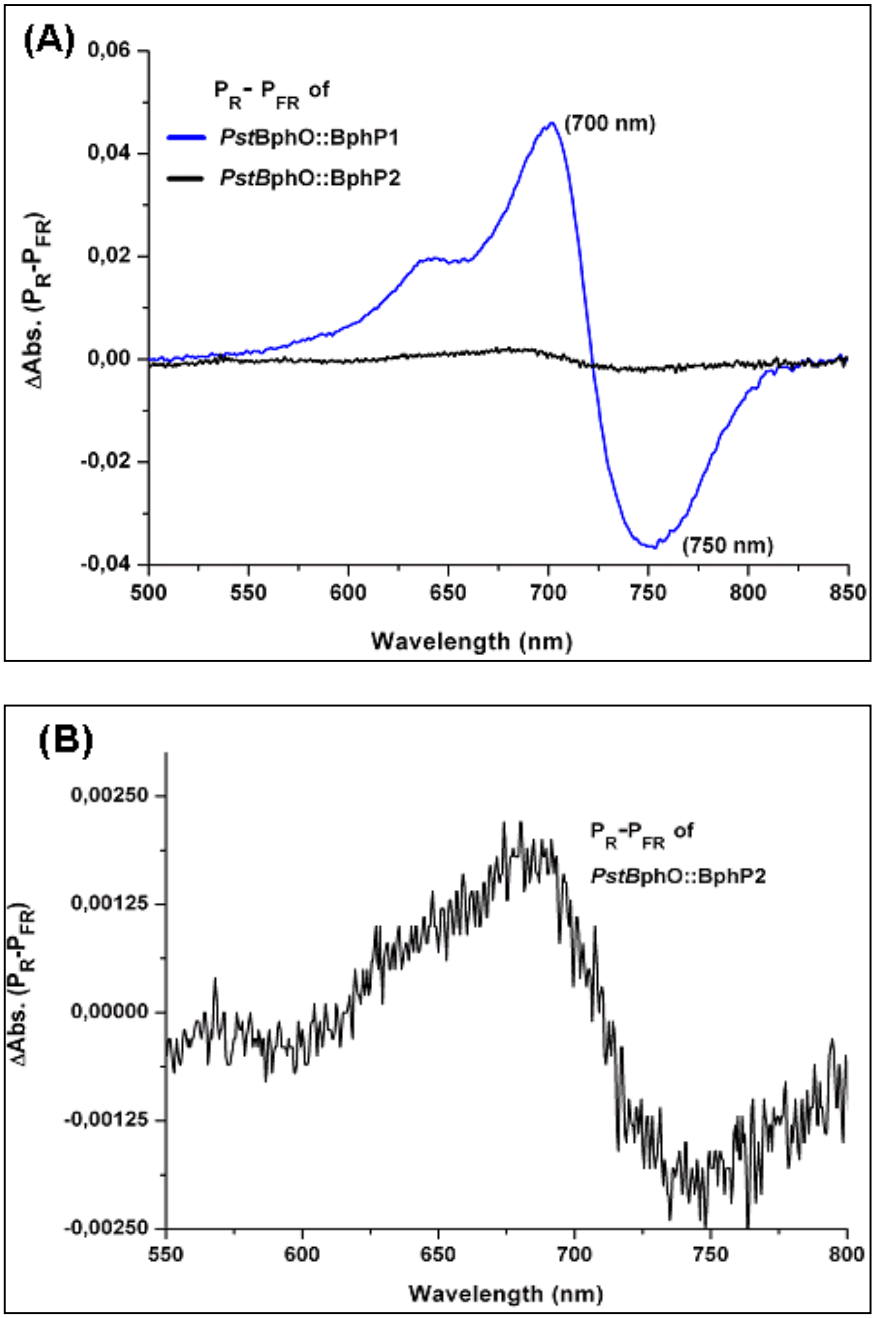

Figure 38: Difference (ΔP_R-P_{FR}) spectra of (A) operon of *PstbphO*:: *bphP1* (blue spectrum), and the identically constructed *PstbphO::bphP2* operon (black spectrum); (B) difference absorption spectrum of *PstbphO::bphP2* (from A) after His tag purification.

In addition, point mutations were performed in the *bphP2* gene to exchange the 2nd and 3rd cysteine to serine in the *PstbphO::bphP2*, but the operon still failed to produce the photoactive phytochrome-2. The nearly complete failure to generate a photoactive *Pst*BphP2 and the observation of significantly improved amount and quality in the case of the *Pst*BphP1 phytochrome is a strong indication that the heme oxygenase supports a correct folding of the phytochrome into the three dimensional structure prior to or during chromophore binding. For that, an operon-regulated expression of both partners is clearly advantageous, but not sufficient, as demonstrated by the operon generation with the *Pst*BphP2 phytochrome encoding gene. This study showed that a complex formation in case of BphO-BphP1 facilitates the release of BV but not in case of BphO-BphP2. One has thus to state that the found and identified heme oxygenase is specific in its interactions for the phytochrome-1 in *P. syringae pv tomato*.

3.3.2.7 Interactions between *Pst*BphO and *Pst*BphP1 during expression

For *Pst*BphP1, a higher yield and better photochemical properties under operon expression-conditions has been achieved, whereas a complete failure to generate a chromophore-assembled chromoprotein, was observed for *Pst*BphP2. The cloning strategy of the *PstbphO::bphP1* operon yielded a strep-tag at the N-terminal end of the *Pst*BphO and a His-tag at the C-terminal end of *Pst*BphP1. It was thus possible to employ either tag for affinity purification. Interestingly, no matter which tag was used, we detect both proteins in the eluted fractions containing the purified proteins (Figure 39). Making use of the strep tag, a nearly equal amount of *Pst*BphO and *Pst*BphP1 is detected by gel electrophoresis (Figure 39, left), whereas under conditions of His-tag purification, the recombinant phytochrome (Figure 39, right) is found in much larger amounts than the heme oxygenase. For both purification conditions, the identity of the proteins was verified by a MALDI-TOF analysis of the tryptic digests.

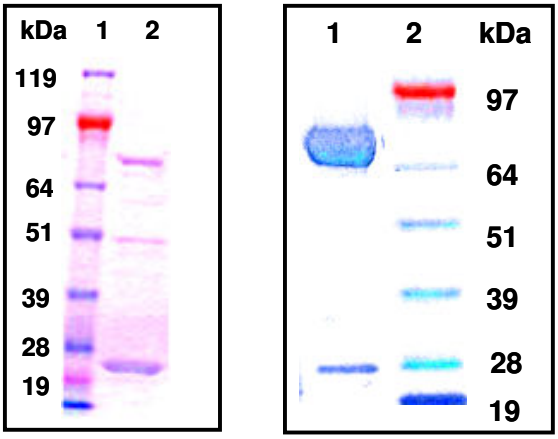

Figure 39: SDS-PAGE analysis of *Pst*BphO::BphP1 expressed in *E. coli and* purified using the strep-tag (left) and the His tag (right), after sample concentration. Lane 1 (left) and 2 (right), protein molecular weight marker with sizes (in kDa) indicated on the side.

3.3.2.8 Tryptic digestion of recombinant *Pst*BphO::BphP1 protein

The protein bands in the SDS-PAGE separations were excised manually and placed into polypropylene 96-well plates. Automated in-gel digests and sample preparation for MALDI-TOF MS was performed using the robotic liquid-handling system FREEDOM EVO-150 Base (Tecan). MALDI-TOF MS was then used to identify the subunit and peptide composition and the molecular mass of the purified protein (Figure 40). The peptides of the gel bands were compared to the predicted peptides of *Pst*BphO and *Pst*BphP1 (Figures 41 and 42). The percentage of similarities of peptides fragments from gel-digestion of protein is compared with the theoretically expected peptide fragments of *Pst*BphO and *Pst*BphP1, is given in Table 10.

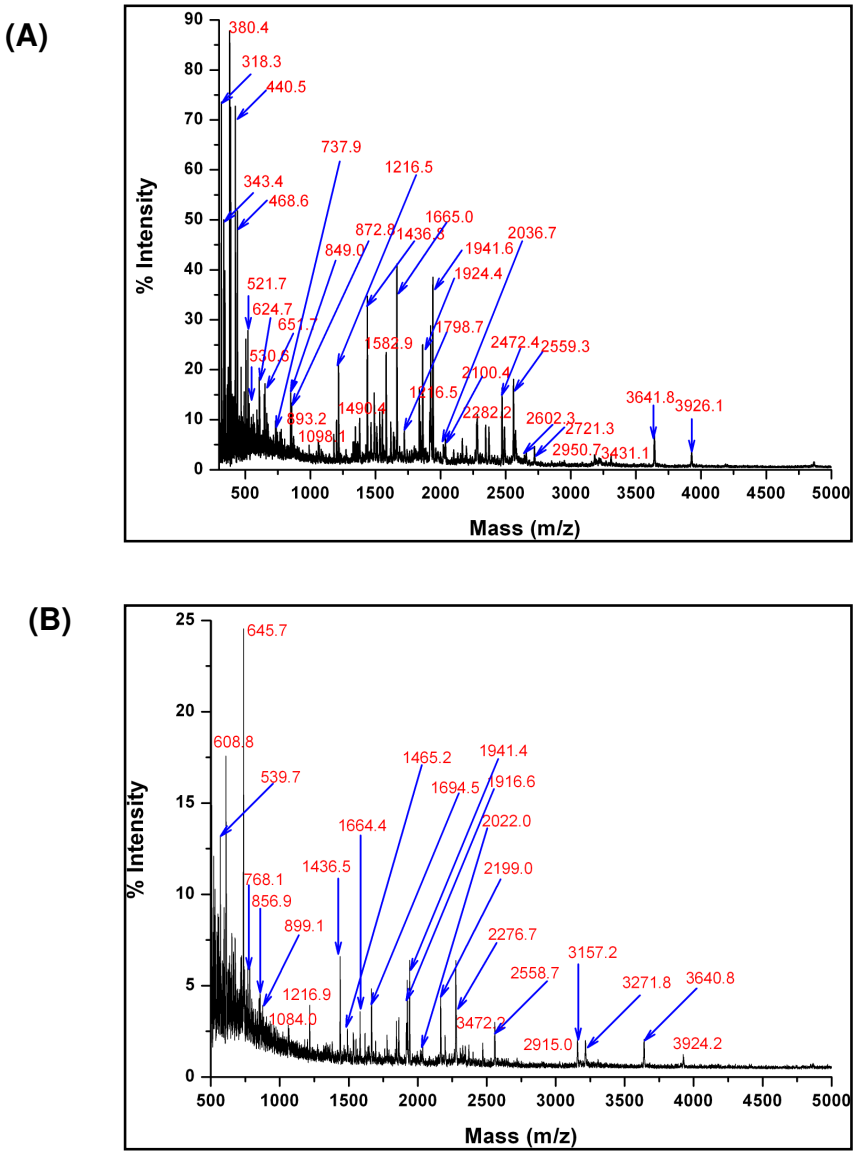

Figure 40: The MALDI-TOF MS molecular mass analysis and identification of peptides from gel-plugs of the recombinant proteins *Pst*BphO::BphP1 after gel electrophoresis and in-gel digest. (A) The uppermost migrated gel-band (from Fig. 39, right) after His-tag purification; and (B) the uppermost migrated gel-band (from Fig. 39, left) after strep-tag purification.

*Pst*BphO

MPASFSPVTP PKLIGALRAE TNQLHVQLEK RM**PFFSSVLD HALYLR**LLQA
YYGFYAPLEA ALR**DSTFMPR** ALTPDDR**IKT CVLVKDLCAL GMSEHDIRQL**
PQCTQLPITN SPGACLGVMY VLEGATLGGQ VLRREVLKRL GLDEYSGAAF
LDVYGAETGP RWKVFLNHLD AVPRGVEFTE AAAHAAHSTF ACFEHWLDGQ
EVLL

*Pst*BphP1

MSQLDKDAFE VLLANCADEP IQFPGAIQPH GLLFTLK**EPE LTILQVSANV**
QSVLGKVPDQ LAGQTLDCVL GAGWAEVIR**S TSANDSLVDV PRLLMSVEGV**
EFEALLHRSQ EALVLELEIQ DKAAQAISYS ERTGNMGRML R**QLHAAADLQ**
TLYEVSVREI QR**MTGYDR**VL IYR**FEEEGHG QVIAEASAPA MELFNGLFFP**
ASDIPEQARE LYRRNWLR**II PDANYTPVPL VPQLRPDTQQ QLDLSFSTLR**
SVSPIHCQYM K**NMGVLSSMS VSLIQGGK**LW GLISCGHR**TP LYVSHELR**SA
CQAIGQVLSL QISAMEALEV SR**QRETK**IQT LQQLHQMMAT SDTDVFDGLA
QQPQLLMDLV GATGVAIIED R**QTHCYGNCP EPSDIR**ALHT WMMAGGEPVY
ASHHLSSVYP PGEAYQTLAS GVLAMSLPKP VDNGVIWFRP EVK**QSVQWSG**
DPNKPLNLDA SDNTLRLQPR TSFEIWKVEM TGIATKWSHG DVFAANDLRR
SALENDLARQ VSKEQQAVRA RDELVAVVSH DLRNPMTVIS MLCGMMQK**SF**
SSDGPHTSRR ISTAIDTMQQ AASRMNVLLE DLLDTSKIEA GRYTITPQPL
EVSQIFEEAY TLLAPLAMDK SIEISFNAEP DIKVNADPER LFQVLSNLIG
NAIKFTPK**LG RIGVAAMSNG DEVVFTVRDS GEGIPPEQLP HIFERYWTVK**
EGNPTGTGLG LYISQGIIKA HGGELAAQSQ VGHGSEFRFT VPIAH

Figure 41: The identified peptide fragments (in blue) after gel digestion of the upper gel-band of *Pst*BphO::BphP1 from His-tag purification (Figure 39, right gel, upper gel band). The theoretically expected peptide fragments were compared with the experimentally obtained peptides which show a 63 % similarity with *Pst*BphO (upper) and 55% similarity with *Pst*BphP1 (lower).

*Pst*BphO

MPASFSPVTP PKLIGALRAE TNQLHVQLEK RMPFFSSVLD **HALYLR**LLQA
YYGFYAPLEA ALR**DSTFMPR ALTPDDR**IK**T CV**L**VK**DLCAL GMSEHDIR**QL**
PQCTQLPITN SPGACLGVMY VLEGATLGGQ VLRREVLKRL GLDEYSGAAF
LDVYGAETGP RWKVFLNHLD AVPRGVEFTE AAAHAAHSTF ACFEHWLDGQ
EVLL

*Pst*BphP1

MSQLDKDAFE VLLANCADEP IQFPGAIQPH GLLFTLK**EPE LTILQVSANV**
QSVLGKVPDQ LAGQTLDCVL GAGWAEVIRS TSANDSLVDV PR**LLMSVEGV**
EFEALLHRSQ EALVLELEIQ DKAAQAISYS ER**TGNMGRML R**QLHAAADLQ
TLYEVSVREI QR**MTGYDR**VL IYR**FEEEGHG QVIAEASAPA MELFNGLFFP**
ASDIPEQARE LYRRNWLRII PDANYTPVPL VPQLRPDTQQ QLDLSFSTLR
SVSPIHCQYM KNMGVLSSMS VSLIQGGKLW GLISCGHR**TP LYVSHELR**SA
CQAIGQVLSL QISAMEALEV SR**QRETK**IQT LQQLHQMMAT SDTDVFDGLA
QQPQLLMDLV GATGVAIIED RQTHCYGNCP EPSDIRALHT WMMAGGEPVY
ASHHLSSVYP PGEAYQTLAS GVLAMSLPKP VDNGVIWFRP EVK**QSVQWSG**
DPNKPLNLDA SDNTLRLQPR TSFEIWKVEM TGIATKWSHG DVFAANDLRR
SALENDLARQ VSKEQQAVRA RDELVAVVSH DLRNPMTVIS MLCGMMQK**SF**
SSDGPHTSR**R ISTAIDTMQQ AASRMNVLLE DLLDTSKIEA GR**YTITPQPL
EVSQIFEEAY TLLAPLAMDK SIEISFNAEP DIKVNADPER LFQVLSNLIG
NAIK**FTPKLG RIGVAAMSNG DEVVFTVRDS GEGIPPEQLP HIFER**YWTVK
EGNPTGTGLG LYISQGIIKA HGGELAAQSQ VGHGSEFRFT VPIAH

Figure 42: The identified peptide fragments (in blue) after gel digestion of the upper gel-band of *Pst*BphO::BphP1 from strep-tag purification (Figure 39, left gel, upper gel band). The theoretically expected peptide fragments were compared with the experimentally obtained peptides which show a 52 % similarity with *Pst*BphO (upper) and 49% similarity with *Pst*BphP1 (lower).

Table 10: Comparison of the molecular mass of peptides of gel plugs obtained after in gel digest and MALDI-TOF analysis with respect to peptides of *Pst*BphP1 and *Pst*BphO.

No.	Types of Purification	Gel band #	Comparision with	% of similarities of peptides
1	His-tag	1st/upper	*Pst*BphP1	53
2	His-tag	1st/upper	*Pst*BphO*	55
3	His-tag	1st/upper	*Pst*BphP1	63
4	His-tag	1st/upper	*Pst*BphO*	46
5	His-tag	1st/upper	*Pst*BphP1	51
6	His-tag	1st/upper	*Pst*BphO*	45
7	His-tag	2nd/lower	*Pst*BphP1**	63
8	His-tag	2nd/lower	*Pst*BphO	64
9	His-tag	2nd/lower	*Pst*BphP1**	50
10	His-tag	2nd/lower	*Pst*BphO	53
11	Strep-tag	1st/upper	*Pst*BphP1	49
12	Strep-tag	1st/upper	*Pst*BphO*	38
13	Strep-tag	1st/upper	*Pst*BphP1	33
14	Strep-tag	1st/upper	*Pst*BphO*	33
15	Strep-tag	1st/upper	*Pst*BphP1	41
16	Strep-tag	1st/upper	*Pst*BphO*	52
17	Strep-tag	2nd/middle	*Pst*BphP1***	18
18	Strep-tag	2nd/middle	*Pst*BphO***	38
19	Strep-tag	3rd/lower	*Pst*BphP1**	29
20	Strep-tag	3rd/lower	*Pst*BphO**	54

*molecular mass of peptides of the upper gel band of His- and strep-tag purification showed similarities with *Pst*BphO. **molecular mass of peptides of the lower gel band of His- and strep-tag purification showed similarities with *Pst*BphP1. ***molecular mass of middle gel band of His- tag purification showed similarities with *Pst*BphP1 and *Pst*BphO.

3.3.2.9 Complex formation between *Pst*BphO::BphP1

The percentage of similarities of peptides of the uppermost gel-band after His-tag purification has shown similarity of 63% and 55% with *Pst*BphP1 and *Pst*BphO, respectively (Figure 41). Similarly, peptides contained in the uppermost gel-band after strep-tag purification has shown 49% and 52% similarity with *Pst*BphP1 and *Pst*BphO, respectively (Figure 42). Other migrated gel-bands also have shown some similarities with *Pst*BphP1 and *Pst*BphO (Table 10).

The findings repesented above for the different use of either of the two tags indicates a complex formation to generate a large amount of chromophore-loaded phytochrome in a photochemically active form. The proteins eluted from the strep-tag purification reflect the current situation, as it is found with the heme oxygenase: the enzyme is complex-forming with a phytochrome molecule during chromophore-loading. On the other hand, the proteins eluted via the His tag purification also contain the complex between the heme oxygenase and the phytochrome, but in addition this fraction shows a large amount of phytochrome molecules that had already been BV-loaded and released from the complex.

Section 3.4

3.4 Effects of light on blue/red light photoreceptors inactivated mutants from *Pseudomonas syringae pv tomato* DC3000.

The *P. syringae pv tomato* strain DC3000 is both an important agricultural pathogen and a valuable model organism for studying plant-pathogen interactions [164]. This plant pathogen carries one gene, encoding a blue light sensing photoreceptor and two genes encoding proteins with red/far red light sensitivity. Following studies on the photochemial properties of these photoreceptors, a study of the regulatory function of these photoreceptor gene products requires the generation of insertional knock out mutants. As the commonly applied protocol of gene transfer by conjugation / homologous recombination is time-consuming process of low-efficiency, an alternative method was developed and employed here.

3.4.1 Generation of gene-inactivated mutant strains of *P. syringae pv tomato*

In order to analyze the regulatory role of the red-light sensor *bphPs,* the blue-light sensor pspto_2896 and *bphO* (responsible for the chromophore production for bphPs) genes in *P. syringae* pv *tomato* DC3000, we have generated five mutant strains carrying interposon cassettes within the coding regions of *bphP1*, *bphP2*, *bphO*, and pspto_2896. To generate gene-inactivated mutants, we have initially used the traditional method using suicide plasmids and conjugation, which is laborious, time consuming and of low efficiency. We have thus developed and applied a convenient and fast approach that allows creating interposon as well as point mutations of the corresponding photoreceptors genes by employing linear DNA constructs. In order to document the advantages of this novel method (at least for *P. syringae tomato*), we have compared both the novel and the traditional (conjugation) method. A mutant strain, pspto_1902 (*bphP1Δ)*, was generated by using a suicide plasmid and by direct insertion of linear, double stranded DNA. After the confirmation of positive mutants we have studied the effect of blue and red light on these mutants.

3.4.1.1 Construction of a pspto1902::Ω-Spc^r strain (*bphP1Δ*) by conjugation method

To inactivate the *bphP1* gene that encodes a red- and far-red light phytochrome-type photoreceptor, the recombinant plasmid pUC*bphP1*::Ω-Sp^r encompassing the spectinomycin cassette (Ω-Spc) within *bphP1* was generated. The construct was generated by PCR-amplifying a 3070-bp DNA fragment encompassing the target gene (*bphP1*, chromosomal positions 2077242 to 2080311). The forward PCR primer (PhP1) was designed to contain an *Eco*RI site on its 5' end that is present in the chromosome itself. The same site, *Eco*RI, was added to the rear primer (PhP2). The resulting PCR product was cloned into vector pJET1.2 generating pUC*bphP1*. An antibiotic cassette (Ω-Sp) isolated from pHP45-Ω by *Sma*I digestion was ligated into the linearized pUC*bphP1* vector (using an *Eco*RV site located within the gene) resulting in pUC*bphP1*::Ω-Spc^r. The construct pUC*bphP1*::Ω-Spc^r was hydrolyzed by EcoRI and the *bphP1*::Ω-Spc^r construct was cloned into the suicide vector pSUP202.

To generate a *P. syringae bphP1* mutant strain, the plasmid pSUP*bphP1*::Ω-Spc^r was subsequently introduced into *E. coli* S17-1 for conjugation into *P. syringae* pv. *tomato* DC3000. For conjugation, cells of *E. coli* S17-1 carrying pSUP*bphP1*::Ω-Spc^r and of *P. syringae tomato* were mixed in a ratio of 1:2. The mixture was dropped on LB agar and cells were cultivated for 24 hours at 30 ^oC for conjugation. Afterwards, the cell mass was scraped from the plate, washed with 1 ml PBS buffer, centrifuged, and resuspended in 2 ml of PBS buffer. Aliquots of 100 µl of the suspension were plated on KB-Agar containing spectinomycin (100 µg/ml) and nalidixic acid (5 µg/ml) and incubated at 30 ^oC for 48 hours. Nalidixic acid was used to select *P. syringae tomato* against *E. coli* S17-1. Exconjugants were streaked for isolation on the same medium and subsequently characterized for proper pspto_1902::ΩSpc^r insertion by PCR amplification and sequencing.

Conjugation between *E. coli* S17-1 carrying pSUP*bphP1*::Ω-Sp^r and *P. syringae* WT strain DC3000 yielded several colonies on a KB plate containing spectinomycin (100 µg/ml) and nalidixic acid (5 µg/ml). Routinely, *ca*. 200 or more exconjugant colonies

were obtained per plate. The colonies were re-streaked on KB agar containing spectinomycin (100 µg/ml) and were grown overnight at 30 °C. Since *P. syringae* colonies appear greenish caused by siderophore production [165] the colour of colonies was analyzed to identify recombinant *Pseudomonas* clones after conjugation. However, even after extended incubation at the room temperature there was no visible colour change of exconjugant colonies which would be indicative for *P. syringae* cells.

Several additional attempts of conjugation only resulted in the growth of *E. coli* S17-1 colonies carrying the suicide plasmid. After screening more than 10,000 exconjugants we finally obtained about 16 exconjugants that were *P. syringae* pv. *tomato* DC3000. Among them, ten colonies contained a single crossover event and only six were double crossover mutants as was proven by PCR amplification.

This commonly used conjugation method uses suicide plasmids, which is much more laborious, time consuming and as documented here of low efficiency. A simple and time efficient method would be most welcomed to functionally analyze many ORFs and newly identified genes.

3.4.1.2 Generation of gene-inactivated mutant strains by insertion of linear DNA in *P. syringae pv tomato*

A convenient and fast approach method was developed in this study to create interposon- as well as point mutations of the corresponding photoreceptors genes by employing linear DNA constructs. Five mutant strains of *bphP1*, *bphP2*, *bphO*, and pspto_2896 were generated using the new method. The bphO- and the pspto_2896 genes encode a heme oxygenase and a blue light-sensitive photoreceptor, respectively. The generation of these constructs that allows inactivation of different genes is described following.

3.4.1.2.1 Construction of the LOV (pspto_2896) inactivated strain (*LOVΔ*) of *P. syringae pv tomato*

The gene pspto_2896 has recently been shown to encode a regulatory protein containing a functional LOV input domain, fused to a sensor kinase and a response regulator output domain [126]. For inactivation of this gene, the recombinant plasmid pJETpstLOV::Km^r was generated. In brief, this construct was obtained by PCR-amplifying a 2044-bp region between the genome positions 3258886 and 3260929 from genomic DNA using primers LP1 and LP2. A *Pst*I restriction site was inserted at the 5'-end of LP1 while the LP2 (rear primer) was designed such that it would amplify a DNA portion containing another *Pst*I restriction site from the chromosome near the rear end of the amplification product. The amplification product was cloned into the pJET1.2 cloning vector (pJETpspto2896). The amplified region carried also a *Bst*Z17I restriction site, into which a kanamycin resistance cassette (Km^r), isolated from pBSL15 by *Sma*I digestion, was ligated, creating pJETpstLOV::Km^r.

This plasmid pJETpstLOV::Km^r harbors the kanamycin cassette in two different orientations (polar and non-polar); these clones were named pJETpstLOV::Km^{r}A and pJETpstLOV::Km^{r}B. Additionally, two point mutations were introduced in the LOV domain region of the constructs, and also the deletion of a cysteine residue (Cys70) of the chromophore-binding motif N**C**RFLQ (C in bold) in the LOV domain

was performed. Changes in the HK were performed by converting the functional (phosphorylated) histidine residue (His132) into leucine. These additional point mutations were performed to ensure the inactivation of chromophore-binding sites of the sensor domains, as it was demonstrated for several recombinant photoreceptors that the chromophore-binding domain showed photochemical activity [77], even if the C-terminally located signaling domain was modified or even truncated [166;167].

The linear DNA fragment containing pstLOV::Km^r that was used for transformation was produced by *Pst*I restriction digestion of pJETpstLOV::Km^r (Figure 43) and transformed into wild type *Pseudomonas syringae tomato* by electroporation.

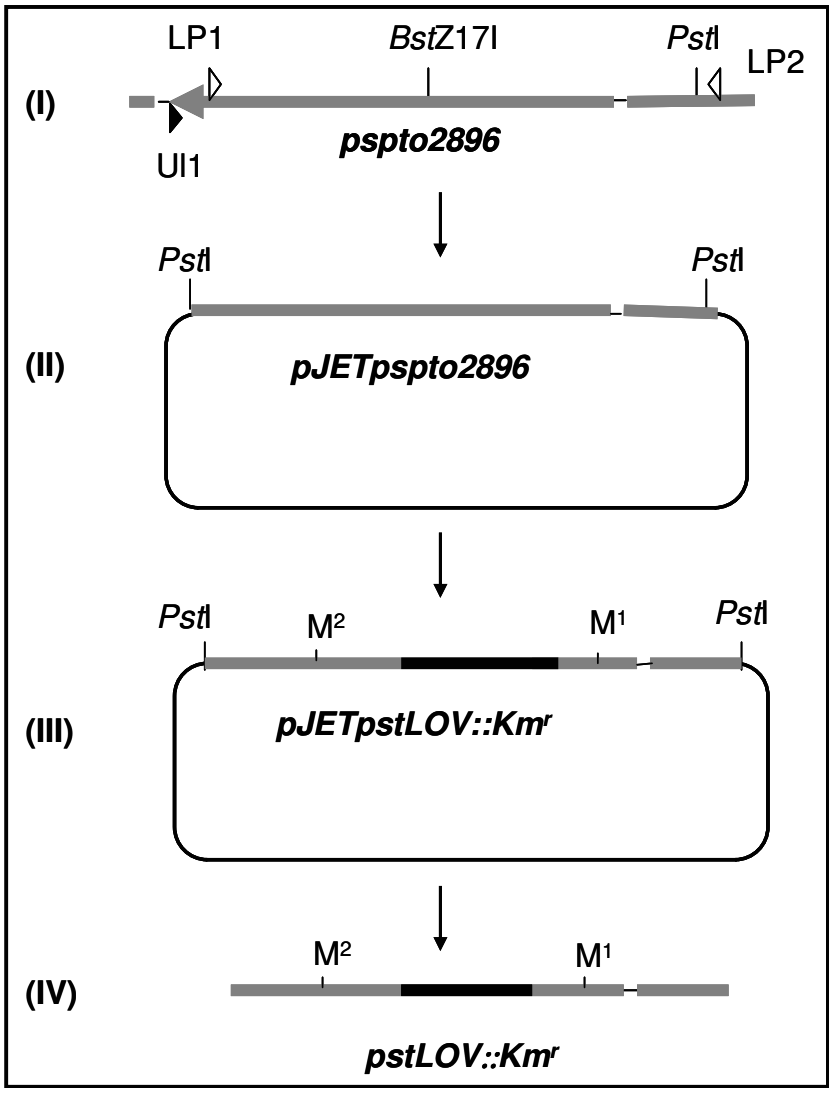

Figure 43: Strategy for the generation of mutations in *pspto_2896* in *P. syringae* pv. *syringae* DC3000. (I) *pspto_2896* and an adjacent part of DNA was amplified using LP1 and LP2, and (II) cloned into pJET1.2 creating pJETpspto2896. (III) A kanamycin resistance cassette was inserted into the *Bst*Z17I site (within the LOV domain) of *pspto_2896*. In this same constrct, the cysteine residue, responsible for the binding of FMN chromophore and photoadduct formation in LOV proteins was deleted in the construct (M^1). Similarly, a histidine residue from the histidine kinase domain was changed into a lysine residue (H132/L, M^2). These mutations were introduced separately. (IV) The construct was digested with the restriction enzyme *Pst*I to generate the linear fragment with antibiotic cassette. Primers Ul1 and LP2 were used

for verification of the mutation in the chromosome. The position of the inserted antibiotics cassette is indicated as a black bar.

This approach yielded quite a number of transformants (15 colonies) that showed capability to grow on agar plates (supplemented with Kanamycin). The positive outcome from this experiment was further confirmed by colony PCR and RT-PCR. A PCR performed with primers (Ul1 and LP2) complementary to DNA regions upstream and downstream of the target gene (not included in the knockout construct) resulted in expected products (Figure 44). The obtained PCR product was sequenced to confirm the insertional inactivation and the point mutation introduced into the functional residues.

We were also considering the possibility that the gene disruption might still allow a read-through, yielding a partial gene (product) that might provide some residual function to the transformed organism. Therefore, the inactivation of the LOV gene was confirmed by transcriptional analysis of *pspto_2896*. Reverse transcription of *pspto_2896* mRNA was carried out from total RNA, extracted from wild type and pstLOV::Km^r strains. The RT-PCR primers for the amplification of the whole gene and the selected region of 459 bp within the gene encompassing a part of the LOV domain yielded the expected product for WT *P. syringae* DC3000 (Figure 44). The *LOVΔ* (mutant strain) did not produce any amplification product in RT PCR analysis confirming the inactivation of the target gene.

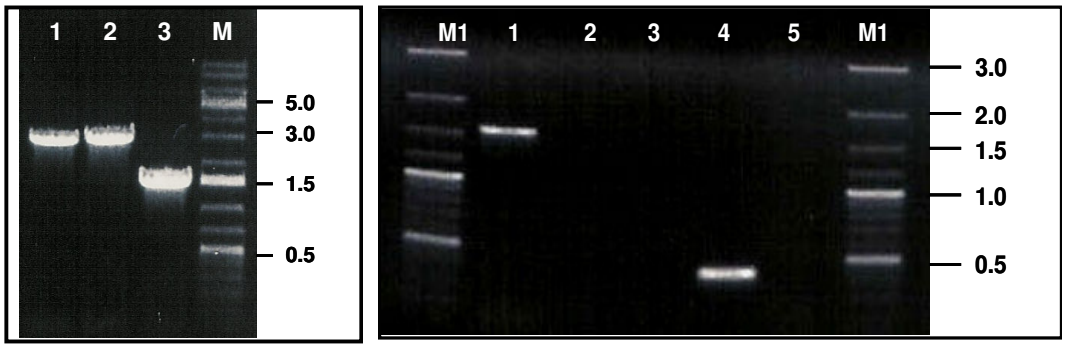

Figure 44: Agarose gel-based verification of the mutant strain using PCR and RT-PCR. (A) PCR-based confirmation of *pspto_2896* mutants. The PCR product from two different mutant strains (lanes 1 and 2) and from the wild type strain (lane 3) is shown (obtained with primers UI1 and LP2). The wild type DNA fragment exhibits the expected size of approximately 1.5 kb whereas the DNA fragment derived from mutant strains showed an additional 1.2 kb insert. (B) RT-PCR of wild type and *pspto_2896* mutant strains. Total RNA was reverse-transcribed using gene specific primers. The cDNA was amplified using *pspto_2896* gene specific primers (pspto2896_for and pspto2896_rev) (lanes 1,2,3) and a pair of primers (LOVa and LOVb) amplifying the inner region (459 bp) of the LOV domain (lanes 4,5). Lane 1 refers to the wild type (WT) strain, lane 2 shows the negative control (the reaction components were as in lane 1, but without reverse transcriptase), lane 3 shows the mutant strain (*LOVΔ*), lane 4 refers to the wild type strain and lane 5 shows the mutant (*LOVΔ*). Lane 1 (WT) showed the expected product, lane 5, *LOVΔ* (mutant strain) did not produce any amplification product in RT PCR analysis confirming the inactivation of the target gene.

3.4.1.2.2 Construction of a heme oxygenase-encoding gene mutant strain (*bphOΔ)*

Heme oxygenases degradate heme groups and generate biliverdin. Thereby, they act a central part of cellular metabolism. For a gene disrupture, the plasmid pETHO::Km^r was constructed. A 615-bp region of the *P. syringae* pv. *tomato* DC3000 genome (chromosomal positions from 2077011 to 2077625) containing the gene *pspto_1901* encoding the heme oxygenase was PCR-amplified using primers HO1 and HO2, carrying *Nde*I and *Bam*HI restriction sites, respectively. The amplicon was digested with *Nde*I and *Bam*HI and cloned into the corresponding site of pET14. The resulting plasmid, pETHO was digested with the restriction enzyme *Stu*I. Subsequently, a kanamycin resistance cassette, derived from pBSL15 by *Sma*I digestion, was inserted into the corresponding *Stu*I site of the *pspto_1901* gene in pETHO. The resulting construct, pETHO::Km^r contained the two opposite orientation of cassette, were designated as pETHO::Km^{r}A and pETHO::Km^{r}B. pETHO::Km^{r}A/B containing the Km^r interposon was digested with *Nde*I and *Bam*HI to produce a linearized DNA fragment which after gel purification was transformed into wild *type P. syringae tomato* by the electroporation method. The positive clones were confirmed by colony PCR and sequencing of the heme oxygenase gene (Figure 45).

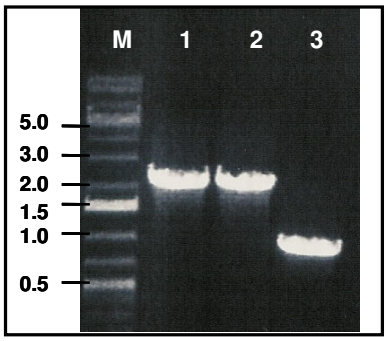

Figure 45: Confirmation of heme oxygenase mutants (*bphOΔ*) by PCR using primers HOU1 and HOU2. Lanes 1 and 2 show the mutant products, whereas lane 3 is the amplification product obtained from the wild type strain.

3.4.1.2.3 Construction of a *bphP1* (bacterial phytochrome-1) mutant strain (*bphP1Δ)*

To inactivate the phytochrome-encoding *bphP1* gene, the recombinant plasmid pJET*bphP1*::Ω-Sp^r encompassing the spectinomycin cassette (Ω-Spc) within *bphP1* was generated.

A 3070-bp DNA fragment encompassing the target gene encoding the bacterial phytochrome (*bphP1*) (chromosomal positions from 2077242 to 2080311) was amplified using the genomic DNA. The forward PCR primer (PhP1) was designed to contain an *Eco*RI site on its 5' end from the chromosome itself. The rear primer (PhP2) was designed to carry an *Eco*RI recognition site at its 5' end. The resulting PCR product was cloned into the vector pJET1.2, thus generating pJET*bphP1*. An antibiotic cassette (Ω-Sp) isolated from pHP45-Ω by *Sma*I digestion was ligated into the linearized pJET*bphP1* construct (linearization by *Eco*RV digestion) resulting in pJET*bphP1*::Ω-Spc^r. Within the recombinant plasmid, the residue (Cys16) responsible for chromophore binding and functioning of the protein was changed into Ser by point mutation. The construct carrying the gene flanked by the antibiotic cassette (*bphP1*::Ω-Spc^r) was *Eco*RI digested and the resulting linear DNA fragment was electroporated into wild type *P. syringae tomato* (Figure 46).

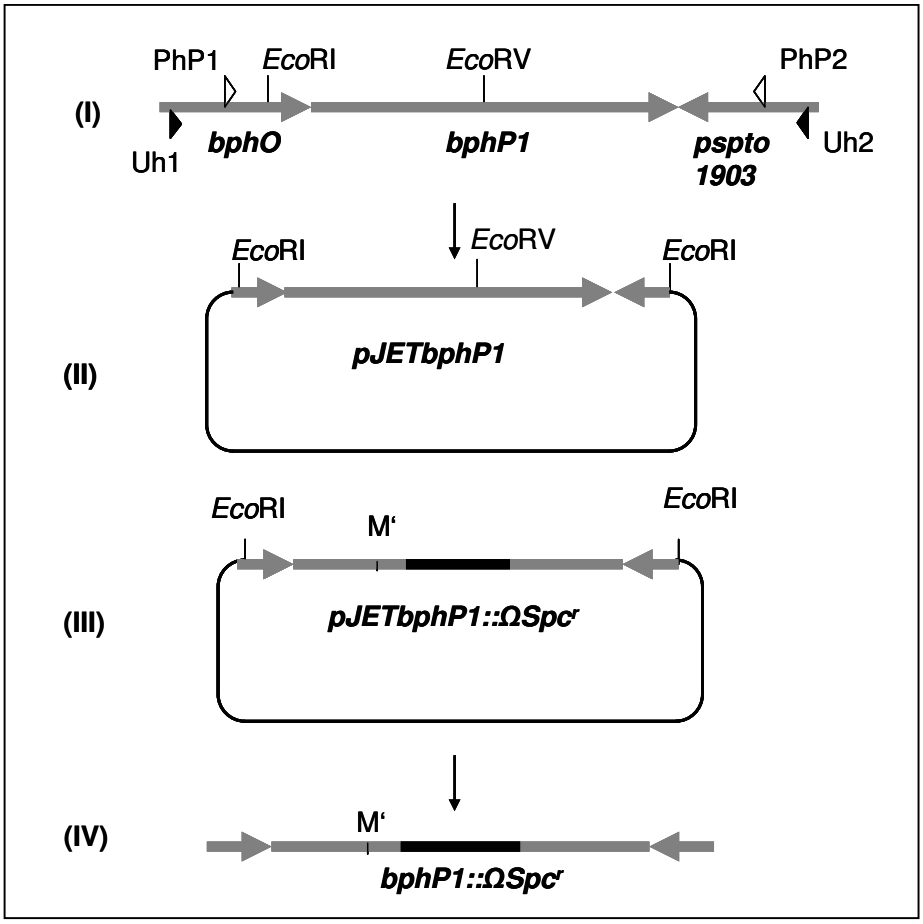

Figure 46: Strategy for the generation of a *pspto_1902* (*bphP1Δ*) mutant strain using linear DNA constructs. (I) A pair of the primers PhP1 and PhP2 was used to amplify a region of chromosomal DNA encompassing the *bphP1* gene which (II) was ligated into pJET1.2 creating pJET*bphP1*. A spectinomycin resistance (Ω-spc) cassette was introduced into the *EcoR*V site of *bphP1* (II/III). Also, (III) a point mutation (M') was introduced converting the chromophore-binding cysteine into a serine residue (C/S). (IV) The construct was digested with *Eco*RI generating a linear DNA ready for electro-transformation. Uh1 and Uh2 were the primers used for verification of the mutation in the chromosome (IV). The position of the inserted antibiotics cassette is indicated as a black bar.

Those transformants (36 colonies) that grew on spectinomycin-agar plates were further confirmed by colony PCR. A PCR performed with primers (Uh1 and Uh2) complementary to DNA regions upstream and downstream of the target gene (not included in the knockout construct) yielded the expected results (Figure 47). The obtained PCR product was sequenced to confirm the insertional inactivation and the point mutation of the functional residue

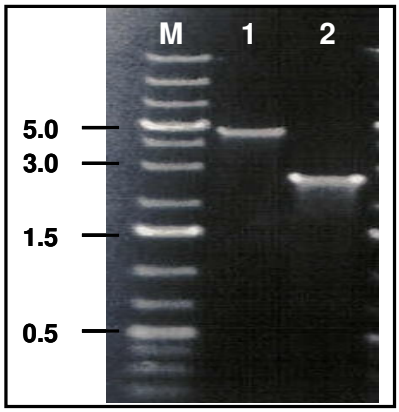

Figure 47: Agarose gel- based confirmation of the mutant strain (*bphP1Δ*) by PCR. Lanes 1 and 2 show the PCR amplification products from mutant and wild type strains, respectively, using primers Uh1 and Uh2.

3.4.1.2.4 Construction of *bphP2* (bacterial phytochrome-2) encoding gene inactivated mutant strain *(bphP2 Δ)*

To inactivate the phytochrome-encoding *bphP2* gene, the recombinant plasmid pUC*bphP2*::Gm encompassing the gentamycine cassette (Gm^r) within *bphP2* was generated.

A 3477-bp DNA fragment encompassing the target gene encoding the bacterial phytochrome (*bphP2*) (chromosomal positions from 2943323 to 2946800) was amplified using the genomic DNA. The forward PCR primer (P2pUCF) was designed to contain an *Eco*RI site on its 5' end from the chromosome itself. An *Eco*RI recognition site was added to the 5' end of the rear primer (P2pUCR). The resulting

PCR product was cloned into vector pUC18, generating pUC*bphP2*. An antibiotic cassette (Gm^r) isolated from pWKR202 by *Bam*HI digestion was ligated into the linear pUC*bphP2* construct (linearization by *Bgl*II digestion), resulting in pUC*bphP2*::Gm^r. Within the recombinant plasmid, potential residues essential for chromophore binding (Cys16, Cys47 and Cys55) were changed by point mutations to serine. The construct carrying the gene flanked by the antibiotic cassette (*bphP2*::Gm^r) was *Eco*RI digested and the resulting linear DNA fragment was ectroporated into wild type *P. syringae*. The positive mutants *(bphP2 Δ)* were confirmed by colony PCR (Figure 48) and sequencing.

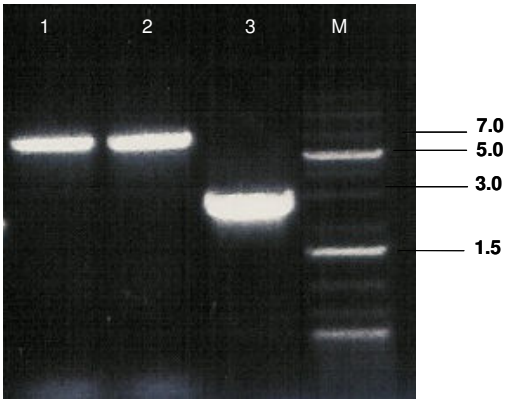

Figure 48: Confirmation of the mutant strain (*bphP2Δ*) by PCR. Lanes 1 and 2 show the PCR amplification products from mutant which is 6 kb (*bphP2* gene and Gm^R cassette) and lane 3 shows the PCR product of the wild type strain as control which is only 3 kb.

3.4.1.2.5 Construction of a double gene-inactivated mutant strain *(bphP1Δ/ bphP2Δ)*

To inactivate the phytochrome-encoding genes, *bphP1* and *bphP2*, a mutant (*bphP1Δ bphP2Δ*) was generated. For this approach, the linear DNA fragment of *Eco*RI-digested pUC*bphP2*::Gm^r, was electroporated into the *bphP1Δ* mutant strain

of *P. syringae*. The positive mutants were confirmed by colony-PCR and sequencing.

Furthermore, to inactivate all three photoreceptors, *bphP1*, *bphP2* and the LOV-encoding genes for the blue and red/far red light photoreceptor were disrupted and combined. For this approach, the linear DNA fragment of LOV::Km^r was electroporated into the *bphP1Δ bphP2Δ* mutant strain. The positive mutants *bphP1ΔbphP2ΔLOVΔ* were confirmed by colony PCR and sequencing.

3.4.2 Effect of light on photoreceptor mutants

Light is probably the most dominating external factor influencing plant growth and development, and an appropriate light environment is also required for the establishment of a complete set of resistance responses in several plant-pathogen interactions [168]. The response to changes of the light conditions involves a variety of receptors that can modulate gene expression, enzyme activity and motility of the organism. Motility changes in response to the alteration of light quality and quantity are ubiquitous features of bacteria. Three distinct types of responses to light were described [169;170]. A phototactic response involves an orientated movement of a cell towards or away from a light source. The scotophobic response (fear of darkness) is characterized by a tumbling or reversal of movement in changes of light intensity, photokinesis is the response in alteration of the rate of motility caused by differences in the light intensity.

Pseudomonas syringae pv tomato is a motile bacterium with polar flagella (Figure 49). The flagella enable the cell to swim in low-density agar medium (<0.4%). In addition, *P. syringae tomato* is also able to propagate at surface interfaces by twitching motility which is mediated by type IV pili [171]. Twitching motility is believed to result from the extension and retraction of the pilus filament, which propels the cells across a surface. Besides swimming and twitching, several gram negative bacteria are able to propagate on semi-solid surfaces (i.e., 0.4 to 1.0% agar) in a coordinated manner by swarming motility. Swarmer cells, which are usually

elongated and hyperflagellated, derived from vegetative cells probably after sensing the viscosity of the surface or in response to nutritional signals [172].

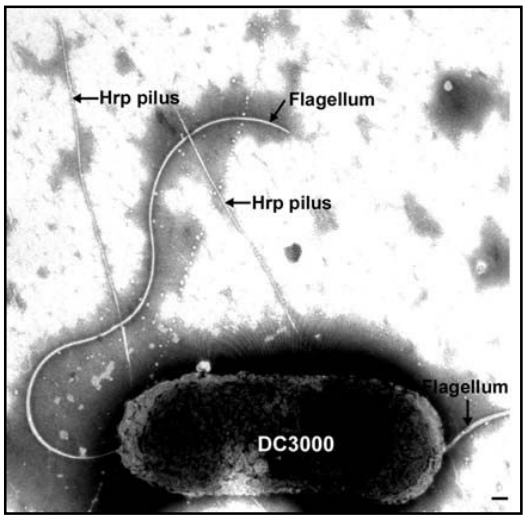

Figure 49: A transmission electron microscope image of the *Pseudomonas syringae pv tomato* DC3000 with polar flagella and Hrp (Hypersensitive reaction and pathogenicity) pili. The flagella and pili are involved in motility and virulence [173].

The pspto_2896 mutant strains (*LOVΔ*A and *LOVΔB)* were tested for the motility in blue light (447 nm), and all the other mutants were tested under red/ far red (625, 660, 720, 740 nm) light for changes in their motility. For these experiments, the cultures of the analyzed strains were grown in KB medium and adjusted to an optical density at 600 nm of 1.0. 5 µl of these cultures were streaked on a straight line on the surface of the KB plates or were placed into soft agar (0.4% wt/vol) for controlling of their swarming motility. The plates were incubated at 30℃ for 48 to 72 h.

A preliminary inspection of all mutated strains revealed differences in the growth behaviour compared to the WT cells. The blue light mutant strains (*LOVΔA and LOVΔB*) were grown under continuous lateral irradiation with blue light (447 nm).

Whereas the mutant cells grow in all directions irrespective of the light, the wild type shows reduced growth of the colony, which was more obvious in the direction of the blue light (Figure 50). In case of *LOVΔA* and *LOVΔB*, the wild-type cells responded to blue light by reduced growth while the mutant cells seem to be unable to detect blue light and grow vigorously in all directions.

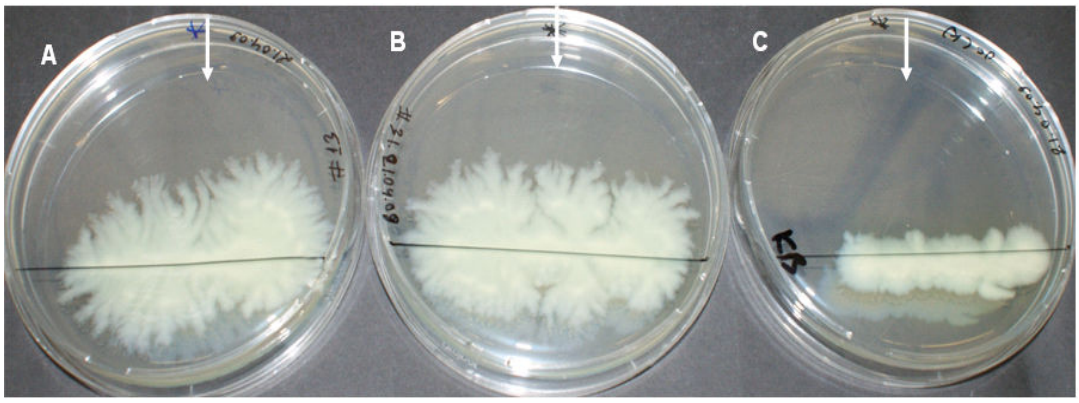

Figure 50: Phenotypes associated with the mutation of the LOV domain- coding gene. Motility of *P. syringae* pv *tomato* DC3000 strains was tested on KB medium containing 0.4% agar under blue-light irradiation (447nm). Five µl of cells from each strain were separately spotted on a line on the plate and incubated for 48 hours at 30 °C. Direction of irradiation is shown by white arrows. (A) *LOV∆A* (polar-mutant), (B) *LOV∆B* (nonpolar-mutant) and (C) wild type (control).

The *bphP1Δ* mutant grown under continuous irradiation of 660 nm, 625 nm, 740 nm and 720 nm red and far red lights showed a wild type comparable phenotype when grown under identical conditions (Figure 51). The insertional knockout mutant, *bphP1Δ* shows more proliferation of colonies than the wild-type cells under continuous irradiation with different red/far red light condition. When grown in darkness, the wild-type strain exhibits a better swarming motility than *bphP1Δ* (Figures 52A and B). Finally, under continuous white light, both, wild type and mutant showed comparable behavior (Figures 52C and D). The comparable growth behavior in white light, however, might be compromised as the continuous white light irradiation caused a temperature rise in the incubator and induced desiccation of the plates after 24 hours, which is about the time that *P. syringae tomato* needs to grow.

The *bphP2Δ* mutant grown under irradiation of red light (625 and 660 nm) and far red light (720 and 740 nm) revealed a comparable phenotype as the wild type (Figure 53), which is also similar to the *bphP1Δ* mutant. Similar phenotypes were found also for the *bphOΔ* and the double knockout mutant *bphP1Δ bphP2Δ*, which were grown under continuous 740 nm and 625 nm irradiation for 36 hours (Figures 54 and 55).

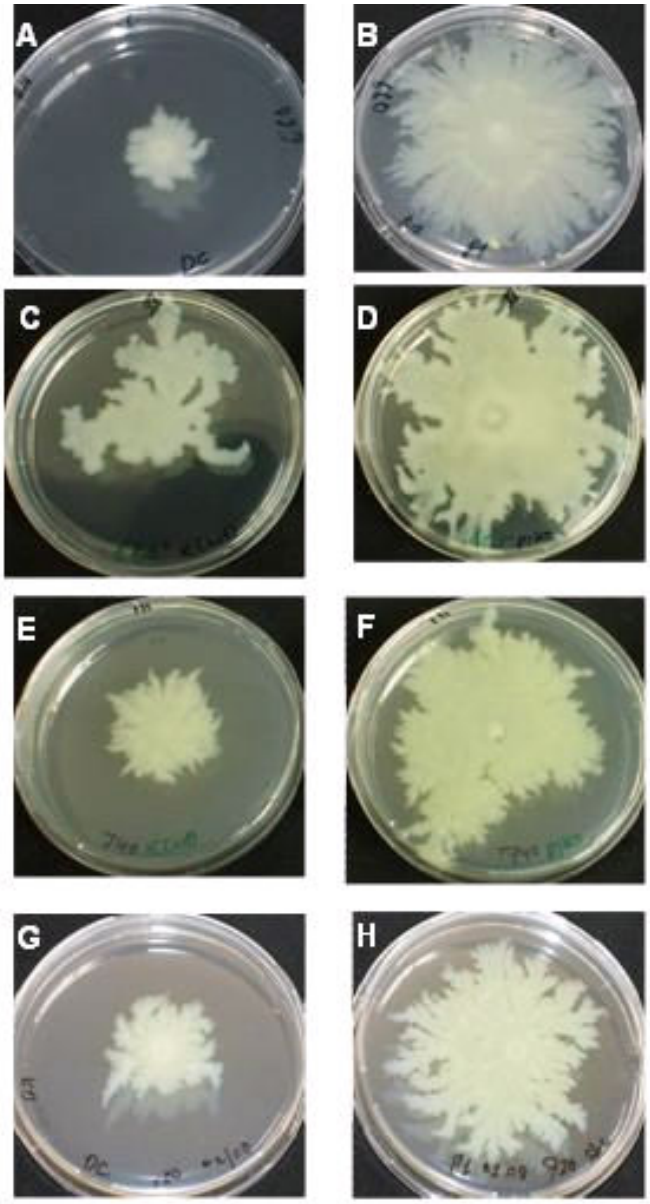

Figure 51: Effect of red and far red light on *P. syringae pv tomato* strains. WT (left plates) as control and knockout mutant *bphP1Δ* (right plates) were incubated on 0.4% agar plates at 30^0C for 48 hours, grown under continuous irradiation of A and B: 660 nm; C and D: 625 nm; E and F: 740 nm; and, G and H: 720 nm. (Source of irradiation of light is lateral but reflected all over the plate)

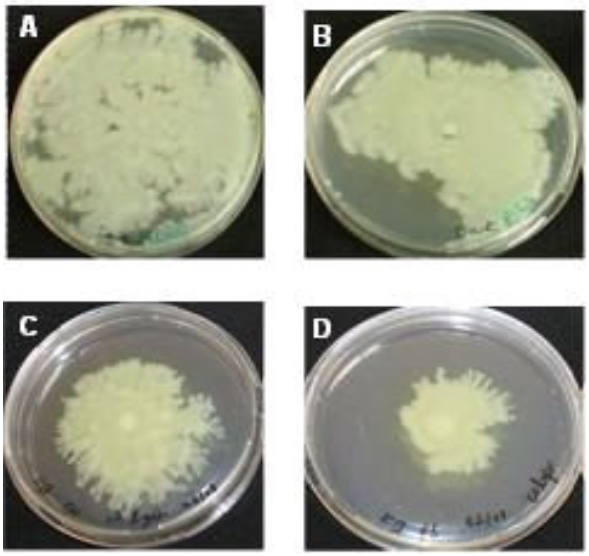

Figure 52: Effect of white light on *P. syringae pv tomato* strains. WT (left plates) and knockout mutant *bphP1Δ* (right plates) were incubated on 0.4% agar plates at 30^0C for e 48 hours, grown under A and B: darkness; and, C and D: white light.

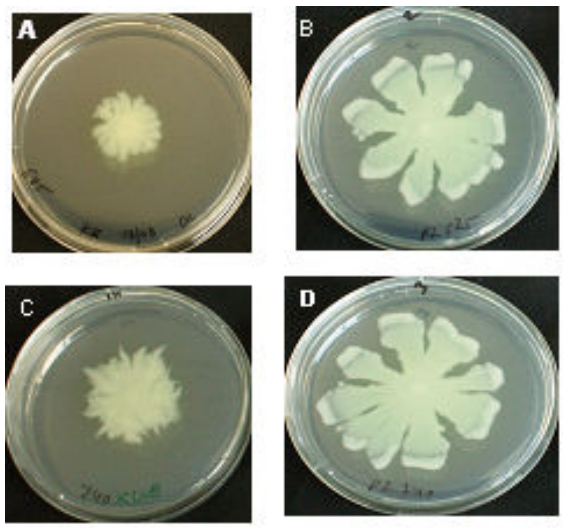

Figure 53: Effect of red and far red light on *P. syringae pv tomato* strains. WT (left plates) as control and knockout mutant *bphP2Δ* (right plates) were incubated on 0.4% agar plates under A and B: 625 nm; and, C and D: 740 nm at 30^0C. Photographs were taken after 48 hours.

Figure 54: Effect of far red light (740 nm) on *P. syringae pv tomato* strains. A: Wild type; B: knockout mutant *bphOΔ;* and C: *bphP1Δ bphP2Δ* (double knockout mutant) were incubated on 0.4% agar plates for 36 hours at 30^0C.

Figure 55: Effect of red light (625 nm) on *P. syringae pv tomato* strains. A: Wild type; B: knockout mutant *bphOΔ;* and C: *bphP1ΔbphP2Δ* (double knockout mutant) were incubated on 0.4% agar plates for 36 hours at 30^0C

All these mutants showed a growth behaviour or phenotypes comparable with wild type cells. Both, the mutants and the wild type demonstrated swarming motility, but the mutants cells grew more vigorously in all directions than wild type which gave a reduced growth under irradiation.

Phototactic responses have been described in detail for many microorganisms including *Rhodospirillum centenum* [174], *Halobacterium salinarum, Ectothiorhodospira halophila* [175] or cyanobacteria such as *Synechocystis*

PCC6803 [176;177]. In case of our study, there was no clear evidence of phototactic response of *P. syringae tomato* wild type, and also for the here generated mutants *LOVΔ, bphOΔ, bphP1Δ, bphP2Δ* and *bphP1ΔbphP2Δ*. However, as far as performed here, the *LOVΔ* and *bphP1Δ* mutants revealed a distinct phenotype in swarmer cells such that these mutants have grown in all the direction whereas wild type cells remained as a small colony when grown in continuous blue-light (447 nm), but intrestingly also under red/ far red light, respectively. Therefore, the light effect found in the present study could be defined as a photokinesis response which is an alteration in the rate of motility caused by differences in light intensity. The direction and irradiation is not relevant for a photokinetic response, whereas it is a critical determinant in phototaxis [174]. A similar type of response was reported for *Agrobacterium tumefaciens* [178].

3.4.3 Effect of mutations on infectivity on plants

According to its biological function as a plant pathogen, infectivity tests of the WT or mutated *P. syringae* strains on Arabidopsis were performed. *Arabidopsis* plants were grown under short days, and their leaves were inoculated with bacteria by bathing in buffer contained wild type or mutant strains of *P. syringae*. Afterwards, the plants were transferred to either continuous light or darkness. The leaves were harvested 24, 48, or 72 hours after surface inoculation and the numbers of colony-forming units (CFU) per unit leaf were calculated. Each data point is taken from at least 19 plants in at least 5 different experiments with mean and standard error (SE). The result presented here are from pspto_2896 mutant strains (*LOVΔ*A and *LOVΔB)* and pspto_1902 (*bphP1Δ*) mutant (Figure 56). For other mutant strains the experiment is still going on.

When the bacteria grow on white light-exposed leaves, the two LOV-mutant strains (*LOVΔ*A and *LOVΔB)* show enhanced growth compared to the wild-type (WT) strain and the phytochrome-1 mutant (*bphP1Δ*). These differences are not observed when the plants are transferred to dark after inoculation. Darkness increases bacterial

growth in the WT and to a lesser extent in the phytochrome mutant, but not in the LOV mutants.

Our preliminary experiments of plant-mutant interaction indicate that light perceived by the LOV-domain photoreceptor reduces bacterial growth, whereas no such effect is observed for the phytochrome photoreceptor.

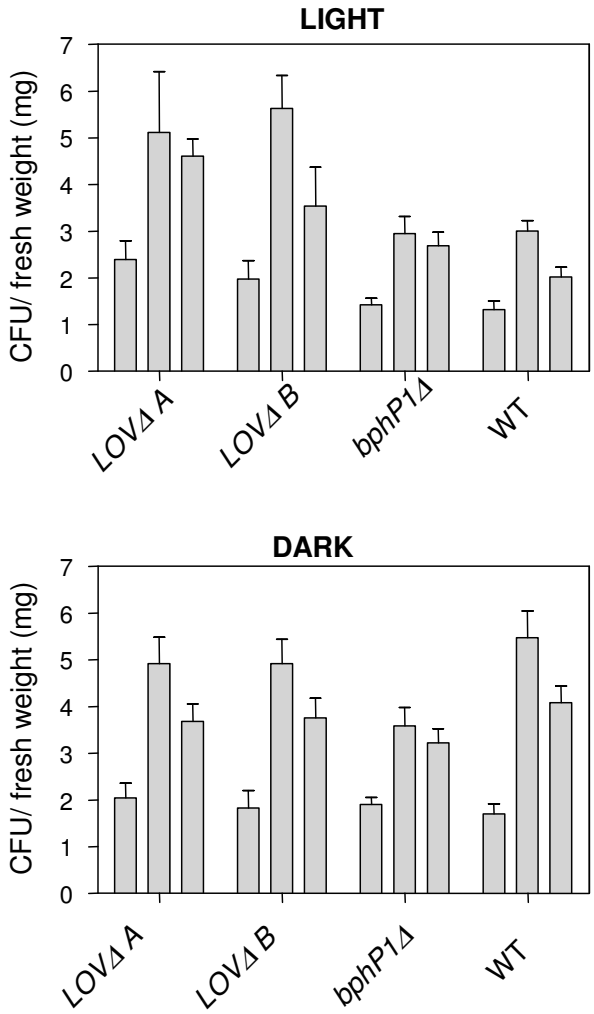

Figure 56: The number of colony-forming units (CFU) per unit leaf (fresh weight) after surface inoculation with the blue-light photoreceptor- (pspto_2896) *LOVΔA* and *LOVΔB* (both orientations) and the phytochrome (*bphP1Δ*) mutant, and with the wild-type (WT) strain of *P. syringae pv tomato*. Wild-type plants were grown under short days, inoculated and transferred to either continuous light (top) or continuous darkness (bottom). The three columns correspond to leaves harvested 1, 2 or 3 days after inoculation. Each data point is mean and standard error (SE) of at least 19 plants harvested in 5 different experiments.

4. Conclusion

Phytochromes are red-/far-red-light photoreceptors in plants and cyanobacteria but have recently been discovered in non-photosynthetic bacteria and in fungi. They carry an open-chain tetrapyrrole (bilin) prosthetic group which is covalently bound to the protein. In this work the phytochromes from cyanobacteria *Calothrix* PCC7601 and plant pathogen *Pseudomonas syringae pv tomato* DC3000 were studied, an attempt to understand the red/ far red biological photoreceptor system in bacterial world.

(a) Domain interaction in Cyanobacterial phytochromes CphA/CphB from *Calothrix* PCC7601

The phytochromes from the cyanobacterium *Calothrix* PCC7601 were investigated for the essential protein domains required to maintain the spectral integrity. The filamentous cyanobacterium *Calothrix* PCC7601 expresses CphA and CphB phytochromes. CphA phytochrome possesses a canonical cysteine within a conserved amino-acid sequence motif to which phycocyanobilin (PCB) is bound covalently. CphB which is similar to other BphPs lacking the canonical cysteine residue carries an N-terminally located cysteine as an alternative binding site for biliverdin (BV). Heterologous expression of *Calothrix* CphA phytochrome in *E. coli* and reconstitution of the recombinant apoprotein with PCB as a chromophore resulted in a chromoprotein showing absorption maxima (λ_{max}) of P_R 663 nm and P_{FR} of 710 nm upon far-red and red light irradiation. Similarly, CphB apoprotein, after reconstitution with chromophore (BV), showed the photoconversion of λ_{max} of P_R 704 nm and P_{FR} of 750 nm. In both cases, the C-terminally truncated CphA-PGP (PAS-GAF-PHY, with the N-terminal 515 amino-acids) and CphB-PGP (with the N-terminal 537 amino-acids) showed the similar photochromocity as the full-length proteins (CphA-PGP: λ_{max} of P_R 663 nm and P_{FR} of 710 nm, CphB-PGP: λ_{max} of P_R 704 nm and P_{FR} of 750 nm). These truncated proteins, lacking the HK domain were more stable than their full-length counterparts. In case of CphA-PG (PAS-GAF, N-terminal 357 amino-acids) and CphB-PG (N-terminal 357 amino-acids), the apoproteins

showed the assembly of chromophore phycocyanobilin (PCB) and biliverdin (BV), respectively, but the P_R and P_{FR} forms showed significant shifts due to the instability and a misfolding of the protein, as is deduced from the overall yield of photoactive protein. The deletion of the "PHY" domains caused a blue-shift of the P_R and P_{FR} absorption of CphA-PG, λ_{max} = 658 and 698 nm, respectively, and also increased the amount of unproperly folded apoprotein. In CphB-PG, however, it practically impaired the formation of P_{FR}, i.e., showing a very low oscillator strength absorption band, whereas the P_R form remains unchanged. One can clearly conclude that removal of the phy domain in CphB has a significant effect on the chromophore conformation and thereby on the spectral properties.

(b) *In vitro* study of novel hybrid (fused blue and red light photo-sensor) kinase protein

Following approaches in optogenetics, a hybrid protein was constructed by fusing the PAS domain of LOV (blue light photoreceptor) from *P. syringae pv tomato* DC3000 with the HK domain of cyanobacterial phytochrome CphA. This reprogrammed sensor LOV-kinase shall serve as a model system for a naturally non-existing hybrid protein in order to learn whether artificially combined protein domains (light-sensing and signaling) can be arranged at will, retaining their respective biochemical functionality. This fusion of domains from blue- and red-sensing biological photoreceptor retained the typical photochemical properties of *Pst*LOV, i.e, functioning furtheron as a blue-light photoreceptor.

(c) Red/far red photoreceptors of *P. syringae pv tomato* DC3000

Recent genome sequence data of the model plant pathogen *Pseudomonas syringae* pv tomato DC3000 has revealed the presence of two red/far red sensing putative phytochrome photoreceptor (*Pst*BphP1 and *Pst*BphP2) and one blue-light photoreceptor (*Pst*LOV). As *P. syringae* is an also economically important plant pathogen, its photoreceptors were characterized *in vitro* and for their impact in the bacterium's lifestyle. The bacterial phytochromes from *P. syringae pv tomato* (*Pst*BphPs) were recombinantly expressed in *E. coli* and characterized *in vitro.* Both

phytochromes show the general modular architecture of a three domain chromophore-binding region (PAS-GAF-PHY) that is followed by a histidine kinase domain at the C-terminal part. *PstbphP1* is arranged in an operon with a preceding gene encoding a heme oxygenase (*PstbphO*), whereas *PstbphP2* is followed by a response regulator. Heterologous expression of the heme oxygenase yielded a green protein (λ_{max} = 650 nm), indicative for bound biliverdin. Heterologous expression of *PstbphP1* and *PstbphP2* yielded the apoproteins for both phytochromes, however, only in case of *Pst*BphP1 a holoprotein was formed upon addition of biliverdin. The two phytochromes were also co-expressed with *Pst*bphO as a two-plasmid approach yielding a fully assembled holoprotein for *Pst*BphP1 (λ_{max} 700 nm and 750 nm for P_R and P_{FR} state, respectively), whereas again for *Pst*BphP2 no chromophore absorbance could be detected. An even further increased yield for *Pst*BphP1 was obtained when the operon *PstbphO::PstbphP1* was expressed in *E. coli*. A construct placing the gene for *Pst*BphP2 exactly at the position of *PstbphP1* in this operon again gave the negative result such that no phytochrome-2 chromoprotein was formed. The reason for the improved yield for the operon expression *PstbphO::PstbphP1* is the formation of a complex formed between both proteins during biosynthesis. As a result, the folding, chromoprotein formation and spectral quality of phytochrome-1 is apparently strongly dependent on a complex formed to the heme oxygenase. This interaction is dependent on precise interactions, as identical arrangements for the gene encoding phytochrome-2 do not lead to chromophore incorporation under no circumstances.

(d) Generation of insertional knock-out mutants of phytochromes and blue-light receptor (LOV) in *P. syringae pv tomato DC3000*

As a logical follow-up, the regulatory function of these red/ far red and blue light photoreceptor genes were studied *in vivo* by generating insertional knockout mutants. The most important outcome from this project is the development of a facile, efficient and time-saving transformation protocol to introduce simply linear, double stranded DNA into the bacterium. This procedure will speed up investigations on the function of single genes for the physiology of the microorganism. As the

commonly applied protocol of gene transfer by conjugation / homologous recombination is known to be a time-consuming process of low-efficiency, an alternative method was developed in this study to create interposon- as well as point mutations of the corresponding photoreceptors genes by employing linear DNA constructs. In this study interposon- as well as point mutations of the corresponding photoreceptors genes were created by employing linear DNA constructs. Five mutant strains of *bphP1Δ*, *bphP2Δ*, *bphOΔ*, pspto_2896 (*LOVΔ*) and double mutant strain of *bphP1ΔbphP2Δ* were generated using the new method to study the regulatory function of these photoreceptor gene. The bphO- and the pspto_2896 (LOV) genes encode a heme oxygenase and a blue light-sensitive photoreceptor, respectively.These mutant strains are used for the following study:

(i) Effects of light on blue/red light photoreceptors inactivated mutants from *P. syringae pv tomato* DC3000

All the generated mutant strains were tested for motility under continuous blue, red and far red lights. The *bphP1Δ* mutant grown under continuous irradiation of 660 nm, 625 nm, 740 nm and 720 nm red and far red lights showed a wild type comparable phenotype. The insertional knockout mutant, *bphP1Δ* shows more proliferation of colonies than the wild-type cells in the different red/far red light irradiations. When grown in darkness, the wild-type strain exhibits a better swarming motility than *bphP1Δ.* The blue light mutant strain (*LOVΔ*) grown under continuous lateral irradiation with blue light (447 nm), spred in all directions irrespective of the light, but the wild type shows reduced growth of the colony, which was more obvious in the direction of the blue light. The wild-type cells respond to blue light by reduced growth while the mutant cells seem to be unable to detect blue light and grow vigorously in all directions. Similar phenotypes were found also for the *bphP2Δ, bphOΔ* and the double knockout mutant *bphP1Δ bphP2Δ*, which were grown under continuous 740 nm and 625 nm irradiation. Although still in its infancy, the data obtained so far clear demosntrate an effect of the photoreceptors on the growth behavior of this plant pathogen.

(ii) Effect of mutations on infectivity on plants

Investigations of light control on the infectivity of *P. syringae* on plants have been started in collaboration (Prof. J. Casal, Univ. Buenos Aires, Argentina). The results obtained so far indicate that light perceived by the LOV-domain photoreceptor reduces bacterial growth, whereas no such effect is observed for the phytochrome photoreceptor.

5. References

[1] Butler,W.L., Norris,K.H., Siegelman,H.W., & Hendricks,S.B. (1959) Detection, Assay, and Preliminary Purification of the Pigment Controlling Photoresponsive Development of Plants. *Proc Natl Acad Sci USA* **45,** 1703-1708.

[2] Lamparter,T., Mittmann,F., Gärtner,W., Börner,T., Hartmann,E., & Hughes,J. (1997) Characterization of recombinant phytochrome from the cyanobacterium *Synechocystis*. *Proc Natl Acad Sci USA* **94,** 11792-11797.

[3] Bhoo,S.H., Davis,S.J., Walker,J., Karniol,B., & Vierstra,R.D. (2001) Bacteriophytochromes are photochromic histidine kinases using a biliverdin chromophore. *Nature* **414,** 776-779.

[4] ASTM (2006) *Book of standard: standard tables for reference solar spectral irradiances: direct normaland hemispherical on 37° tilted surface*. Book of Standards vol. 14.04.ASTM International, West Conshohocken, PA,USA.

[5] Naylor,M.F. & Farmer,K.C. Sun damage and Prevention. Electronic citation 2000. The Internet Dermatology Society.

[6] Batschauer,A. (2003) *Photoreceptors and Light Signalling (Ed. A. Batschauer)*. Royal Society of Chemistry, Cambridge.

[7] Schäfer,E. & Nagy,F. (2006) *Photomorphogenesis in Plants and Bacteria : Function and Signal Transduction Mechanisms, 3rd ed (Eds.:Schafer,E. and Nagy,F.)*, 3 edn. Springer, Dordrecht.

[8] Briggs W.R. & Spudich,J.L. (2005) *Handbook of Photosensory Receptors*. Wiley-VCH,Weinheim.

[9] Spudich,J.L., Yang,C.S., Jung,K.H., & Spudich,E.N. (2000) Retinylidene proteins: Structures and functions from archaea to humans. *Annu Rev Cell Dev Biol* **16,** 365-392.

[10] Schegk,E.S. & Oesterhelt,D. (1988) Isolation of a prokaryotic photoreceptor - sensory rhodopsin from halobacteria. *Embo J* **7,** 2925-2933.

[11] Sakmar,T.P. (2002) Structure of rhodopsin and the superfamily of seven-helical receptors: the same and not the same. *Curr Opin Cell Biol* **14,** 189-195.

[12] Engel,A. & Gaub,H.E. (2008) Structure and mechanics of membrane proteins. *Ann Rev Biochem* **77,** 127-148.

[13] Yoshizawa,T. (1984) Photophysiological functions of visual pigments. *Adv Biophys* **17,** 5-67.

[14] Kort,R., Hoff,W.D., VanWest,M., Kroon,A.R., Hoffer,S.M., Vlieg,K.H., Crielaard,W., VanBeeumen,J.J., & Hellingwerf,K.J. (1996) The xanthopsins: A new family of eubacterial blue-light photoreceptors. *Embo J* **15,** 3209-3218.

[15] Meyer,T.E. (1985) Isolation and characterization of soluble cytochromes, ferredoxins and other chromophoric proteins from the halophilic phototrophic bacterium *Ectothiorhodospira-Halophila*. *Biochim Biophys Acta* **806,** 175-183.

[16] Sprenger,W.W., Hoff,W.D., Armitage,J.P., & Hellingwerf,K.J. (1993) The eubacterium *Ectothiorhodospira-halophila* is negatively phototactic, with a wavelength dependence that fits the absorption-spectrum of the photoactive yellow protein. *J Bacteriol* **175,** 3096-3104.

[17] Jiang,Z.Y., Swem,L.R., Rushing,B.G., Devanathan,S., Tollin,G., & Bauer,C.E. (1999) Bacterial photoreceptor with similarity to photoactive yellow protein and plant phytochromes. *Science* **285,** 406-409.

[18] Kyndt,J.A., Meyer,T.E., & Cusanovich,M.A. (2004) Photoactive yellow protein, bacteriophytochrome, and sensory rhodopsin in purple phototrophic bacteria. *Photochem Photobio Sci* **3,** 519-530.

[19] Sancar,A. (2004) Photolyase and cryptochrome blue-light photoreceptors. *Adv Protein chem* **69,** 73-100.

[20] Lin,C.T. & Todo,T. (2005) The cryptochromes. *Genome Biol* **6,** 220.

[21] Iseki,M., Matsunaga,S., Murakami,A., Ohno,K., Shiga,K., Yoshida,K., Sugai,M., Takahashi,T., Hori,T., & Watanabe,M. (2002) A blue-light-activated adenylyl cyclase mediates photoavoidance in *Euglena gracilis*. *Nature* **415,** 1047-1051.

[22] Brudler,R., Hitomi,K., Daiyasu,H., Toh,H., Kucho,K., Ishiura,M., Kanehisa,M., Roberts,V.A., Todo,T., Tainer,J.A., & Getzoff,E.D. (2003) Identification of a new cryptochrome class: Structure, function, and evolution. *Mol Cell* **11,** 59-67.

[23] Worthington,E.N., Kavakli,I.H., Berrocal-Tito,G., Bondo,B.E., & Sancar,A. (2003) Purification and characterization of three members of the photolyase/cryptochrome family blue-light photoreceptors from *Vibrio cholerae*. *J Biol Chem* **278,** 39143-39154.

[24] Gomelsky,M. & Klug,G. (2002) BLUF: a novel FAD-binding domain involved in sensory transduction in microorganisms. *Trends Biochem Sci* **27,** 497-500.

[25] Masuda,S. & Bauer,C.E. (2002) AppA is a blue light photoreceptor that antirepresses photosynthesis gene expression in *Rhodobacter sphaeroides*. *Cell* **110,** 613-623.

[26] Liscum,E. & Briggs,W.R. (1995) Mutations in the Nph1 locus of Arabidopsis disrupt the perception of phototropic stimuli. *Plant Cell* **7,** 473-485.

[27] Christie,J.M., Salomon,M., Nozue,K., Wada,M., & Briggs,W.R. (1999) LOV (light, oxygen, or voltage) domains of the blue-light photoreceptor phototropin (nph1): Binding sites for the chromophore flavin mononucleotide. *Proc Natl Acad Sci USA* **96,** 8779-8783.

[28] Christie,J.M. (2007) Phototropin blue-light receptors. *Annu. Rev. Plant Biol.* **58,** 21-45.

[29] Huala,E., Oeller,P.W., Liscum,E., Han,I.S., Larsen,E., & Briggs,W.R. (1997) *Arabidopsis* NPH1: A protein kinase with a putative redox-sensing domain. *Science* **278,** 2120-2123.

[30] Losi,A. (2004) The bacterial counterparts of plant phototropins. *Photochem. Photobiol Sci* **3,** 566-574.

[31] Somers,D.E., Schultz,T.F., Milnamow,M., & Kay,S.A. (2000) ZEITLUPE encodes a novel clock-associated PAS protein from Arabidopsis. *Cell* **101,** 319-329.

[32] Zikihara,K., Iwata,T., Matsuoka,D., Kandori,H., Todo,T., & Tokutomi,S. (2006) Photoreaction cycle of the light, oxygen, and voltage domain in FKF1 determined by low-temperature absorption spectroscopy. *Biochemistry* **45,** 10828-10837.

[33] Demarsy,E. & Fankhauser,C. (2009) Higher plants use LOV to perceive blue light. *Curr Opin Plant Biol* **12,** 69-74.

[34] Gaba,V., Black,M., & Attridge,T.H. (1984) Photocontrol of hypocotyl elongation in de-etiolated *Cucumis sativus,* long-term, fluence rate-dependent responses to blue light. *Plant Physiol* **74,** 897-900.

[35] Vierstra,R.D. & Quail,P.H. (1982) Proteolysis Alters the Spectral Properties of 124 K Dalton Phytochrome from *Avena*. *Planta* **156,** 158-165.

[36] Hershey,H.P., Barker,R.F., Idler,K.B., Lissemore,J.L., & Quail,P.H. (1985) Analysis of cloned cDNA and genomic sequences for phytochrome - complete amino-acid-sequences for 2 gene-products expressed in etiolated *Avena*. *Nucleic Acids Res* **13,** 8543-8559.

[37] Yeh,K.C., Wu,S.H., Murphy,J.T., & Lagarias,J.C. (1997) A cyanobacterial phytochrome two-component light sensory system. *Science* **277,** 1505-1508.

[38] Davis,S.J., Vener,A.V., & Vierstra,R.D. (1999) Bacteriophytochromes: Phytochrome-like photoreceptors from nonphotosynthetic eubacteria. *Science* **286,** 2517-2520.

[39] Starostzik,C. & Marwan,W. (1995) A photoreceptor with characteristics of phytochrome triggers sporulation in the true slime-mold *Physarum Polycephalum*. *FEBS Lett* **370,** 146-148.

[40] Karniol,B., Wagner,J.R., Walker,J.M., & Vierstra,R.D. (2005) Phylogenetic analysis of the phytochrome superfamily reveals distinct microbial subfamilies of photoreceptors. *Biochem J* **392,** 103-116.

[41] Jorissen,H.J.M.M., Quest,B., Remberg,A., Coursin,T., Braslavsky,S.E., Schaffner,K., de Marsac,N.T., & Gärtner,W. (2002) Two independent, light-sensing two-component systems in a filamentous cyanobacterium. *Eur J Biochem* **269,** 2662-2671.

[42] Lagarias,J.C. & Rapoport,H. (1980) Chromopeptides from phytochrome the structure and linkage of the Pr form of the phytochrome chromophore. *J Am Chem Soc* **102,** 4821-4828.

[43] Hübschmann,T., Börner,T., Hartmann,E., & Lamparter,T. (2001) Characterization of the Cph1 holo-phytochrome from *Synchocystis sp* PCC 6803. *Eur J Biochem* **268,** 2055-2063.

[44] Tasler,R., Moises,T., & Frankenberg-Dinkel,N. (2005) Biochemical and spectroscopic characterization of the bacterial phytochrome of *Pseudomonas aeruginosa*. *FEBS J* **272,** 1927-1936.

[45] Blumenstein,A., Vienken,K., Tasler,R., Purschwitz,J., Veith,D., Frankenberg-Dinkel,N., & Fischer,R. (2005) The *Aspergillus nidulans* phytochrome FphA represses sexual development in red light. *Curr Biol* **15,** 1833-1838.

[46] Lamparter,T., Carrascal,M., Michael,N., Martinez,E., Rottwinkel,G., & Abian,J. (2004) The biliverdin chromophore binds covalently to a conserved cysteine residue in the N-terminus of *Agrobacterium* phytochrome Agp1. *Biochemistry* **43,** 3659-3669.

[47] Wagner,J.R., Brunzelle,J.S., Forest,K.T., & Vierstra,R.D. (2005) A light-sensing knot revealed by the structure of the chromophore-binding domain of phytochrome. *Nature* **438,** 325-331.

[48] Dammeyer,T. & Frankenberg-Dinkel,N. (2008) Function and distribution of bilin biosynthesis enzymes in photosynthetic organisms. *Photochem. Photobio Sci* **7,** 1121-1130.

[49] Hahn,J., Strauss,H.M., Landgraf,F.T., Gimenez,H.F., Lochnit,G., Schmieder,P., & Hughes,J. (2006) Probing protein-chromophore interactions in Cph1 phytochrome by mutagenesis. *FEBS J* **273,** 1415-1429.

[50] Lamparter,T., Esteban,B., & Hughes,J. (2001) Phytochrome Cph1 from the cyanobacterium *Synechocystis* PCC6803 - Purification, assembly, and quaternary structure. *Eur J Biochem* **268,** 4720-4730.

[51] Gärtner,W. & Braslavasky,S.E. The phytochromes: spectroscopy and function. In Photoreceptors and light signaling. Batschauer, A. 137-180. 2003. Cambrige, UK, Royal Society of Chemistry.

[52] Essen,L.O., Mailliet,J., & Hughes,J. (2008) The structure of a complete phytochrome sensory module in the Pr ground state. *Proc Natl Acad Sci USA* **105,** 14709-14714.

[53] Yang,X., Kuk,J., & Moffat,K. (2008) Crystal structure of *Pseudomonas aeruginosa* bacteriophytochrome: Photoconversion and signal transduction. *Proc Natl Acad Sci USA* **105,** 14715-14720.

[54] Tenhunen,R., Marver,H.S., & Schmid,R. (1969) Microsomal heme oxygenase characterization of enzyme. *J Biol Chem* **244,** 6388-6394.

[55] Wilks,A. (2002) Heme oxygenase: Evolution, structure, and mechanism. *Antioxid Redox Sign* **4,** 603-614.

[56] Schmitt,M.P. (1997) Transcription of the *Corynebacterium diphtheriae* hmuO gene is regulated by iron and heme. *Infect Immun* **65,** 4634-4641.

[57] Skaar,E.P., Gaspar,A.H., & Schneewind,O. (2004) IsdG and IsdI, heme-degrading enzymes in the cytoplasm of *Staphylococcus aureus*. *J Biol Chem* **279,** 436-443.

[58] Frankenberg-Dinkel,N. (2004) Bacterial heme oxygenases. *Antioxid Redox Sign* **6,** 825-834.

[59] Cornejo,J., Willows,R.D., & Beale,S.I. (1998) Phytobilin biosynthesis: cloning and expression of a gene encoding soluble ferredoxin-dependent heme oxygenase from *Synechocystis sp*. PCC 6803. *Plant J* **15,** 99-107.

[60] Wegele,R., Tasler,R., Zeng,Y.H., Rivera,M., & Frankenberg-Dinkel,N. (2004) The heme oxygenase(s)-phytochrome system of *Pseudomonas aeruginosa*. *J Biol Chem* **279,** 45791-45802.

[61] Vierstra,R.D. (1993) Illuminating phytochrome functions. *Plant Physiol* **103,** 679-684.

[62] Chen,M., Tao,Y., Lim,J., Shaw,A., & Chory,J. (2005) Regulation of phytochrome B nuclear localization through light-dependent unmasking of nuclear-localization signals. *Curr Biol* **15,** 637-642.

[63] Montgomery,B.L. & Lagarias,J.C. (2002) Phytochrome ancestry: sensors of bilins and light. *Trends Plant Sci* **7,** 357-366.

[64] Rockwell,N.C. & Lagarias,J.C. (2010) A brief history of phytochromes. *Chemphyschem* **11,** 1172-1180.

[65] Rockwell,N.C. & Lagarias,J.C. (2006) The structure of phytochrome: A picture is worth a thousand spectra. *Plant Cell* **18,** 4-14.

[66] Ikeuchi,M. & Ishizuka,T. (2008) Cyanobacteriochromes: a new superfamily of tetrapyrrole-binding photoreceptors in cyanobacteria. *Photochem Photobio Sci* **7,** 1159-1167.

[67] Ulijasz,A.T., Cornilescu,G., von Stetten,D., Cornilescu,C., Escobar,F.V., Zhang,J.R., Stankey,R.J., Rivera,M., Hildebrandt,P., & Vierstra,R.D. (2009) Cyanochromes are blue/green light photoreversible photoreceptors defined by a stable double cysteine linkage to a phycoviolobilin-type chromophore. *J Biol Chem* **284,** 29757-29772.

[68] Borthwick,H.A., Hendricks,S.B., Parker,M.W., Toole,E.H., & Toole,V.K. (1952) A reversible photoreaction controlling seed germination. *Proc Natl Acad Sci USA* **38,** 662-666.

[69] Clack,T., Mathews,S., & Sharrock,R.A. (1994) The phytochrome apoprotein family in *Arabidopsis* is encoded by 5 Genes - the sequences and expression of phyD and phyE. *Plant Mol Biol* **25,** 413-427.

[70] Quail,P.H. (2002) Phytochrome photosensory signalling networks. *Nat Rev Mol Cell Biol* **3,** 85-93.

[71] Pratt,L.H. (1995) Phytochromes - Differential properties, expression patterns and molecular evolution. *Photochem Photobiol* **61,** 10-21.

[72] Mathews,S. (2006) Phytochrome-mediated development in land plants: red light sensing evolves to meet the challenges of changing light environments. *Mol Ecol* **15,** 3483-3503.

[73] Aukerman,M.J., Hirschfeld,M., Wester,L., Weaver,M., Clack,T., Amasino,R.M., & Sharrock,R.A. (1997) A deletion in the PHYD gene of the Arabidopsis Wassilewskija ecotype defines a role for phytochrome D in red/far-red light sensing. *Plant Cell* **9,** 1317-1326.

[74] Franklin,K.A. & Quail,P.H. (2010) Phytochrome functions in *Arabidopsis* development. *J Exp Bot* **61,** 11-24.

[75] Esteban,B., Carrascal,M., Abian,J., & Lamparter,T. (2005) Light-induced conformational changes of cyanobacterial phytochrome Cph1 probed by limited proteolysis and autophosphorylation. *Biochemistry* **44,** 450-461.

[76] Yoon,J.M., Hahn,T.R., Cho,M.H., Jeon,J.S., Bhoo,S.H., & Kwon,Y.K. (2008) The PHY domain is required for conformational stability and spectral integrity of the bacteriophytochrome from *Deinococcus radiodurans*. *Biochem Bioph Res Co* **369,** 1120-1124.

[77] Sharda,S., Shah,R., & Gärtner,W. (2007) Domain interaction in cyanobacterial phytochromes as a prerequisite for spectral integrity. *Eur Biophys J* **36,** 815-821.

[78] Hübschmann,T., Jorissen,H.J.M.M., Börner,T., Gärtner,W., & de Marsac,N.T. (2001) Phosphorylation of proteins in the light-dependent signalling pathway of a filamentous cyanobacterium. *Eur J Biochem* ***268*****,** 3383-3389.

[79] Stock,A.M., Robinson,V.L., & Goudreau,P.N. (2000) Two-component signal transduction. *Annu Rev Biochem* **69,** 183-215.

[80] Zhao,K.H., Ran,Y., Li,M., Sun,Y.N., Zhou,M., Storf,M., Kupka,M., Bohm,S., Bubenzer,C., & Scheer,H. (2004) Photochromic biliproteins from the cyanobacterium *Anabaena sp* PCC7120: Lyase activities, chromophore exchange, and photochromism in phytochrome AphA. *Biochemistry* **43,** 11576-11588.

[81] Park,C.M., Shim,J.Y., Yang,S.S., Kang,J.G., Kim,J.I., Luka,Z., & Song,P.S. (2000) Chromophore-apoprotein interactions in *Synechocystis s*p PCC6803 phytochrome Cph1. *Biochemistry* **39,** 6349-6356.

[82] Giraud,E., Fardoux,L., Fourrier,N., Hannibal,L., Genty,B., Bouyer,P., Dreyfus,B., & Vermeglio,A. (2002) Bacteriophytochrome controls photosystem synthesis in anoxygenic bacteria. *Nature* **417,** 202-205.

[83] Herdman,M., Coursin,T., Rippka,R., Houmard,J., & de Marsac,N.T. (2000) A new appraisal of the prokaryotic origin of eukaryotic phytochromes. *J Mol Evol* **51,** 205-213.

[84] Wagner,J.R., Zhang,J.R., Brunzelle,J.S., Vierstra,R.D., & Forest,K.T. (2007) High resolution structure of *Deinococcus* bacteriophytochrome yields new insights into phytochrome architecture and evolution. *J Biol Chem* **282,** 12298-12309.

[85] Yang,X., Stojkovic,E.A., Kuk,J., & Moffatt,K. (2007) Crystal structure of the chromophore binding domain of an unusual bacteriophytochrome, RpBphP3, reveals residues that modulate photoconversion. *Proc Natl Acad Sci USA* **104,** 12571-12576.

[86] Lamparter,T., Michael,N., Mittmann,F., & Esteban,B. (2002) Phytochrome from *Agrobacterium tumefaciens* has unusual spectral properties and reveals an N-terminal chromophore attachment site. *Proc Natl Acad Sci USA* **99,** 11628-11633.

[87] Vuillet,L., Kojadinovic,M., Zappa,S., Jaubert,M., Adriano,J.M., Fardoux,J., Hannibal,L., Pignol,D., Vermeglio,A., & Giraud,E. (2007) Evolution of a bacteriophytochrome from light to redox sensor. *Embo J* **26,** 3322-3331.

[88] Karniol,B. & Vierstra,R.D. (2003) The pair of bacteriophytochromes from Agrobacterium tumefaciens are histidine kinases with opposing photobiological properties. *Proc Natl Acad Sci USA* **100,** 2807-2812.

[89] West,A.H. & Stock,A.M. (2001) Histidine kinases and response regulator proteins in two-component signaling systems. *Trends Biochem Sc* **26,** 369-376.

[90] Karniol,B. & Vierstra,R.D. (2004) The HWE histidine kinases, a new family of bacterial two-component sensor kinases with potentially diverse roles in environmental signaling. *J Bacteriol* **186,** 445-453.

[91] Catlett,N.L., Yoder,O.C., & Turgeon,B.G. (2003) Whole-genome analysis of two-component signal transduction genes in fungal pathogens. *Eukaryot Cell* **2,** 1151-1161.

[92] Kehoe,D.M. & Grossman,A.R. (1996) Similarity of a chromatic adaptation sensor to phytochrome and ethylene receptors. *Science* **273,** 1409-1412.

[93] Terauchi,K., Montgomery,B.L., Grossman,A.R., Lagarias,J.C., & Kehoe,D.M. (2004) RcaE is a complementary chromatic adaptation photoreceptor required for green and red light responsiveness. *Mol Microbiol* **51,** 567-577.

[94] Mutsuda,M., Michel,K.P., Zhang,X.F., Montgomery,B.L., & Golden,S.S. (2003) Biochemical properties of CikA, an unusual phytochrome-like histidine protein kinase that resets the circadian clock in *Synechococcus elongatus* PCC7942. *J Biol Chem* **278,** 19102-19110.

[95] Ivleva,N.B., Gao,T.Y., Liwang,A.C., & Golden,S.S. (2006) Quinone sensing by the circadian input kinase of the cyanobacterial circadian clock. *Proc Natl Acad Sci USA* **103,** 17468-17473.

[96] Narikawa,R., Kohchi,T., & Ikeuchi,M. (2008) Characterization of the photoactive GAF domain of the CikA homolog (SyCikA, Slr1969) of the cyanobacterium *Synechocystis sp* PCC6803. *Photochemi Photobiol Sci* **7,** 1253-1259.

[97] Bhaya,D., Takahashi,A., & Grossman,A.R. (2001) Light regulation of type IV pilus-dependent motility by chemosensor-like elements in *Synechocystis* PCC6803. *Proc Natl Acad Sci USA* **98,** 7540-7545.

[98] Ng,W.O., Grossman,A.R., & Bhaya,D. (2003) Multiple light inputs control phototaxis in *Synechocystis* sp strain PCC6803. *J Bacteriol* **185,** 1599-1607.

[99] Yoshihara,S., Katayama,M., Geng,X.X., & Ikeuchi,M. (2004) Cyanobacterial phytochrome-like PixJ1 holoprotein shows novel reversible photoconversion between blue- and green-absorbing forms. *Plant Cell Physiol* **45,** 1729-1737.

[100] Ishizuka,T., Shimada,T., Okajima,K., Yoshihara,S., Ochiai,Y., Katayama,M., & Ikeuchi,M. (2006) Characterization of cyanobacteriochrome TePixJ from a thermophilic cyanobacterium *Thermosynechococcus elongatus* strain BP-1. *Plant Cell Physiol* **47,** 1251-1261.

[101] Narikawa,R., Fukushima,Y., Ishizuka,T., Itoh,S., & Ikeuchi,M. (2008) A novel photoactive GAF domain of cyanobacteriochrome AnPixJ that shows reversible green/red photoconversion. *J Mol Biol* **380,** 844-855.

[102] Thümmler,F., Rudiger,W., Cmiel,E., & Schneider,S. (1983) Chromopeptides from Phytochrome and Phycocyanin - Nmr-Studies of the Pfr and Pr Chromophore of Phytochrome and E,Z Isomeric Chromophores of Phycocyanin. *Z Naturforsch A* **38,** 359-368.

[103] Rüdiger,W., Thümmler,F., Cmiel,E., & Schneider,S. (1983) Chromophore Structure of the Physiologically Active Form (Pfr) of Phytochrome. *Proc Natl Acad Sci USA* **80,** 6244-6248.

[104] Andel,F., Lagarias,J.C., & Mathies,R.A. (1996) Resonance Raman analysis of chromophore structure in the lumi-R photoproduct of phytochrome. *Biochem* **35,** 15997-16008.

[105] Müller,M.G., Lindner,I., Martin,I., Gärtner,W., & Holzwarth,A.R. (2008) Femto-second kinetics of photoconversion of the higher plant photoreceptor phytochr ome carrying native and modified chromophores. *Biophys J* **94,** 4370 - 4382.

[106] Gensch,T., Churio,M.S., Braslavsky,S.E., & Schaffner,K. (1996) Primary quantum yield and volume change of phytochrome-A phototransformation determined by laser-induced optoacoustic spectroscopy. *Photochem Photobiol* **63,** 719-725.

[107] Foerstendorf,H., Benda,C., Gärtner,W., Storf,M., Scheer,H., & Siebert,F. (2001) FTIR studies of phytochrome photoreactions reveal the C=O bands of the chromophore: Consequences for its protonation states, conformation, and protein interaction. *Biochemistry* **40,** 14952-14959.

[108] Matysik,J., Hildebrandt,P., Schlamann,W., Braslavsky,S.E., & Schaffner,K. (1995) Fourier-transform resonance raman-spectroscopy of intermediates of the phytochrome photocycle. *Biochemistry* **34,** 10497-10507.

[109] Remberg,A., Lindner,I., Lamparter,T., Hughes,J., Kneip,C., Hildebrandt,P., Braslavsky,S.E., Gärtner,W., & Schaffner,K. (1997) Raman spectroscopic and light-induced kinetic characterization of a recombinant phytochrome of the cyanobacterium *Synechocystis*. *Biochemistry* **36,** 13389-13395.

[110] Ulijasz,A.T., Cornilescu,G., Cornilescu,C.C., Zhang,J.R., Rivera,M., Markley,J.L., & Vierstra,R.D. (2010) Structural basis for the photoconversion of a phytochrome to the activated Pfr form. *Nature* **463,** 250-254.

[111] Bischoff,M., Hermann,G., Strehlow,D., & Rentsch,S. (2002) Femtosecond studies of the phototransformation process in phytochrome. *Rec Res Dev in Appl Phy* **5,** 107-120.

[112] Schumann,C., Gross,R., Michael,N., Lamparter,T., & Diller,R. (2007) Sub-picosecond mid-infrared spectroscopy of phytochrome Agp1 from *Agrobacterium tumefaciens*. *Chemphyschem* **8,** 1657-1663.

[113] Heyne,K., Herbst,J., Stehlik,D., Esteban,B., Lamparter,T., Hughes,J., & Diller,R. (2002) Ultrafast dynamics of phytochrome from the cyanobacterium *Synechocystis,* reconstituted with phycocyanobilin and phycoerythrobilin. *Biophys J* **82,** 1004-1016.

[114] Schwinte,P., Gärtner,W., Sharda,S., Mroginski,M.A., Hildebrandt,P., & Siebert,F. (2009) The photoreactions of recombinant phytochrome CphA from the cyanobacterium *Calothrix* PCC7601: A low-temperature UV-Vis and FTIR study. *Photochem Photobiol* **85,** 239-249.

[115] Rohmer,T., Lang,C., Bongards,C., Gupta,K.B.S.S., Neugebauer,J., Hughes,J., Gärtner,W., & Matysik,J. (2010) Phytochrome as molecular machine: revealing chromophore action during the Pfr -> Pr photoconversion by magic-angle spinning NMR spectroscopy. *J Am Chem Soc* **132,** 4431-4437.

[116] Foerstendorf,H., Lamparter,T., Hughes,J., Gärtner,W., & Siebert,F. (2000) The photoreactions of recombinant phytochrome from the cyanobacterium *Synechocystis*: A low-temperature UV-Vis and FT-IR spectroscopic study. *Photochem Photobiol* **71,** 655-661.

[117] Schmitz,O., Katayama,M., Williams,S.B., Kondo,T., & Golden,S.S. (2000) CikA, a bacteriophytochrome that resets the cyanobacterial circadian clock. *Science* **289,** 765-768.

[118] Wilde,A., Churin,Y., Schubert,H., & Börner,T. (1997) Disruption of a *Synechocystis* sp. PCC6803 gene with partial similarity to phytochrome genes alters growth under changing light qualities. *FEBS Lett* **406,** 89-92.

[119] Wilde,A., Fiedler,B., & Börner,T. (2002) The cyanobacterial phytochrome Cph2 inhibits phototaxis towards blue light. *Mol Microbiol* **44,** 981-988.

[120] Fiedler,B., Broc,D., Schubert,H., Rediger,A., Börner,T., & Wilde,A. (2004) Involvement of cyanobacterial phytochromes in growth under different light qualities and quantities. *Photochem Photobiol* **79,** 551-555.

[121] Hübschmann,T., Yamamoto,H., Gieler,T., Murata,N., & Börner,T. (2005) Red and far-red light alter the transcript profile in the cyanobacterium *Snechocystis* sp PCC6803: Impact of cyanobacterial phytochromes. *FEBS Lett* **579,** 1613-1618.

[122] Yeh,K.C. & Lagarias,J.C. (1998) Eukaryotic phytochromes: Light-regulated serine/threonine protein kinases with histidine kinase ancestry. *Proc Natl Acad Sci USA* **95,** 13976-13981.

[123] Matsushita,T., Mochizuki,N., & Nagatani,A. (2003) Dimers of the N-terminal domain of phytochrome B are functional in the nucleus. *Nature* **424,** 571-574.

[124] Tsien,R.Y. (2010) Nobel lecture: constructing and exploiting the fluorescent protein paintbox. *Integrat Biol* **2,** 77-93.

[125] Zhang,J.A., Wu,X.J., Wang,Z.B., Chen,Y., Wang,X., Zhou,M., Scheer,H., & Zhao,K.H. (2010) Fused-gene approach to photoswitchable and fluorescent biliproteins. *Angewandte Chemie-Intl Ed* **49,** 5456-5458.

[126] Cao,Z., Buttani,V., Losi,A., & Gärtner,W. (2008) A blue light inducible two-component signal transduction system in the plant pathogen *Pseudomonas syringae pv. tomato*. *Biophys J* **94,** 897-905.

[127] Simon,R., Priefer,U., & Pühler,A. (1983) A broad host range mobilisation system for *in vivo* genetic engineering: transposon mutagenesis in gram negative bacteria. *Biotechnology* **1,** 784-791.

[128] Bullock,W.O., Fernandez,J.M., & Short,J.M. (1987) Xl1-Blue - A high-efficiency plasmid transforming reca *Escherichia coli* strain with beta-galactosidase selection. *Biotechniques* **5,** 376-379.

[129] Prentki,P. & Krisch,H.M. (1984) Invitro insertional mutagenesis with a selectable DNA fragment. *Gene* **29,** 303-313.

[130] Drepper,T., Gross,S., Yakunin,A.F., Hallenbeck,P.C., Masepohl,B., & Klipp,W. (2003) Role of GlnB and GlnK in ammonium control of both nitrogenase systems in the phototrophic bacterium *Rhodobacter capsulatus*. *Microbiology* **149,** 2203-2212.

[131] Alexeyev,M.F., Shokolenko,I.N., & Croughan,T.P. (1995) Improved antibiotic-resistance gene cassettes and omega-elements for *Escherichia coli* vector construction and *in-vitro* deletion insertion mutagenesis. *Gene* **160,** 63-67.

[132] Kunkel,T., Tomizawa,K., Kern,R., Furuya,M., Chua,N.H., & Schäfer,E. (1993) In-Vitro Formation of A photoreversible adduct of phycocyanobilin and tobacco apophytochrome-B. *Eur J Biochem* **215,** 587-594.

[133] Higa,A. & Mandel,M. (1970) Actinomycin sensitive mutants of *Escherichia coli* K-12. *Mol Gen Genet* **108,** 41-46.

[134] Cohen,S.N., Chang,A.C.Y., & Hsu,L. (1972) Nonchromosomal antibiotic resistance in bacteria - genetic transformation of *Escherichia coli* by R-factor DNA. *Proc Natl Aca Sci USA* **69,** 2110-2114.

[135] McDonagh,A.F., Palma,L.A., & Lightner,D.A. (1980) Blue-light and bilirubin excretion. *Science* **208,** 145-151.

[136] Kufer,W. & Scheer,H. (1979) Studies on plant bile pigments-V. Chemical modification of biliprotein chromophores. *Z Nature Forsch C* **34,** 776-781.

[137] Jahn,O., Hesse,D., Reinelt,M., & Kratzin,H.D. (2006) Technical innovations for the automated identification of gel-separated proteins by MALDI-TOF mass spectrometry. *Anal Bioanal Chem* **386,** 92-103.

[138] Larkin,M.A., Blackshields,G., Brown,N.P., Chenna,R., McGettigan,P.A., McWilliam,H., Valentin,F., Wallace,I.M., Wilm,A., Lopez,R., Thompson,J.D., Gibson,T.J., & Higgins,D.G. (2007) Clustal W and clustal X version 2.0. *Bioinformatics* **23,** 2947-2948.

[139] de Castro,E., Sigrist,C.J.A., Gattiker,A., Bulliard,V., Langendijk-Genevaux,P.S., Gasteiger,E., Bairoch,A., & Hulo,N. (2006) ScanProsite: detection of PROSITE signature matches and ProRule-associated functional and structural residues in proteins. *Nucleic Acids Res* **34,** W362-W365.

[140] Letunic,I., Copley,R.R., Pils,B., Pinkert,S., Schultz,J., & Bork,P. (2006) SMART 5: domains in the context of genomes and networks. *Nucleic Acids Res* **34,** D257-D260.

[141] Rozen,S. & Skaletsky,H. (2000) Primer3 on the WWW for general users and for biologist programmers. *Methods Mol Biol* **132**.

[142] Jones,D.T. (1999) Protein secondary structure prediction based on position-specific scoring matrices. *J Mol Biol* **292,** 195-202.

[143] Quest,B. & Gärtner,W. (2004) Chromophore selectivity in bacterial phytochromes - Dissecting the process of chromophore attachment. *Eur J Biochem* **271,** 1117-1126.

[144] Quest,B., Hübschmann,T., Sharda,S., de Marsac,N.T., & Gärtner,W. (2007) Homologous expression of a bacterial phytochrome - The cyanobacterium Fremyella diplosiphon incorporates biliverdin as a genuine, functional chromophore. *FEBS J* **274,** 2088-2098.

[145] Gärtner,W., Hill,C., Worm,K., Braslavsky,S.E., & Schaffner,K. (1996) Influence of expression system on chromophore binding and preservation of spectral properties in recombinant phytochrome A. *Eur J Biochem* **236,** 978-983.

[146] Schmidt,P., Gensch,T., Remberg,A., Gärtner,W., Braslavsky,S.E., & Schaffner,K. (1998) The complexity of the P-r to P-fr phototransformation kinetics is an intrinsic property of native phytochrome. *Photochem Photobiol* **68,** 754-761.

[147] Jorissen,H.J.M.M. Spectroscopic and functional characterization of recombinant phytochromes from the lower plants *Anemia phyllitidis* and *Mougeotia scalaris* and the cyanobacterium *Calothrix* PCC760. Ph. D. thesis, MPI für Strahlenchemie, Mülheim (Ruhr). Gerhard-Mercator-Universität Duisburg, p.94. 2001.

[148] Pawson,T. & Nash,P. (2003) Assembly of cell regulatory systems through protein interaction domains. *Science* **300,** 445-452.

[149] Galperin,M.Y. (2004) Bacterial signal transduction network in a genomic perspective. *Environ Microbiol* **6,** 552-567.

[150] Lavin,J.L., Kiil,K., Resano,O., Ussery,D.W., & Oguiza,J.A. (2007) Comparative genomic analysis of two-component regulatory proteins in *Pseudomonas syringae*. *Bmc Genomics* **8**:397

[151] Swartz,T.E., Tseng,T.S., Frederickson,M.A., Paris,G., Comerci,D.J., Rajashekara,G., Kim,J.G., Mudgett,M.B., Splitter,G.A., Ugalde,R.A., Goldbaum,F.A., Briggs,W.R., & Bogomolni,R.A. (2007) Blue-light-activated histidine kinases: Two-component sensors in bacteria. *Science* **317,** 1090-1093.

[152] Purcell,E.B., Siegal-Gaskins,D., Rawling,D.C., Fiebig,A., & Crosson,S. (2007) A photosensory two-component system regulates bacterial cell attachment. *Proc Natl Acad Sci USA* **104,** 18241-18246.

[153] Avila-Perez,M., Vreede,J., Tang,Y.F., Bende,O., Losi,A., Gärtner,W., & Hellingwerf,K. (2009) *In Vivo* mutational analysis of YtvA from *Bacillus subtilis* mechanism of light activation of the general stress response. *J Biol Chem* **284,** 24958-24964.

[154] Taylor,B.L. & Zhulin,I.B. (1999) PAS domains: Internal sensors of oxygen, redox potential, and light. *Microbiol Mol Biol Rev* **63,** 479-506.

[155] Deisseroth,K., Feng,G.P., Majewska,A.K., Miesenbock,G., Ting,A., & Schnitzer,M.J. (2006) Next-generation optical technologies for illuminating genetically targeted brain circuits. *J Neurosci* **26,** 10380-10386.

[156] Shimizu-Sato,S., Huq,E., Tepperman,J.M., & Quail,P.H. (2002) A light-switchable gene promoter system. *Nat Biotechnol* **20,** 1041-1044.

[157] Levskaya,A., Chevalier,A.A., Tabor,J.J., Simpson,Z.B., Lavery,L.A., Levy,M., Davidson, E.A., Scouras,A., Ellington,A.D., Marcotte,E.M., & Voigt,C.A. (2005) Synthetic biology: engineering *Escherichia coli* to see light. *Nature* **438,** 441-442

[158] Lee,J., Natarajan,M., Nashine,V.C., Socolich,M., Vo,T., Russ,W.P., Benkovic,S.J., & Ranganathan,R. (2008) Surface sites for engineering allosteric control in proteins. *Science* **322,** 438-442.

[159] Strickland,D., Moffat,K., & Sosnick,T.R. (2008) Light-activated DNA binding in a designed allosteric protein. *Proc Natl Acad Sci USA* **105,** 10709-10714.

[160] Möglich,A., Ayers,R.A., & Moffat,K. (2009) Design and signaling mechanism of light-regulated histidine kinases. *J Mol Biol* **385,** 1433-1444.

[161] Ratliff,M., Zhu,W.M., Deshmukh,R., Wilks,A., & Stojiljkovic,I. (2001) Homologues of neisserial heme oxygenase in gram-negative bacteria: Degradation of heme by the product of the pigA gene of *Pseudomonas aeruginosa*. *J Bacteriol* **183,** 6394-6403.

[162] Caignan,G.A., Deshmukh,R., Wilks,A., Zeng,Y.H., Huang,H.W., Moenne-Loccoz,P., Bunce,R.A., Eastman,M.A., & Rivera,M. (2002) Oxidation of heme to beta- and delta-biliverdin by *Pseudomonas aeruginosa* heme oxygenase as a consequence of an unusual seating of the heme. *J Am Chem Soc* **124,** 14879-14892.

[163] Lamparter,T., Carrascal,M., Michael,N., Martinez,E., Rottwinkel,G., & Abian,J. (2004) The biliverdin chromophore binds covalently to a conserved cysteine residue in the N-terminus of *Agrobacterium* phytochrome Agp1. *Biochemistry* **43,** 3659-3669.

[164] Quirino,B.F. & Bent,A.F. (2003) Deciphering host resistance and pathogen virulence: the *Arabidopsis/Pseudomonas* interaction as a model. *Mol Plant Pathol* **4,** 517-530.

[165] Jones,A.M., Lindow,S.E., & Wildermuth,M.C. (2007) Salicylic acid, yersiniabactin, and pyoverdin production by the model phytopathogen *Pseudomonas syringae* pv. *tomato* DC3000: Synthesis, Regulation, and Impact on Tomato and *Arabidopsis* host plants. *J Bacteriol* **189,** 6773-6786.

[166] Losi,A. & Gärtner,W. (2008) Bacterial bilin- and flavin-binding photoreceptors. *Photochem Photobio Sci* **7,** 1168-1178.

[167] Pathak,G.P., Ehrenreich,A., Losi,A., Streit,W.R., & Gärtner,W. (2009) Novel blue light-sensitive proteins from a metagenomic approach. *Environ Microbiol* **11,** 2388-2399.

[168] Roberts,M.R. & Paul,N.D. (2006) Seduced by the dark side: integrating molecular and ecological perspectives on the inflence of light on plant defence against pests and pathogens. *New Phytol* **170,** 677-699.

[169] Häder,D.P. (1987) Photosensory behavior in prokaryotes. *Microbiol Rev* **51,** 1-21.

[170] Gest,H. (1995) Phototaxis and other sensory phenomena in purple photosynthetic bacteria. *Fems Microbiol Rev* **16,** 287-294.

[171] Mattick,J.S. (2002) Type IV pili and twitching motility. *Ann Rev Microbiol* **56,** 289-314.

[172] Harshey,R.M. (1994) Bees aren't the only ones - swarming in gram-negative bacteria. *Mol Microbiol* **13,** 389-394.

[173] Katagiri,F., Thilmony,R., & He,S. (2002) The *Arabidopsis thaliana-Pseudomonas syringae* interaction. In The *Arabidopsis* (Meyerowitz, E.M. & Somerville,C.R., eds), American Society of Plant Biologists, Rockville, MD, USA.

[174] Jiang,Z.Y., Rushing, B.G., Bai, Y., Gest,H., & Bauer,C.E. (1998) Isolation of *Rhodospirillum centenum* mutants defective in phototactic colony motility by transposon mutagenesis. *J Bacteriol* **180,** 1248-1255.

[175] Hellingwerf,K.J. (2002) The molecular basis of sensing and responding to light in microorganisms. *Antonie Van Leeuwenhoek* **81,** 51-59.

[176] Yoshihara,S. & Ikeuchi,M. (2004) Phototactic motility in the unicellular cyanobacterium *Synechocystis* sp PCC6803. *Photochem Photobiol Sci* **3,** 512-518.

[177] Burriesci, M. & Bhaya,D. (2008) Tracking phototactic responses and modeling motility of *Synechocystis* sp strain PCC6803. *J Photoch Photobiol B* **91,** 77-6.

[178] Oberpichler, I., Rosen,R., Rasouly,A., Vugman,M., Ron,E.Z., & Lamparter,T. (2008) Light affects motility and infectivity of *Agrobacterium tumefaciens*. *Environ Microbiol* **10,** 2020-2029.

Die hier vorgelegte Dissertation habe ich eigenständig und ohne unerlaubte Hilfe angefertigt. Die Dissertation wurde in der vorgelegten oder in ähnlicher Form noch bei keiner anderen Institution eingereicht. Ich habe bisher keine erfolglosen Promotionsversuche unternommen.

Mülheim an der Ruhr,

Rashmi Shah